ABSTRACT

Monte Carlo Simulations using Infrared Improved DGLAP-CS Theory

Samuel J. Joseph, Ph.D.

Chairperson: Bennie F.L. Ward, Ph.D.

A large number of Z and W bosons will be produced at the LHC. A careful study of their properties in the presence of QCD background processes, will be important in studying the Standard Model more rigorously and to uncover new physics which may appear through radiative corrections or through new tree level processes with suppressed couplings. In order to reach the 1% attendant theoretical precision tag on processes such as single Z and W production, more precise Monte Carlos need to be developed. As a step towards this goal a new set of infrared (ir) improved DGLAP-CS kernels was developed by Ward.

For this work we implemented these infrared improved kernels in HERWIG6.5 to create a new program HERWIRI1.0. We discuss the phenomological implications of our new Monte Carlo HERWIRI1.0. Specifically we compared $pp \to$ 2-jets $+ X$ and $pp \to Z/\gamma^* + X \to \ell^+\ell^- + X'$, with $\ell = e, \mu$, results obtained by HERWIG6.5 and HERWIRI1.0. The three main quantities that we compared were the p_t, energy fraction and rapidity distributions. We made these comparisons at $\sqrt{s} = 14$ TeV, the highest LHC energies. Comparisons were also made for π^+ production in $pp \to$ 2-jets $+ X$ at this energy. As expected, the IR-improved spectra were generally softer.

As a test of HERWIRI1.0 a comparison of the p_t and rapidity distribution data from FNAL at $\sqrt{s} = 1.96$ TeV for the process $p\bar{p} \rightarrow Z/\gamma^* \rightarrow e^+e^- + X$ was made. We found that the softer part of these observed spectra were better described by HERWIRI1.0. This represents a new chapter in precision Monte Carlo simulations for hadron-hadron high energy collisions because the IR-improved kernels do not require an explicit cut-off.

Monte Carlo Simulations using Infrared Improved DGLAP-CS Theory

by

Samuel J. Joseph, ICTP Dipl., M.Phil., BSc.

A Dissertation

Approved by the Department of Physics

____

Gregory A. Benesh, Ph.D., Chairperson

Submitted to the Graduate Faculty of
Baylor University in Partial Fulfillment of the
Requirements for the Degree
of
Doctor of Philosophy

Approved by the Dissertation Committee

Bennie F.L. Ward, Ph.D. , Chairperson

Gerald B. Cleaver, Ph.D.

Robert Piziak, Ph.D.

Dwight P. Russell, Ph.D

Anzhong Wang, Ph.D.

Accepted by the Graduate School
August 2009

J. Larry Lyon, Ph.D., Dean

Page bearing signatures is kept on file in the Graduate School.

TABLE OF CONTENTS

LIST OF FIGURES

LIST OF TABLES

ACKNOWLEDGMENTS

Any work of this extent could not be completed without the help of others. Firstly, I would like to express my gratitude to my advisor Dr. B.F.L. Ward who for five years gave of his time and effort to make me the best physicist possible. Even through his professional difficulties he made sure that my education was not neglected.

Special thanks to Dr. M. Kalmykov, Dr. S. Majhi and Dr. S. Yost for the assistance they have given me.

I would like to acknowledge my committee members, Dr. Cleaver, Dr. Piziak, Dr.Russell and Dr. Wang who volunteered of their time, in spite of all their other duties.

From the insightful discussions I had with Victor Guerrero ranging from cricket to the meaning of quantum mechanics, I would like to express my gratitude.

I would also like to express thanks to my parents, Richard and Yolande Joseph, who never stopped believing in me.

DEDICATION

To Crystal Archer, the love of my life.

CHAPTER ONE

Introduction

The turn on of the Large Hadron Collider (LHC) has bought renewed interest in the development of precision Monte Carlo generators. Luminosity processes, such as single heavy boson production is one of the main areas of interest. At the LHC the use of massive vector bosons as standard candles have been proposed where their yields will be used to compute, or provide an alternative definition of collider integrated luminosities. If we presume the LHC luminosity experimental error to reach 2% [3] then the attendant theoretical precision tag on a single vector boson production should be $^2/_3 - 1\%$.

To achieve this desired level of accuracy $QED \otimes QCD$ exponentiation (a theory of the simultaneous resummation of multiple gluon and multiple photon radiative effects) was used to derive a set of infrared (IR) improved DGLAP kernels [2, 4, 5, 6, 7, 8, 9, 10, 11, 12]. Using this theory we can realize systematically the needed higher order corrections on an event by event basis in the presence of parton showers to the desired accuracy. In this work we implemented these kernels in HERWIG6.5 [13, 14] to create a new Monte Carlo event generator HERWIRI1.0.

1.1 Standard Model

The Standard Model is a comprehensive theory which explains most of the fundamental microscopic interactions we observe [15, 16, 17, 18, 19, 20, 21, 22, 23, 24, 25]. The Standard Model describes three out of the four known forces of nature, the strong, electromagnetic and weak interactions. Gravity has not yet being incorporated into the Standard Model but its effect on fundamental particle process are negligible at the energy scales we can access. This model is a gauge invariant generalization of Quantum Electrodynamics (QED) based on the group $SU(3) \otimes SU(2) \otimes U(1)_Y$. It describes the world in terms of matter fermions and force bosons (cf. table B.1 and table B.2).

The matter particles of the Standard Model, which are are all spin 1/2, are the quarks and leptons. The quarks are the constituents of protons, neutrons and all hadrons. They have both colour and electro-weak charges. The leptons have electro-weak but no colour charge. The quarks and leptons come in three families with identical quantum numbers but different masses:

$$\begin{pmatrix} u^\alpha \\ d^\alpha \end{pmatrix}_L, u_R^\alpha, d_R^\alpha, \begin{pmatrix} c^\alpha \\ s^\alpha \end{pmatrix}_L c_R^\alpha, s_R^\alpha, \begin{pmatrix} t^\alpha \\ b^\alpha \end{pmatrix}_L, t_R^\alpha, b_R^\alpha,$$
$$\begin{pmatrix} \nu_e \\ e \end{pmatrix}_L, e_R, \begin{pmatrix} \nu_\mu \\ \mu \end{pmatrix}_L \mu_R, \begin{pmatrix} \nu_\tau \\ \tau \end{pmatrix}_L \tau_R, \tag{1.1}$$

where the subscripts L and R refer to the left and right handed components respectively. These are defined by

$$\psi_L = \frac{1-\gamma_5}{2}\psi \tag{1.2}$$

and

$$\psi_R = \frac{1+\gamma_5}{2}\psi, \tag{1.3}$$

where ψ is any of the leptons. Here, α denotes colour in the triplet representation of $SU(3)$ colour.

In QED the electromagnetic force between two electrons is due to the exchange of one or more photons emitted by one electron and absorbed by the other. Similarly we have quark-quark interaction mediated by gluon exchange cf. fig. (1.1).

The force carriers of the Standard Model, which are spin 1, are the photon γ, the weak interaction gauge bosons W^+, W^- and Z and the eight gluons g. The spin 0 Higgs particle mediates a force as well, proportional to the fermion masses, therfeore it has yet to be observed directly.

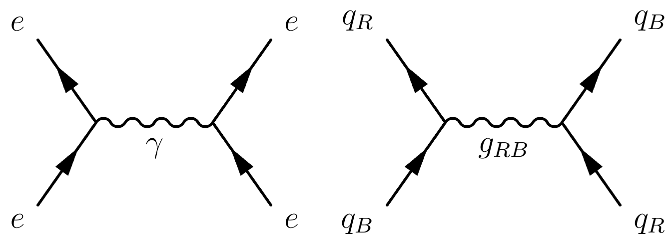

Figure 1.1: Electron-electron interaction due to virtual photon exchange, and quark-quark interaction due to virtual gluon exchange.

Electric charge and colour charge are conserved due to the exact conservation of the corresponding symmetry generators; hence the photons and gluons are massless. On the other hand, the weak bosons W^+, W^-, and Z have large masses implying that the corresponding symmetries are broken. In the Standard Model this symmetry breaking is due to the Higgs mechanism [26, 27] which predicts the physical spectrum of one spin 0 particle, the Higgs boson. This particle has not yet been observed but there is a tremendous experimental effort underway to discover it.

The weak interactions are parity violating. This is incorporated into the Standard Model by associating the left handed and right handed fermion components to different representations of the gauge group. This means that the doublets in eqn. (1.1) are assumed to transform in the fundamental representation of an $SU(2)$ group whereas the right handed partners are taken to be singlets in this group. It is assumed that there are no right handed neutrinos in the Standard Model. Recent observations of small neutrino masses would require addition of a $SU(3) \otimes SU(2) \otimes U(1)_Y$ gauge singlet ν_R to each generation [28].

To construct the Lagrangian, we need to construct the covariant derivative of the various fields. Consider the electron family where

$$\psi_e = \begin{pmatrix} \nu_e \\ e \end{pmatrix}_L . \tag{1.4}$$

The covariant derivatives are then constructed as follows

$$D_\mu \psi_e = (\partial_\mu + igW^r_\mu t_r)\psi_e \tag{1.5}$$

where W^r_μ, $r = 1, 2, 3$ are the gauge fields and t_r are the $SU(2)$ generators in the reducible representation of ψ_e. Since the right handed electron is a singlet of this $SU(2)$, its covariant derivative will be identical to its ordinary derivative

$$D_\mu e_R = \partial_\mu e_R. \tag{1.6}$$

Finally we need to take into consideration the $U(1)$ transformation properties of the various fields. Under the action of $U(1)$ we require the following behaviour

$$\psi_e \rightarrow e^{iy_L\theta(x)}\psi_e, \quad e_R \rightarrow e^{iy_R\theta(x)}e_R. \tag{1.7}$$

To make the derivative covariant with respect to these transformations, we must introduce a new gauge field B_μ and write

$$D_\mu \psi_e = (\partial_\mu - igW^r_\mu t_r + ig^{'} y_L B_\mu)\psi_e \tag{1.8}$$

and

$$D_\mu e_R = (\partial_\mu + ig^{'} y_R B_\mu)e_R \tag{1.9}$$

where $g^{'}$ is the $U(1)$ coupling constant.

Thus the Lagrangian for the gauge fields and the fermions is given by

$$\mathcal{L}_{\text{symm}} = -\frac{1}{4}\sum_{r=1}^{3} F^r_{\mu\nu}F^{r\mu\nu} - \frac{1}{4}B_{\mu\nu}B^{\mu\nu} + \bar{\psi}_L i\gamma^\mu D_\mu \psi_L + \bar{\psi}_R i\gamma^\mu D_\mu \psi_R, \tag{1.10}$$

which contains only gauge bosons and fermions, where we have

$$B_{\mu\nu} = \partial_\mu B_\nu - \partial_\nu B_\mu \tag{1.11}$$

and

$$F^r_{\mu\nu} = \partial_\mu W^r_\nu - \partial_\nu W^r_\mu - g\epsilon_{rst}W^s_\mu W^t_\nu \tag{1.12}$$

are the gauge antisymmetric tensors and ϵ_{rst} are the $SU(2)$ group structure constants.

The $SU(2)$ generators have the following commutation relation

$$[t^r_L, t^s_L] = i\epsilon_{rst} t^t_L \quad \text{and} \quad [t^r_R, t^s_R] = i\epsilon_{rst} t^t_R \tag{1.13}$$

with normalization $\mathrm{Tr}\,[t^r t^s] = \frac{1}{2}\delta^{rs}$ in the fundamental representation of $SU(2)$. Finally the electric charge is given by

$$Q = t^3_L + \frac{1}{2} Y_L = t^3_R + \frac{1}{2} Y_R. \tag{1.14}$$

The physical photon A_μ and the Z boson Z_μ are a linear orthogonal normalized combination of B_μ and W^3_μ,

$$\begin{aligned} A_\mu &= \cos\theta_W B_\mu + \sin\theta_W W^3_\mu \\ Z_\mu &= -\sin\theta_W B_\mu + \cos\theta_W W^3_\mu. \end{aligned} \tag{1.15}$$

This equation defines the weak mixing angle θ_W. Using eqn. (1.14) and the fact that the photon couples to the right and left fermions with the same strength equal to the electric charge e we obtain

$$g \sin\theta_W = g^{'} \cos\theta_W = e, \tag{1.16}$$

which implies

$$\tan\theta_W = \frac{g^{'}}{g}. \tag{1.17}$$

The fermion matter fields are described through their left and right handed components

$$\psi_{L,R} = \left[(1 \mp \gamma_5)/2\right]\psi, \quad \bar{\psi}_{L,R} = \bar{\psi}\left[(1 \pm \gamma_5)/2\right]. \tag{1.18}$$

In the electroweak sector, as we have noted, ψ_L and ψ_R transform differently under the gauge group, ψ_R are singlets and ψ_L are doublets. So the Standard-Model is a chiral theory. We therefore cannot write mass terms of the form $\bar{\psi}_L \psi_R + \mathrm{h.c}$ in the symmetric limit. Fermion masses and W and Z masses have to be introduced by a different mechanism, the Higgs mechanism.

The fermion and gauge boson masses in the Standard Model are generated through the elaborate mechanism of spontaneous symmetry breaking. This mechanism involves the introduction of a scalar field ϕ which is a doublet of the $SU(2)$ group.

The gauge principle and requirement of renormalizabilty fixes the Higgs Lagrangian to be

$$\mathcal{L}_{\text{Higgs}} = (D_\mu\phi)^\dagger(D^\mu\phi) - V(\phi^\dagger\phi) - \bar{\psi}_L\Gamma\psi_R\phi - \bar{\psi}_R\Gamma^\dagger\psi_L\phi, \tag{1.19}$$

where ϕ is the Higgs column vector which perhaps transforms as a reducible representation of the gauge group. The matrices Γ which contain the coupling constants make the Yukawa couplings invariant under the Lorentz and gauge groups. The potential $V(\phi^\dagger\phi)$ must be symmetric under $SU(2)\otimes U(1)$ and be renormalizable. These requirements fix V to be

$$V(\phi^\dagger\phi) = -\frac{1}{2}\mu^2\phi^\dagger\phi + \frac{1}{4}\lambda(\phi^\dagger\phi)^2. \tag{1.20}$$

The covariant derivative of ϕ is defined as

$$D_\mu\phi = (\partial_\mu + igW_\mu^r t_r + ig^{'}y_\phi B_\mu)\phi. \tag{1.21}$$

We get spontaneous symmetry breaking if the minimum of V is obtained for non-vanishing ϕ vacuum expectation values. The vacuum expectation value (VEV) of ϕ, the position of the minimum, is denoted by ν and is defined as

$$\langle 0|\phi(x)|0\rangle = \nu \neq 0. \tag{1.22}$$

To break the symmetry spontaneously, we need a scalar field that transforms under $SU(2)\otimes U(1)$. We assign the scalar field a charge of $1/2$ under the $U(1)$ symmetry so that ϕ transforms as

$$\phi \to e^{i\alpha^a t^a}e^{i\beta/2\phi}, \quad t^a = \sigma^a/2. \tag{1.23}$$

If the field ϕ acquires a vacuum expectation value of the form

$$\langle\phi\rangle = \frac{1}{\sqrt{2}} \begin{pmatrix} 0 \\ \nu \end{pmatrix}, \tag{1.24}$$

then a gauge transformation with

$$\alpha^1 = \alpha^2 = 0, \quad \alpha^3 = \beta \tag{1.25}$$

leaves $\langle\phi\rangle$ invariant. This theory will contain one massless gauge boson and three massive gauge bosons.

We now work out the gauge boson masses. These terms come from the square of eqn. (1.8) evaluated at the scalar field vacuum expectation value of eqn. (1.24). We obtain

$$\Delta\mathcal{L} = \frac{1}{2}(0 \quad \nu) \left(gW_\mu^A t^A + \frac{1}{2}g^{'} B_\mu\right) \left(gW^{b\mu} t^a + \frac{1}{2}g^{'} B^\mu\right) \begin{pmatrix} 0 \\ \nu \end{pmatrix}. \tag{1.26}$$

Using $t^a = \sigma/2$ we obtain

$$\Delta\mathcal{L} = \frac{1}{2}\frac{\nu^2}{4} \left[g^2 \left(A_\mu^1\right)^2 + g^2 \left(A_\mu^2\right)^2 + \left(-gA_\mu^3 + g^{'} B_\mu\right)^2\right]. \tag{1.27}$$

This gives three massive vector bosons.

$$W_\mu^\pm = \frac{1}{\sqrt{2}} \left(W_\mu^1 \mp iW_\mu^2\right) \quad \text{with mass} \quad m_W = g\frac{\nu}{2} \tag{1.28}$$

$$Z_\mu^0 = \frac{1}{\sqrt{g^2 + g^{'2}}} \left(gW_\mu^3 - g^{'} B_\mu\right) \quad \text{with mass} \quad m_Z = \sqrt{g^2 + g^{'2}}\frac{\nu}{2}. \tag{1.29}$$

Finally the massless vector field which is orthogonal to Z_μ is massless:

$$W_\mu = \frac{1}{\sqrt{g^2 + g^{'2}}} \left(g^{'} W_\mu^3 + gW + \mu\right) \quad \text{with mass} \quad m = 0. \tag{1.30}$$

We now come to the $SU(3)$ part of the gauge group [29, 30]. The $SU(3)$ factor describes the theory of strong interaction known as Quantum Chromodynamics (QCD). Each flavour u, d, s, c, t and b of quarks are assumed to transform in the fundamental 3-dimensional representation of this group. So QCD is a non-abelian gauge theory with gauge group $SU(3)$ coupled to quarks in the fundamental representation. The quanta of the $SU(3)$ gauge field are called gluons. The charge of QCD is called colour. Colour is a conserved quantum number with three values labeled red, green and blue, with quarks carrying colours or red, green and blue and antiquarks carrying the respective anti-colours.

Consider the u quark and let us denote its field by a 4-component Dirac spinor field $u(x)$. Each spinor component of this field will transform as a triplet of $SU(3)$. This fact together with the requirement of renormalizability and Lorentz invariance fixes the structure of the Lagrangian uniquely to be

$$\mathcal{L} = -\frac{1}{4}G^a_{\mu\nu}G^{a\mu\nu} + \bar{u}(i\gamma^\mu D_\mu - m)u, \tag{1.31}$$

where m is the mass of the quark. The covariant derivative is defined by

$$D_\mu u = \partial_\mu u - ig_s A^a_\mu \lambda_a u \tag{1.32}$$

and

$$G^a_{\mu\nu} = \partial_\mu A^a_\nu - \partial_\nu A^a_\mu + g_s f_{abc} A^b_\mu A^c_\nu, \tag{1.33}$$

where g_s is the $SU(3)$ coupling constant and f_{abc} its structure constant. The last term $g_s f_{abc} A^b_\mu A^c_\nu$ means that gluons are self interacting, through three and four point vertices. This will give rise to asymptotic freedom at high energies and strong interactions at low energies. Here, λ_a generate the triplet representation of $SU(3)$ colour.

The Lagrangian is invariant under

$$u(x) \to u^{'}(x) = e^{i\Lambda(x)}u(x), \tag{1.34}$$

where

$$\Lambda(x) = \Lambda^a(x)\lambda_a, \tag{1.35}$$

with Λ^a, $a = 1, \cdots, 8$ are arbitrary real functions.

We introduce other flavours of quarks in the QCD Lagrangian by

$$\mathcal{L} = -\frac{1}{4}\sum_{A=1}^{8} G^{A\mu\nu}G^{A}_{\mu\nu} + \sum_{j=1}^{n_f} \bar{q}_j \left(i\not{D} - m_j\right) q_j, \tag{1.36}$$

where, q_j are the quark fields (of n_f different flavours) with mass m_j and $\not{D} = \gamma^\mu D_\mu$, where γ^μ are the Dirac matrices. The generators obey the commutation relations

$$\left[t^a, t^b\right] = i f_{abc} t^c, \tag{1.37}$$

where f_{abc} are the complete antisymmetric structure constants of the fundamental representation of $SU(3)$ normalized by

$$\text{Tr}\,\left[t^a t^b\right] = \frac{\delta^{ab}}{2}. \tag{1.38}$$

Equation (1.37) defines the Lie algebra of the group.

We can also define a set of $(N^2 - 1) \times (N^2 - 1)$ matrices that obey the same algebra:

$$(T^A)_{BC} \equiv -i f^{ABC}, \tag{1.39}$$

$$[T^A, T^B] = -f^{ABC} T^C. \tag{1.40}$$

These define the group's adjoint representation.

Also note:

$$\begin{aligned}
\text{Tr}\,(t^A t^B) &= \frac{1}{2}\delta^{AB} \equiv T_R \delta^A & (1.41)\\
\sum_A t^A_{ab} t^A_{bc} &= \frac{N^2-1}{2N}\delta_{ac} \equiv C_F \delta_{ac} & (1.42)\\
\text{Tr}\,(T^C T^D) &= \sum_{A,B} F^{ABC} F^{ABD} = N\delta^{CD} \equiv C_A \delta^{CD}, & (1.43)
\end{aligned}$$

where the constants C_F and C_A are the Casmir operators of the fundamental and adjoint representation of the group respectively. These constants are:

$$\begin{aligned} T_R &= \frac{1}{2}, &(1.44)\\ C_F &= \frac{4}{3}, &(1.45)\\ C_A &= 3. &(1.46) \end{aligned}$$

Quarks also participate in electro-weak interactions so we need to transform them non-trivially with respect to the $SU(2) \otimes U(1)$ subgroup of $SU(3) \otimes SU(2) \otimes U(1)$. Consider the (u, d) family of quark. We assign u_L and d_L to the fundamental two dimensional representation of $SU(2)$. We denote this doublet by a column matrix q

$$q(x) = \begin{pmatrix} u(x) \\ d(x) \end{pmatrix}_L . \tag{1.47}$$

The right handed quarks u_R and d_R are assumed to be $SU(2)$ singlets.

Finally, we need to specify the $U(1)$ representation of the various quarks. Combining all these pieces we get the Standard Model for the electron family of leptons and (u, d) family of quarks.

$$\begin{aligned} \mathcal{L} &= -\frac{1}{4}(G^a_{\mu\nu}G^a_{\mu\nu} + F^r_{\mu\nu}F^{r\mu\nu} + B_{\mu\nu}B^{\mu\nu}) \\ &+ \bar{q}i\gamma^\mu D_\mu q + \bar{u}_R i\gamma^\mu D_\mu u_R + \bar{d}_R i\gamma^\mu D_\mu d_R \\ &+ \bar{\psi}i\gamma^\mu D_\mu \psi_e + \bar{e}_R i\gamma^\mu D_\mu e_R + (h\bar{\psi}_e \phi e_R + \text{hermitian conjugate}) \\ &+ D_\mu \phi^\dagger D^\mu \phi - m^2\phi^\dagger\phi - \frac{\lambda}{4}(\phi^\dagger\phi)^2, \end{aligned} \tag{1.48}$$

where

$$D_\mu q = (\partial_\mu - ig_s A_\mu - igW^r_\mu t_r - i\frac{g^{'}}{2}y_q B_\mu)q, \tag{1.49}$$

and

$$D_\mu u_R = (\partial_\mu - ig_s A_\mu - i\frac{g^{'}}{2}y_{u_R} B_\mu)u_R. \tag{1.50}$$

In order to generate mass terms for the quark fields we have to include Yukawa couplings. To accomplish this we construct all the gauge invariant renormalizable couplings of $(u, d)_L$, u_R, d_R and the Higgs field ϕ. The most general term has the following form

$$\mathcal{L}_{\text{Yukawa}} = f_1 \bar{q}\phi d_R + f_2 \bar{q}\tilde{\phi} u_R + h.c. \tag{1.51}$$

where $\tilde{\phi}$ is given by

$$\tilde{\phi} = \begin{pmatrix} -\phi_2^* \\ \phi_1^* \end{pmatrix}. \tag{1.52}$$

Including all three families of quarks and leptons gives the complete Standard Model Lagrangian after electroweak symmetry breaking, with no explicit Higgs boson.

$$\mathcal{L}_{\text{SM}} = \mathcal{L}_{\text{Dirac}} + \mathcal{L}_{\text{mass}} + \mathcal{L}_{\text{gauge}} + \mathcal{L}_{\text{gauge}/\psi}. \tag{1.53}$$

Here,

$$\mathcal{L}_{\text{Dirac}} = i\bar{e}_L^i \partial\!\!\!/ e_L^i + i\bar{\nu}_L^i \partial\!\!\!/ \nu_L^i + i\bar{e}_R^i \partial\!\!\!/ e_R^i + i\bar{u}_L^i \partial\!\!\!/ u_L^i + i\bar{d}_L^i \partial\!\!\!/ d_L^i + i\bar{u}_R^i \partial\!\!\!/ u_R^i + i\bar{d}_R^i \partial\!\!\!/ d_R^i; \tag{1.54}$$

$$\mathcal{L}_{\text{mass}} = -\nu(\lambda_e^i \bar{e}_L^i e_R^i + \lambda_u^i \bar{u}_L^i u_R^i + \lambda_d^i \bar{d}_L^i d_R^i + \text{h.c.}) - \mathrm{M_W^2 W_\mu^+ W^{-\mu}} - \frac{\mathrm{M_W^2}}{2\cos^2\theta_{\mathrm{W}}} \mathrm{Z_\mu Z^\mu}; \tag{1.55}$$

$$\mathcal{L}_{\text{gauge}} = -\frac{1}{4}(G_{\mu\nu}^a)^2 - \frac{1}{2}W_{\mu\nu}^+ W^{-\mu\nu} - \frac{1}{4}Z_{\mu\nu}Z^{\mu\nu} - \frac{1}{4}F_{\mu\nu}F^{\mu\nu} + \mathcal{L}_{WZA}, \tag{1.56}$$

where

$$\begin{aligned} G_{\mu\nu}^a &= \partial_\mu A_\nu^a - \partial_\nu A_\mu^a - g_s f^{abc} A_\mu^b A_\nu^c \\ W_{\mu\nu}^\pm &= \partial_\mu W_\nu^\pm - \partial_\nu W_\mu^\pm \\ Z_{\mu\nu} &= \partial_\mu Z_\nu - \partial_\nu Z_\mu \\ F_{\mu\nu} &= \partial_\mu A_\nu - \partial_\nu A_\mu, \end{aligned} \tag{1.57}$$

and

$$
\begin{aligned}
\mathcal{L}_{WZA} &= ig_2 \cos\theta_W \left[\left(W_\mu^- W_\nu^+ - W_\nu^- W_\mu^+ \right) \partial^\mu Z^\nu + W_{\mu\nu}^+ W^{-\mu} Z^\nu - W_{\mu\nu}^- W^{+\mu} Z^\nu \right] \\
&+ ie \left[\left(W_\mu^- W_\nu^+ - W_\nu^- W_\mu^+ \right) \partial^\mu A^\nu + W_{\mu\nu}^+ W^{-\mu} A^\nu - W_{\mu\nu}^- W^{+\mu} A^\nu \right] \\
&+ g_2^2 \cos^2\theta_W \left(W_\mu^+ W_\nu^- Z^\mu Z^\nu - W_\mu^+ W^{-\mu} Z_\nu Z^\nu \right) \\
&+ g_2^2 \left(W_\mu^+ W_\nu^- A^\mu A^\nu - W_\mu^+ W^{-\mu} A_\nu A^\nu \right) \\
&+ g_2 e \cos\theta_W \left[W_\mu^+ W_\nu^- \left(Z^\mu A^\nu + Z^\nu A^\mu \right) - W_\mu^+ W^{-\mu} Z_\nu A^\nu \right] \\
&+ \frac{1}{2} g_2^2 \left(W_\mu^+ W_\nu^- \right) \left(W^{+\mu} W^{-\nu} - W^{+\nu} W^{-\mu} \right); \qquad (1.58)
\end{aligned}
$$

and

$$
\mathcal{L}_{\mathrm{gauge}/\psi} = -g_s A_\mu^a J_{(3)}^{\mu a} - g_2 \left(W_\mu^+ J_{W^+}^\mu + W_\mu^- J_{W^-}^\mu + Z_\mu J_Z^\mu \right) - e A_\mu J_A^\mu, \qquad (1.59)
$$

where

$$
\begin{aligned}
J_{(3)}^{\mu a} &= \bar{u}^i \gamma^\mu T_{(3)}^a u^i + \bar{d}^i \gamma^\mu T_{(3)}^a d^i \\
J_{W^+}^\mu &= \frac{1}{\sqrt{2}} \left(\bar{\nu}_L^i \gamma^\mu e_L^i + V^{ij} \bar{u}_L^i \gamma^\mu d_L^j \right) \\
J_{W^-}^\mu &= \left(J_{W^+}^\mu \right)^* \\
J_Z^\mu &= \frac{1}{\cos\theta_W} \left[\frac{1}{2} \bar{\nu}_L^i \gamma^\mu \nu_L^i + \left(-\frac{1}{2} + \sin^2\theta_W \right) \bar{e}_L^i \gamma^\mu e_L^i + \left(\sin^2\theta_W \right) \bar{e}_R^i \gamma^\mu e_R^i \right. \\
&+ \left(\frac{1}{2} - \frac{2}{3} \sin^2\theta_W \right) \bar{u}_L^i \gamma^\mu u_L^i + \left(-\frac{2}{3} \sin^2\theta_W \right) \bar{u}_R^i \gamma^\mu u_R^i \\
&+ \left. \left(-\frac{1}{2} + \frac{1}{3} \sin^2\theta_W \right) \bar{d}_L^i \gamma^\mu d_L^i + \left(\frac{1}{3} \sin^2\theta_W \right) \bar{d}_R^i \gamma^\mu d_R^i \right] \\
J_A^\mu &= (-1)\, \bar{e}^i \gamma^\mu e^i + \left(\frac{2}{3} \right) \bar{u}^i \gamma^\mu u^i + \left(-\frac{1}{3} \right) \bar{d}^i \gamma^\mu d^i. \qquad (1.60)
\end{aligned}
$$

1.3 Calculating in QFT

In particle physics we generally collide two beams with well defined momenta, and observe what comes out. The probability of observing any particular final state can be expressed in terms of the cross section. Another frequently measured quantity is the decay rate.

Let us suppose we have a target consisting of particle a with density ρ_a at rest. We now aim at this target a bunch of particles of type b, with number density ρ_b and velocity v. If ℓ_a and ℓ_b and A are the lengths of the bunches and the cross sectional area common to both bunches of particles then the number of scattering events is proportional to ρ_a, ρ_b, ℓ_a, ℓ_b. The cross section, (σ) which has units of area is defined as

$$\sigma \equiv \frac{\text{Number of scattering events}}{\rho_a \ell_a \rho_b \ell_b A}. \tag{1.61}$$

To compute the event rate in an actual accelerator, we integrate over the beam area.

$$\text{Number of events} = \sigma \ell_\mathrm{a} \ell_\mathrm{b} \int \mathrm{d}^2\mathrm{x} \rho_\mathrm{a}(\mathrm{x}) \rho_\mathrm{b}(\mathrm{x}). \tag{1.62}$$

We can also measure the momenta of the final particles. We now have a differential cross section $d\sigma/(d^3p_1, \cdots, d^3p_n)$, which when integrated over any small $d^3p_1, \cdots d^3, p_n$ gives the cross section for scattering into that region of final state momentum space.

The second measurable quantity is the decay rate Γ of an unstable particle A into a specified final state. It is defined as

$$\Gamma \equiv \frac{\text{Number of decays per unit time}}{\text{Number of A particles present}}. \tag{1.63}$$

The lifetime τ of the particle is then the reciprocal of the sum of its decay rates into all possible final states.

To calculate a scattering cross section, we start from a free field which describes the incoming and outgoing particles and a Hamiltonian that describes how the particles interact with each other. The amplitude for scattering is then the sum of each possible interaction history over all possible intermediate particle states. The number of times this interaction Hamiltonian acts, is the order of the pertubative expansion. The time dependent pertubation theory is known as the Dyson series.

In the canonical quantization formulation the probability amplitude for a transition of a quantum system from the initial state $|i>$ to the final state $|f>$ is given by the matrix element,

$$S_{fi} = \langle f \left| S \right| i \rangle \,, \tag{1.64}$$

where S is the S-matrix given by

$$S = \sum_{n=0}^{\infty} \frac{i^n}{n!} \int \prod_{j=1}^{n} d^4 x_j \mathcal{T} \left[\prod_{j=1}^{n} \mathcal{L}_\nu(x_j) \right] \equiv \sum_{n=0}^{\infty} S^{(n)}, \tag{1.65}$$

where $\mathcal{L}_\nu$ is the interaction Lagrangian and $\mathcal{T}$ signifies the time ordered product of operators.

For two operators $\mathcal{O}_1(x)$ and $\mathcal{O}_2(y)$ that depend on spacetime locations x and y we define

$$\mathcal{T}\left[\mathcal{O}_1\left(x\right)\mathcal{O}_2\left(y\right)\right] := \begin{cases} (-1)^{\mathrm{sgn}(\mathcal{O}_1\mathcal{O}_2)}\mathcal{O}_1(x)\mathcal{O}_2(y) & \text{if } x_0 > y_0 \\ (-1)^{\mathrm{sgn}(\mathcal{O}_1\mathcal{O}_2)}\mathcal{O}_2(y)\mathcal{O}_1(x) & \text{if } x_0 < y_0 \end{cases} \tag{1.66}$$

Here x_0 and y_0 denote the time coordinate of the points x and y and $\mathrm{sgn}(\mathcal{O}_1\mathcal{O}_2)$ is a possible minus sign for Fermi statistics.

A Feynman diagram is a graphical representation of a term in the Wick's expansion of the time ordered product in the n-th order term $S^{(n)}$ of the S-matrix,

$$\mathcal{T} \prod_{j=1}^{n} \mathcal{L}_\nu(x_j) = \sum_{\text{all possible contractions}} (\pm) \mathcal{N} \prod_{j=1}^{n} \mathcal{L}_\nu(x_j), \tag{1.67}$$

where $\mathcal{N}$ signifies the normal product (all creation operators are to the left of all annihilation operators). For a given diagram, Feynman gave a prescription for calculating the amplitude from a field theory Lagrangian. These can be read off from the action defined by

$$S = i \int d^4 x \mathcal{L}. \tag{1.68}$$

In order to derive the Feynman rules, we need to fix the gauge. In covariant gauges we have

$$\mathcal{L}_{\text{gauge}-\text{fixing}} = -\frac{1}{2\lambda} \left(\partial^\mu A^a_\mu \right)^2. \tag{1.69}$$

In non-abelian gauge theory we need to add an extra ghost term. These are an unphysical set of scalar fields that obey Fermi statistics. They are used to cancel the unphysical degrees of freedom which propagate when non-abelian gauge theories are renormalized. So for every diagram with a closed loop of internal gluons, we must add a diagram with them replaced by ghosts.

$$\mathcal{L}_{\text{ghost}} = (\partial_\mu \bar{c}^a)(D^\mu c^a). \tag{1.70}$$

Here c^a is the ghost field with colour index a. Its covariant derivative is

$$D_\mu c^a = (\partial \delta^{ab} - i g_s A_\mu^{ab}) c^b, \quad A_\mu^{ab} = A_\mu^c (t^c)^{ab}, \tag{1.71}$$

where

$$(t^c)^{ab} = i f^{acb}, \tag{1.72}$$

are the generators of the colour group in the adjoint representation.

These changes give the final Lagrangian

$$\mathcal{L} = -\frac{1}{4} \sum_{A=1}^{8} G^{A\mu\nu} G^A_{\mu\nu} + \sum_{j=1}^{n_f} \bar{q}_j \left(i \not{D} - m_j \right) q_j - \frac{1}{2\lambda} \left(\partial^\mu A^a_\mu \right)^2 + \partial_\mu \bar{c}^a)(D^\mu c^a). \tag{1.73}$$

To calculate the cross section for a given process, we must write down all possible diagrams, use the Feynman rules to give us the amplitude $i\mathcal{M}$, use Dirac algebra and trace theorems to calculate $\sum |\mathcal{M}|^2$, where the sum is over all unobserved quantum numbers, divide by the over counting of incoming states, and integrate over phase space:

$$\sigma = \frac{1}{S} \frac{1}{2s} \int d\Gamma \sum |\mathcal{M}|^2 . \tag{1.74}$$

An element of n-body phase space is given by

$$\begin{aligned} d\Gamma &= \prod_{i=1}^{n} \left(\frac{d^4 p_i}{(2\pi)^4} (2\pi)\, \theta(p_{i0}) \delta\left(p_i^2 - m_i^2\right) \right) (2\pi)^4 \delta^4 \left(p_{\text{tot}} - \sum_i^n p_i \right) \\ &= \prod_{i=1}^{n} \left(\frac{d^3 p_i}{(2\pi)^3 2E_i} \right) (2\pi)^4 \delta^4 \left(p_{\text{tot}} - \sum_i^n p_i \right). \end{aligned} \tag{1.75}$$

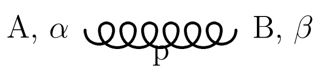

$$= \delta^{ab}\left[-g^{\alpha\beta} + (1-\lambda)\frac{p^\alpha p^\beta}{p^2+i\epsilon}\right]\frac{i}{p^2+i\epsilon}$$

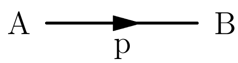

$$= \delta^{AB}\frac{i}{(p^2+i\epsilon)}$$

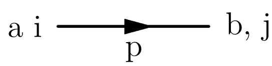

$$= \delta^{ab}\frac{i}{(\not p - m + i\epsilon)_{ji}}$$

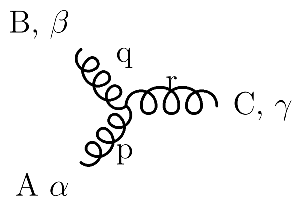

$$= -gf^{ABC}\left[(p-q)^\gamma g^{\alpha\beta} + (q-r)^\alpha g^{\beta\gamma} + (r-p)^\beta g^{\gamma\alpha}\right]$$
$$\text{(all momenta incoming, } p+q+r=0)$$

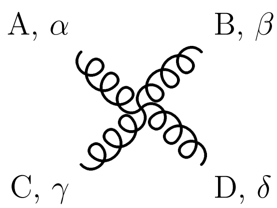

$$\begin{aligned} = &-ig^2 f^{XAC}f^{XBD}\left[g^{\alpha\beta}g^{\gamma\delta} - g^{\alpha\delta}g^{\beta\gamma}\right] \\ &-ig^2 f^{XAD}f^{XBC}\left[g^{\alpha\beta}g^{\gamma\delta} - g^{\alpha\gamma}g^{\beta\delta}\right] \\ &-ig^2 f^{XAB}f^{XCD}\left[g^{\alpha\gamma}g^{\beta\delta} - g^{\alpha\delta}g^{\beta\gamma}\right]\end{aligned}$$

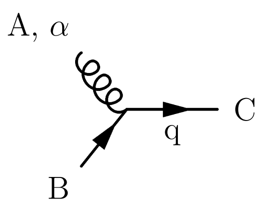

$$= gf^{ABC}q^\alpha$$

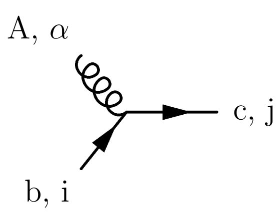

$$= -ig(t^A)_{cb}(\gamma^\alpha)_{ji}$$

Figure 1.2: Feynman rules for QCD. The solid lines represent the fermions, the curly lines the gluons.

In practical calculations we use $\alpha_s = g_s^2/4\pi$ rather than g_s. Along with quark masses g_s is the only parameter in the QCD Lagrangian. These parameters in the Lagrangian are not physically observable quantities. The physical quantities are calculated as a function of the terms in the Lagrangian. By using renormalization theory, we can reformulate the theory in such a way that one physical observable can be written as a function of another. A specific scale, called the renormalization scale μ is chosen at which to define the physical quantities.

By using the fact that varying μ moves physical contributions around within a calculation, but does not change the results of the physical calculation, we can derive an equation for how g_s varies as a function of μ. This forms one of a set of equations that together describes how the the theory varies with the renormalization scale, which formally forms a group.

Consider a dimensionless physical observable R that is a function of only one physical scale Q^2. Assume that this observable is not sensitive to quark masses. After renormalization, R can only be a function of Q^2, μ^2 and $\alpha_s(\mu^2)$. By dimensional analysis, the only way R can depend on the dimensionful variables Q^2 and μ^2 is through their ratio. Therefore

$$R = R(Q^2/\mu^2, \alpha_s(\mu^2)). \tag{1.76}$$

Since R is a physical quantity it must be independent of the value of μ so using the chain rule for partial derivatives we get

$$\begin{aligned}\mu^2 \frac{d}{d\mu^2} R(Q^2/\mu^2, \alpha_s) = 0 \quad &= \quad \left[\mu^2 \frac{\partial}{\partial \mu^2} + \mu^2 \frac{\partial \alpha_s}{\partial \mu^2} \frac{\partial}{\partial \alpha_s}\right] R \\ &\equiv \quad \left[\mu^2 \frac{\partial}{\partial \mu^2} + \beta(\alpha_s) \frac{\partial}{\partial \alpha_s}\right] R.\end{aligned} \tag{1.77}$$

i.e.

$$\beta(\alpha_s) \equiv \mu^2 \frac{\partial \alpha_s}{\partial \mu^2}. \tag{1.78}$$

Let us apply the RGE to some hard process at a large scale Q. Also let

$$t = \log \frac{Q^2}{\mu^2}. \tag{1.79}$$

Eqn. (1.77) becomes

$$\left[-\frac{\partial}{\partial t} + \beta\left(\alpha_s\right) \frac{\partial}{\partial \alpha_s} \right] R = 0, \tag{1.80}$$

where we have set $Q^2 = \mu^2$ at $t = 0$. The solution is

$$R(t, \alpha_s) = R(0, \alpha_s(t)) \tag{1.81}$$

where

$$t = \int_{\alpha_s}^{\alpha_s(t)} \frac{1}{\beta(\alpha_s^{'})} d\alpha_s^{'}. \tag{1.82}$$

Taking d/dt of eqn. (1.82) we obtain

$$1 = \frac{1}{\beta(\alpha_s(t))} \frac{\partial \alpha_s(t)}{\partial t} \tag{1.83}$$

and taking $d/d\alpha_s$ gives

$$0 = -\frac{1}{\beta(\alpha_s)} + \frac{1}{\beta\alpha_s(t)} \frac{\partial \alpha_s(t)}{\partial \alpha_s}. \tag{1.84}$$

These two equations imply

$$\frac{\partial \alpha(t)}{\partial t} = \beta(\alpha(t)), \tag{1.85}$$

$$\frac{\partial \alpha(t)}{\partial \alpha} = \frac{\beta(\alpha(t))}{\beta(\alpha)}. \tag{1.86}$$

By direct calculation one finds

$$\beta(\alpha_s) = -\alpha_s^2 \left(\beta_0 + \beta_1 \alpha_s + \beta_2 \alpha_s^2 + \beta_3 \alpha_s^3 + \cdots \right). \tag{1.87}$$

To one loop, we have

$$\beta_0 = \frac{11 C_A - 4 T_R n_f}{12\pi}, \tag{1.88}$$

where n_f is the number of quark flavours. We note that if $n_f \leq 16$, then $\beta_0 > 0$ in QCD. We see that $\alpha_s(t)$ decreases with Q^2 (eqn. 1.85) if β is negative at small

α_s. Conversely, the coupling increases with decreasing energy. This means that the coupling becomes large at low energies, and one can no longer rely on perturbation theory. Substituting the one loop $\beta(\alpha_s) = -\alpha_s\beta_0$ result into eqn. (1.82), we obtain

$$\alpha_s(Q^2) = \frac{\alpha_s(\mu^2)}{1 + \alpha_s(\mu^2)\beta_0 \ln \frac{Q^2}{\mu^2}}. \tag{1.89}$$

This property of QCD is called asymptotic freedom or anti-screening [31]. Asymptotic freedom implies that a charge of small magnitude catalyzes a cloud of virtual particles that enhances its power. Since these virtual particles themselves carry a charge the process is self reinforcing. This implies that the required energy diverges to infinity. This cannot be the case, so we conclude that the source cannot be produced in the first place. Thus quarks cannot exist on their own and are confined but quarks and antiquarks can form bound states of finite energy. In the region where they overlap the cloud of the source can be canceled by the anticloud of the antisource.

Asymptotic freedom leads to the phenomenon of jets associated with hard or soft radiation. Hard radiation is capable of significantly redirecting the flow of energy and momentum, where as soft radiation produces additional particles moving in the same direction, without deflecting the overall flow.

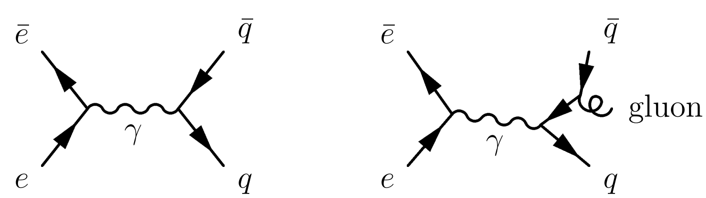

Figure 1.3: Feynman graphs representing the fundamental processes in electron-positron annihilation, as they take place in space time. They show the origin of two-jet and three-jet events.

Consider the processes shown in fig. (1.3). The quark and antiquark move in opposite directions due to the conservation of energy and momentum. If there is no

Figure 1.4: A photograph from the L3 collaboration, showing three jets emerging from electron-positron annihilation at high energy. These jets are the materialization of a quark, antiquark and gluon.

hard radiation, the soft radiation will convert the quark into a spray of hadrons moving in a common direction called a jet as seen in fig. (1.4). Similarly, the antiquarks produces a jet moving in the opposite direction. We should then see a 2-jet event. Sometimes there will be hard radiation, with the quark (or antiquark) emitting a gluon in a significantly new direction and we get a 3-jet event. Occasionally we also get a 4-jet events.

The relative probability of different number of jets, how it varies with the overall energy, the relative frequency of the different angles at which the jets emerge and the total energy can be predicted quantitatively. These predictions agree well with experimental results. Figure (1.5) shows the coupling α_s measured by different experiments at different energies [32]. We see that the coupling changes with the energy scale as predicted by the theory. Therefore we can have some confidence in the correctness of QCD.

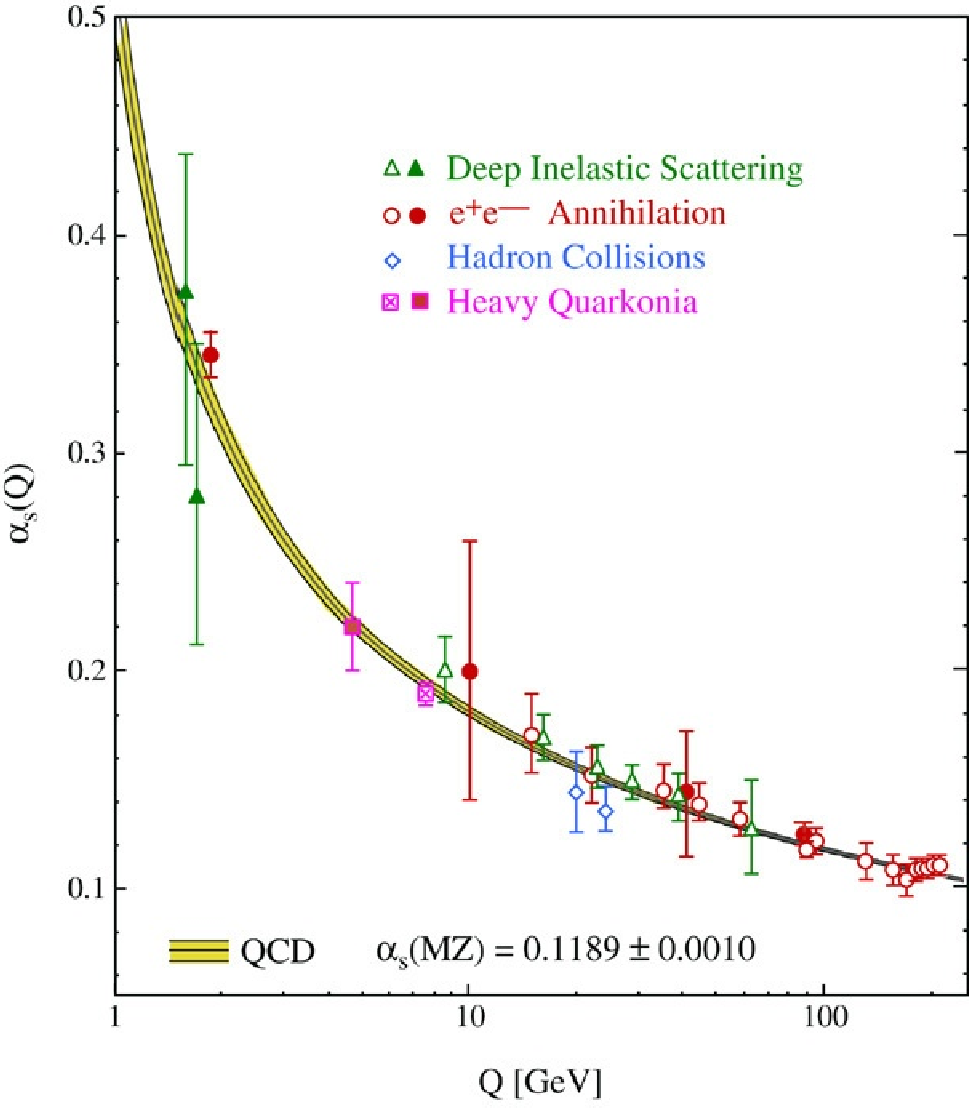

Figure 1.5: Summary of measurements of $\alpha_s(Q)$ as a function of the respective energy scale Q. Open symbols indicate (resummed) NLO, and filled symbols NNLO QCD calculations used in the respective analysis. The curves are the QCD predictions for the combined world average value of $\alpha_s(M_Z)$, in 4-loop approximation and using 3-loop threshold matching at the heavy quark pole masses. $M_c = 1.5$ GeV and $M_b = 4.7$GeV.

1.5 Parton Model

In order to calculate a production cross section, we need to know the distribution of the momentum fraction x of the partons in the incoming hadrons in the relevant kinematic range. These parton distribution functions (PDF's) can not be calculated pertubatively but are determined by global fits to data from deep inelastic scattering (DIS), Drell-Yan(DY) (fig. 1.6), and jet production. Two major groups CTEQ [33] and MRST [34] provide regular updates to the PDF's.

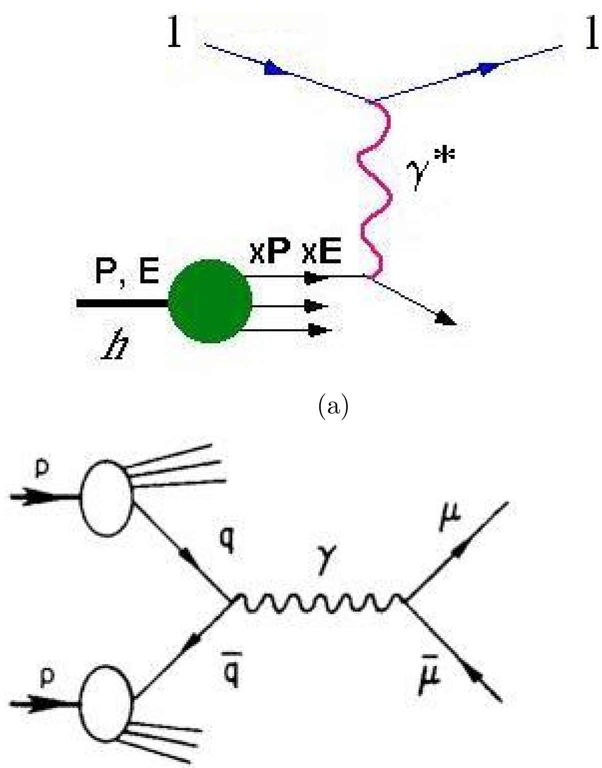

(a)

(b)

Figure 1.6: (a) Deep inelastic scattering. (b) Drell-Yan diagram for the production of massive dimuon pairs in pp collisions.

These parton densities are used to calculate hard processes initiated by hadronic collisions via the Factorization Theorem [35, 36, 37, 38, 39]. Consider a hadronic process of the form $h_1 + h_2 \rightarrow X + all$, where X is some particle or pair of particles which specify the large scale Q^2 relevant for the process. For example, in a $p\bar{p}$ collision, X can be a W, Z or a virtual photon with large Q^2 or a jet at large transverse momentum p_t, or a pair of heavy quark antiquark of mass M. The total collection of gluons and light quark pairs is included in "all". The factorization theorem states that for the cross section or some other sufficiently inclusive distribution we have

$$\sigma(s,\tau) = \sum_{AB} \int dx_1 dx_2 p_{1A}(x_1, Q^2) p_{2B}(x_2, Q^2) \sigma_{AB}(x_1 x_2 s, \tau), \tag{1.90}$$

where $\tau = Q^2/s$ is a scaling variable, p_{iC} are generic parton-C densities inside the hadron h_i, σ_{AB} is the partonic cross section for $h_1 + h_2 \rightarrow X + all$. The factorization theorem is due to the fact that the mass singularities that are associated with the initial legs are universal in nature, so that we can absorb these singularities into the bare parton densities to produce modified parton densities. This means that once the parton densities and α_s are known from other measurements we can predict the rate of any given hard process with no free parameters.

1.6 Experimental Tests

Different aspects of the electroweak sector have been verified (fig. 1.7). The indirect effects of the Z were first observed in 1973 at CERN (European Organization for Nuclear Research) by the Gargamelle collaboration [40, 41]. In 1982 also at CERN, the $W^{\pm}$ and Z were directly produced by the UA1 and UA2 collaborations. [42, 43, 44]. These were subsequently produced at the Tevatron at the Fermi National Accelerator Laboratory (Fermilab). From 1989 LEP, The Large Electron-Positron Collider, with its four experiments: ALEPH, DELPHI, OPAL, L3 studied the precise properties of the standard model [45]. It was found that the couplings of quarks and leptons to the weak gauge bosons $W^{\pm}$ and Z are those predicted by the Standard Model.

From 1995 the energy of LEP was gradually increased to 206 GeV. This phase is referred to as LEP2. The main goal was to search for the Higgs boson, the precise measurement of m_W and the experimental study of the triple gauge vertices $WW\gamma$

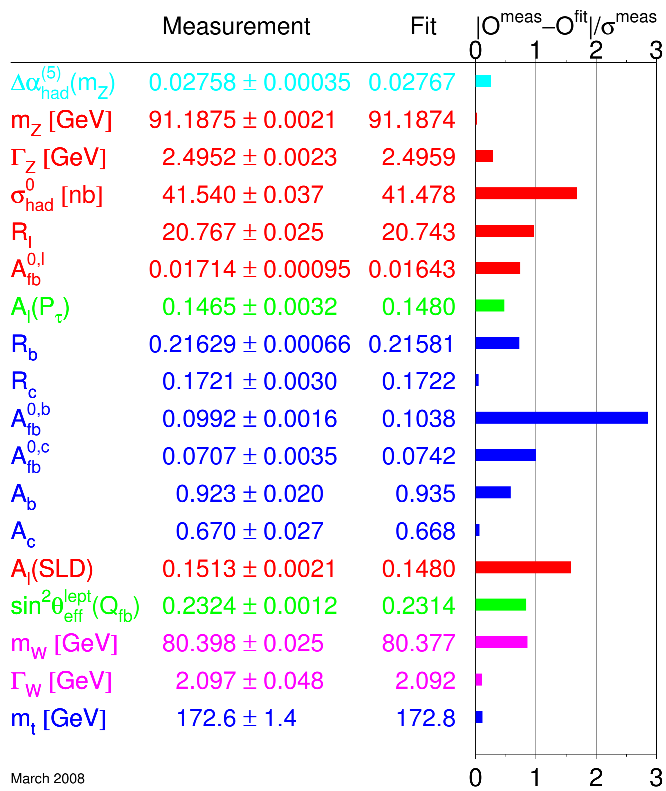

Figure 1.7: Each measured observable (O^{meas}) quantity is compared with the value obtained from the fit (O^{fit}). Also shown graphically is the difference between measurement and fit values in number of standard deviations. Colours indicate groups of similar variables.

and WWZ. The experiment failed to detect the Higgs, but a lower limit was placed on its mass $m_H \gtrsim 114$ GeV. Indirect evidence from precision tests of the Standard Model placed an upper limit of $m_H \lesssim$ at 95% c.l. (fig. 1.8).

In 2002 LEP, was dismantled to make way for a new accelerator, the LHC (LARGE HADRON COLLIDER) which is a proton-proton collider with a center of mass energy of 14 TeV. Two main experiments, ATLAS and CMS, will continue the search for the Higgs boson starting in late 2009. A precise measurement of gauge boson production will be important as a way to test the Standard Model more rigorously and to discover new physics which may appear through radiative corrections and/or through new tree level processes with suppressed couplings. The computational tools such as Monte Carlo event generators used in the analysis therefore need

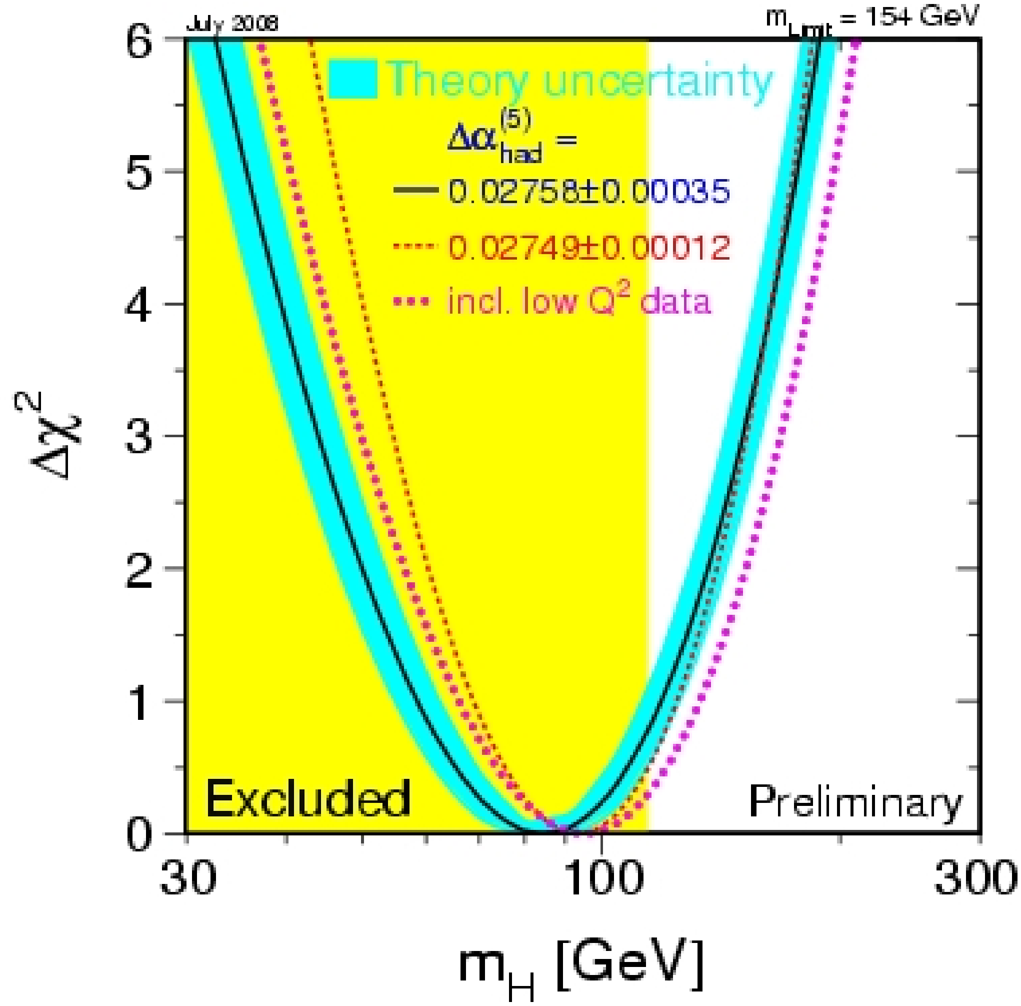

Figure 1.8: $\Delta\chi^2 = \chi^2 - \chi^2_{min}$ vs m_h curve. The line is the result of the fit using all the high-Q^2 data; the band represents an estimate of the theoretical error due to missing higher order corrections. The vertical band shows the 95% CL exclusion limit on m_H from the direct search. The dashed curve is the results obtained using the evaluation of $\alpha^{(5)}_{\text{had}}(m_Z^2)$ from [1]. The dotted curve is the result obtained including all the low-Q^2 data.

to be as precise as possible. In this work, we modified the kernels of HERWIG6.5 so as to improve its infrared behaviour.

A compilation of both Run I and Run II measurements from CDF and DO based on Run II datasets between 72pb^{-1} and 350pb^{-1} is shown in figs. (1.9) and (1.10). We see that they are in reasonable agreement with predictions calculated at NNLO in QCD [46]

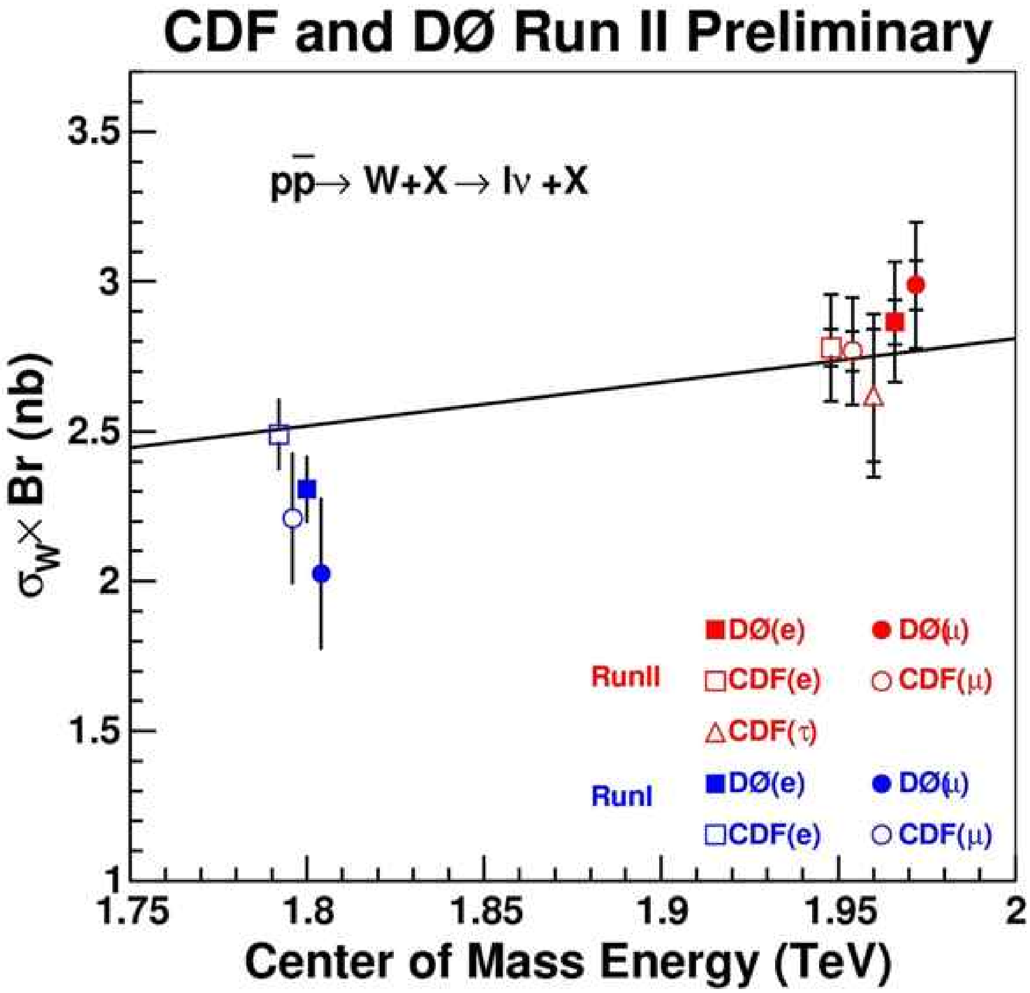

Figure 1.9: A compilation of Run I and II Tevatron results on the measurement of $\sigma_W \times$ BR($W \rightarrow l\nu$). The measurements are compared to NNLO predictions.

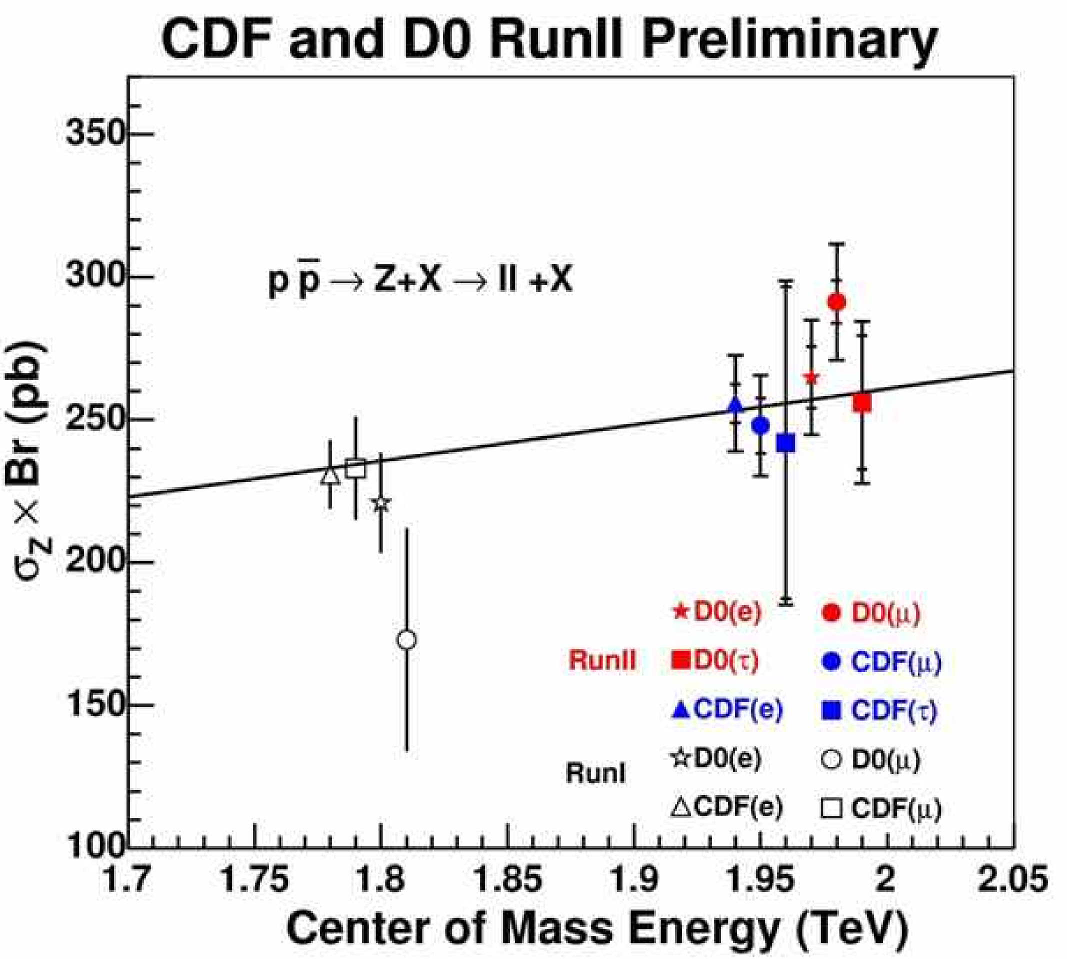

Figure 1.10: A compilation of Run I and II Tevatron results on the measurement of $\sigma_Z \times \mathrm{BR}(Z \to l^+l^-)$. The measurements are compared to NNLO predictions.

CHAPTER TWO

DGLAP-CS Theory

We expect cross sections to scale as powers of Q^2, but this is not the case. Collinear and infrared divergences are responsible for large enhancements in these distributions which need to be resummed. These enhancements are due to the large logarithms from higher order terms arising from singularities of QCD radiative corrections. These enhanced terms can be resummed due to the fact that these singularities factorize [35, 36, 37, 38, 39]. One can therefore formulate recurrence relations that lead to evolution equations. The main set of equations are the DGLAP-CS [47, 48, 49, 50, 51, 52] evolution equations which sum collinear singularities in parton densities and fragmentation functions. This resummation is necessary for a detailed simulation of QCD hard subprocesses, since the lowest order perturbation theory can only give an adequate description of some broad features of the data such as the angular distributions of the jet axes in hadronic jet production.

In Ref.[2], it was found that the resummation of large infrared effects in the kernels of the usual DGLAP-CS theory improved their infrared behavior. A new set of IR-Improved DGLAP-CS kernels were found which gave better control of the accuracy of a given fixed-order calculation throughout the entire phase space of the respective physical process, especially when the prediction is given by Monte Carlo methods. In this work, we implemented these kernels in Herwig6.5 and compared the results to the old kernels. First, we will derive the usual DGLAP-CS kernels following [49].

We start by evaluating the probability of finding a particle B inside a particle A with fraction z of the longitudinal momentum of A in the p_∞ frame to the lowest order in α_s, that is

$$d\mathscr{P}_{BA}(z)dz = \frac{\alpha_s}{2\pi}P_{BA}(z)dzdt. \tag{2.1}$$

Let C be a third particle in the bare vertex where A and B occur. Let D be a given particle and f be any final state. To calculate eqn. (2.1) we proceed by comparing the cross sections depicted in fig. (2.1).

The general S-matrix element is defined as

$$S_{ij} - \delta_{ij} = 2\pi i\delta(E_j - E_i)M_{ij}\prod_k (2E_k)^{-1/2}, \tag{2.2}$$

where the index k runs over all external particles. The contribution to M_{ij} in eqn. (2.2) of a given intermediate state B to the first process in fig. (2.1) is given by

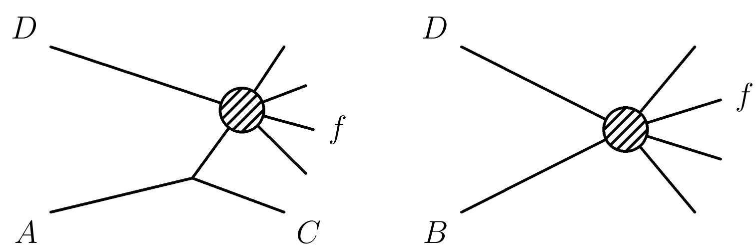

Figure 2.1: (a) Contribution of the B intermediate state to the process $A + D \to C + F$. (b) The process $B + D \to f$.

$$M_{A+D\to C+f} = g_s^2 \frac{V_{A\to B+C}V_{B+D\to f}}{(2E_B)(E_B + E_C - E_A)}, \tag{2.3}$$

where V_{ij} is the invariant matrix element of the interactions (with the factors $(2E_k)^{-1/2}$ removed). For the second figure of (2.1) we have

$$M_{B+D\to f} = g_s V_{B+D\to f}. \tag{2.4}$$

The contribution of a given intermediate state B to the differential cross sections $d\sigma_a$ and $d\sigma_b$ is given by

$$
\begin{aligned}
d\sigma_a &= \frac{g_s^4}{8E_A E_D} \frac{|V_{A\to B+C}|^2 |V_{B+D\to f}|^2}{(2E_B)^2 (E_B + E_C - E_A)^2} \\
&\times\ (2\pi^4)\delta^4(k_A + k_D - k_C - k_f) \frac{d^3 k_C}{(2\pi)^3 (2E_C)} \prod_f \frac{d^3 p_f}{(2\pi)^3 (2E_f)}, \qquad (2.5) \\
d\sigma_b &= \frac{g_s^2}{8E_B E_D} |V_{B+D\to f}|^2 (2\pi)^4 \delta^4(k_B + k_D - k_f) \prod_f \frac{d^3 p_f}{(2\pi)^3 (2E_f)}. \qquad (2.6)
\end{aligned}
$$

Now the differential cross section $d\sigma_a$ is equal to the probability of the B particle being present inside of A with fractional momentum z times the differential cross section of b, i.e.

$$
d\sigma_a = d\mathscr{P}_{BA}(z) dz d\sigma_b, \qquad (2.7)
$$

$d\sigma_a = d\mathscr{P}_{BA}(z)$ can now be calculated by comparing eqn. (2.6) and eqn. (2.5) we deduce

$$
d\mathscr{P}_{BA}(z)dz = \frac{E_B}{E_A} \frac{g_s^2 |V_A \to B + C|^2}{(2E_B)^2 (E_B + E_C - E_A)^2} \frac{d^3 k_C}{(2\pi)^3 (2E_C)}, \qquad (2.8)
$$

where all the masses have being neglected.

Now in the p_∞ frame

$$
\begin{aligned}
k_A &= (P; P, \mathbf{0}), \\
k_B &= \left(zP + \frac{p_\perp^2}{2zP}; zP, \mathbf{p}_\perp\right), \\
k_c &= \left((1-z)P + \frac{p_\perp^2}{2(1-z)P}; (1-z)P, -\mathbf{p}_\perp\right). \qquad (2.9)
\end{aligned}
$$

We therefore have

$$
(2E_B)^2 (E_B + E_C - E_A)^2 = \frac{(p_\perp^2)^2}{(1-z)^2}, \qquad (2.10)
$$

and

$$
\frac{d^3 k_C}{(2\pi)^3 (2E_C)} = \frac{dz d_\perp^2}{16\pi^2 (1-z)}. \qquad (2.11)
$$

Eqn. (2.1) thus becomes

$$
d\mathscr{P}_{BA}(z) = \frac{\alpha_s}{2\pi} \frac{z(1-z)}{2} \overline{\sum_{\text{spins}}} \frac{|V_{A\to B+C}|^2}{p_\perp^2} d\ln p_\perp^2, \qquad (2.12)
$$

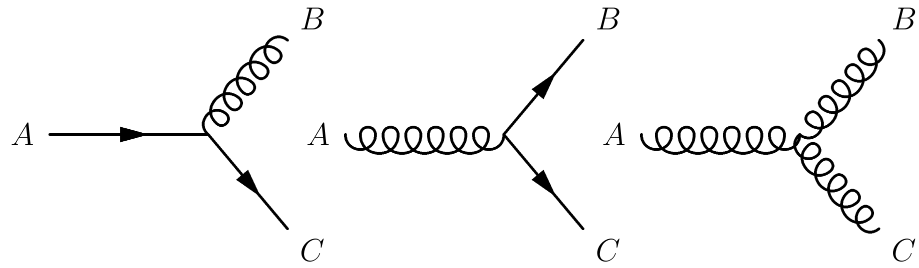

Figure 2.2: The three vertices that contribute to the parton evolution in QCD: The quark gluon vertex which determines P_{Gq} and P_{qq}, the annihilation vertex of a gluon into a quark-antiquark pair which fixes P_{qG}, the three-gluon vertex relevant to determine P_{GG}.

where we sum over the spins of B and C and average over the spins of A. As $p_\perp \to 0$ the ratio $|V/|/p_\perp^2$ does not blow up since in the case we are interested in, $|V|^2$ vanishes linearly in $p_\perp^2$, so that the ratio $|V^2|/p_\perp^2$ is finite at $p_\perp^2 = 0$. In the leading logarithmic approximation $d\ln p_\perp^2$ can be directly interpreted as dt ($t \equiv \ln Q^2/Q_0^2$) since for a virtual mass ($-Q^2$) for particle D the integral in $p_\perp$ has upper limit of order Q^2. So by comparing eqn. (2.12) with eqn. (2.1) we obtain

$$P_{BA}(z) = \frac{1}{2}z(1-z)\overline{\sum_{\text{spins}}}\frac{|V_{A\to B+C}|^2}{p_\perp^2} \quad (z<1). \tag{2.13}$$

We note that P_{BA} only depends on the vertex ABC. When the spin sum is symmetric we have

$$P_{CA} = P_{BA}(1-z) \quad (z<1). \tag{2.14}$$

We are now in a position to calculate the splitting functions of QCD. Firstly, we will use the quark gluon vertex (fig 2.2) in order to evaluate $P_{Gq}(z)$. For this case

$$\overline{\sum_{\text{spins}}}|V_{q\to Gq}|^2 = \frac{1}{2}C_2(R)\text{Tr }(\not{k}_C\gamma_\mu\not{k}_A\gamma_\nu)\overline{\sum_{\text{pol}}}\epsilon^{*\mu}\epsilon^\nu, \tag{2.15}$$

where the factor of $\frac{1}{2}$ comes from the average over the initial quark spin, and we define $C_2(R)$ as

$$C_2(R) = \frac{1}{N}\sum_a t^a t^a = \frac{N^2-1}{2N}, \tag{2.16}$$

which arises from the sum and average over the final and initial states in colour space. To make sure that only physical transverse gluon states are included in the sum, we write

$$\sum_{\text{pol}} \epsilon^* \epsilon \to \delta^{ij} - \frac{k_B^i k_B^j}{k_B^2} \qquad (i,j = 1,2,3). \tag{2.17}$$

Putting it all together gives

$$\overline{\sum_{\text{pol}}} |V_{q \to G+q}|^2 = \frac{2p_\perp^2}{z\,(1-z)} \frac{1+(1-z)^2}{z} C_2(R). \tag{2.18}$$

Combining eqn. (2.13) and eqn. (2.18) gives

$$P_{Gq}(z) = C_2(R) \frac{1+(1-z)^2}{z}. \tag{2.19}$$

Momentum conservation in the vertices imposes constraints on the P functions. At $z < 1$ we have

$$\begin{aligned} P_{qq}(z) &= P_{Gq}(1-z), \\ P_{qG}(z) &= P_{qG}(1-z) \quad (z<1), \\ P_{GG}(z) &= P_{GG}(1-z). \end{aligned} \tag{2.20}$$

These equations are due to the fact that when a quark radiates, it splits into a quark with fraction z of its momentum plus a gluon with fraction $(1-z)$, etc. From eqn. (2.19) and the above symmetry relations we also obtain

$$P_{qq}(z) = C_2(R) \frac{1+z^2}{1-z} \quad (z<1) \tag{2.21}$$

We will now derive P_{qG} from the second vertex in fig. (2.2). Now P_{qG} is proportional to the probability density of finding inside a gluon (averaged over colours) a quark (or an antiquark) of a given flavour of any colour. The sum and average in colour space gives a factor of $1/2$, therefore we have

$$\overline{\sum_{\text{spins}}} |V_{G \to q+\bar{q}}|^2 = \frac{1}{2} \text{Tr}\,(\not{k}_C \gamma_\mu \not{k}_B \gamma_\nu) \frac{1}{2} \sum_{\text{pol}} \epsilon^{*\mu} \epsilon^\nu, \tag{2.22}$$

so using eqn. (2.17) gives

$$\overline{\sum_{\text{spins}}} |V_{G \to q+\bar{q}}|^2 = p_\perp^2 \left(\frac{1-z}{z} + \frac{z}{1-z} \right). \tag{2.23}$$

So from eq. (2.13) we obtain

$$P_{qG}(z) = \frac{1}{2}(z^2 + (1-z)^2). \tag{2.24}$$

This symmetry under the change of z into $(1-z)$ is expected because

$$P_{qG}(z) = P_{\bar{q}G}(1-z) = P_{qG}(1-z) \tag{2.25}$$

by the symmetry relations and the fact that colour and flavour commute. $P_{q^iq^j}$ is diagonal in quark indices because a gluon is emitted without flavour exchange,

$$P_{q^iq^j} = \delta_{ij}P_{qq}. \tag{2.26}$$

When we neglect all masses, the probability of emitting a gluon is the same for all flavours,

$$P_{Gq^i} = P_{Gg} \quad \text{(independent of } i\text{)}. \tag{2.27}$$

Also a gluon creates a massless quark-antiquark pair with equal probability for all flavours. Thus,

$$P_{q^iG} = P_{qG} \quad \text{(independent of } i\text{)}. \tag{2.28}$$

Finally we use the three gluon vertex to calculate $P_{GG}(z)$. This vertex is equal to

$$-igc_{abc}\left[g_{\nu\mu}\left(k_A+k_B\right)_\lambda - g_{\mu\lambda}\left(k_C+k_A\right)_\nu + g_{\lambda\nu}\left(k_C-k_B\right)_\mu\right]. \tag{2.29}$$

This gives the following amplitude

$$\begin{aligned} V_{G\to G+G} &= -c_{abc}\left\{-[(k_A+K_C)\epsilon_B^{*b}](\epsilon_A^a\epsilon_C^{*c})\right. \\ &+ \left.[(k_C-k_B)\epsilon_A^a](\epsilon_C^{*c}\epsilon_B^{*b}) + [(k_A+k_B)\epsilon_C^{*c}](\epsilon_A^a\epsilon_B^{*b})\ \right\} \end{aligned} \tag{2.30}$$

Squaring and summing over the spins gives

$$\overline{\sum_{\text{spins}}}|V_{G\to G+G}|^2 = 4C_2(G)\frac{p_\perp^2}{z\,(1-z)}\left[\frac{1-z}{z} + \frac{z}{1-z} + z\,(1-z)\right]. \tag{2.31}$$

Therefore from eq. (2.13) we obtain

$$P_{GG} = 2C_2(G)\left[\frac{1-z}{z} + \frac{z}{1-z} + z\,(1-z)\right] \quad (z < 1). \tag{2.32}$$

Again we see the symmetry for z going into $(1-z)$.

At $z = 1$ $P_{qq}(z)$ and $P_{GG}(z)$ diverge. We regularize the factor $1/(1-z)$ by reinterpreting it as a distribution $(1-z)_+^{-1}$ defined as follows

$$\int_0^1 \frac{dz f(z)}{(1-z)_+} \equiv \int_0^1 dz \frac{f(z)-f(1)}{1-z} = \int_0^1 dz \ln(1-z)\frac{d}{dz}f(z), \tag{2.33}$$

where $f(z)$ is any test function which is sufficiently regular at the end points and

$$\int_0^1 dz \frac{1}{(1-z)_+} = 0. \tag{2.34}$$

Now the total number of quarks minus antiquarks is conserved, and the probability of finding a quark integrated over all values of z must be one. It therefore follows that

$$\int dz P_{qq}(z) = 0. \tag{2.35}$$

Also, due to momentum conservation of the partons, we have

$$\begin{aligned} \int_0^1 dz z[P_{qq}(z) + P_{Gq}(z)] &= 0, \\ \int dz z[2f P_{qG(z)} + P_{GG}(z)] &= 0. \end{aligned} \tag{2.36}$$

We now add to $P_{qq}(z)$ and P_{GG} a $\delta(z-1)$ function with the coefficient determined by the constraints in eqs. (2.35) and (2.36). We thus find

$$P_{qq}(z) = C_2(R)\left[\frac{1+z^2}{(1-z)_+} + \frac{3}{2}\delta(z-1)\right] \tag{2.37}$$

$$\begin{aligned} P_{GG}(z) &= 2C_2(G)\left[\frac{z}{(1-z)_+} + \frac{1-z}{z} + z(1-z)\right. \\ &+ \left.\left(\frac{11}{12} - \frac{1}{3}\frac{T(R)}{C_2(G)}\right)\delta(z-1)\right], \end{aligned} \tag{2.38}$$

where $C_2(G)$ and $T(R)$ are the Casmir operators for the adjoint representation G of the colour group and for the representation R of the fermions respectively. For

$SU(N)_{\text{colour}}$ with f flavours they are given by

$$\begin{aligned} C_2(G) &= \frac{1}{N^2-1}\sum_{a,b,c} c_{abc}c_{abc} = N, \\ T(R)\delta_{ab} &= \mathrm{Tr}\,(t^a t^b)\frac{1}{2} f\delta_{ab}. \end{aligned} \tag{2.39}$$

Therefore the spitting functions for QCD in the lowest derived from the vertices (Fig. 2.2) are given by:

$$P_{qq}(z) = \frac{4}{3}\left[\frac{1+z^2}{(1-z)_+} + \frac{3}{2}\delta(1-z)\right], \tag{2.40}$$

$$P_{Gq}(z) = \frac{4}{3}\left[\frac{1+(1-z)^2}{z}\right], \tag{2.41}$$

$$P_{qG}(z) = \frac{1}{2}\left[z^2+(1-z)^2\right], \tag{2.42}$$

$$P_{GG}(z) = 6\left[\frac{(1-z)}{z} + \frac{z}{(1-z)_+} + z(1-z) + \left(\frac{11}{12} - \frac{n_f}{18}\right)\delta(1-z)\right], \tag{2.43}$$

2.1 Resummation

Recall that if α_s is small, we can perform calculations in QCD by doing a perturbative expansion. Suppose we have an observable quantity such as a cross section, decay rate etc, or a theoretical quantity like a form factor or a parton distribution. Resummation is an attempt to sum some terms in the perturbative series to all orders. That is, we start from a subset of terms in a finite order perturbative series and construct an all orders expression whose expansion gives these terms back. Suppose we have a quantity $\mathcal{O}$ with the following schematic perturbative expansion.

$$\mathcal{O}_{\mathrm{PT}} = f_{00} + \alpha_s(c_{12}L^2 + c_{11}L + f_{10}) + \alpha_s^2(c_{24}L^4 + c_{23}L^3 + c_{22}L^2 + \cdots + f_{20}) + \cdots\ , \tag{2.44}$$

where α_s is the coupling of the theory, L is some logarithm and f_{i0} represents all terms not containing a power of L. We assume the c_{ij}'s are well behaved. We note that L depends on the quantity under discussion; for example for

$$d\sigma(p\bar{p} \to Z + X)/dp_T^Z \quad \text{then} L = \ln(M_Z/P_T^Z). \tag{2.45}$$

The schematic resummed form of $\mathcal{O}$ may be written as

$$\mathcal{O}_{\rm res} = \exp[Lg_1(\alpha_s L) + g_2(\alpha_s L) + \cdots](f_{00}^{'} + \alpha_s f_{10}^{'} + \cdots), \tag{2.46}$$

where $g_{1,2}$ are known functions. $\mathcal{O}_{\rm res}$ has some special features. Since the residual series $\sum f_{i0}^{'}\alpha_s^i$ is without the resummed logs it is better behaved. The dependence on the resummed logarithm, which is now a series in α_s is under analytical control. This is the main benefit of resummation. Secondly, the resummed form contains an exponential which roughly reflects the Poisson statistics of independent emission. Finally due to technical reasons L is most often not the log of the original variable but of a conjugate variable resulting from the Fourier or other integral transform.

2.2 QED ⊗ QCD Exponentiation

We will present a brief review of the new QCD exponentiation theory developed in [4, 5, 6, 7, 8, 9, 10, 11, 12]. For this derivation we will use the process

$$\bar{Q}^(p_1)Q(q_1) \rightarrow \bar{Q}^{'''}(p_2)\bar{Q}^{''}(q_2) + G_1(k_1) + \cdots + G_n(k_n), \tag{2.47}$$

with the kinematics as shown in fig. (2.3). This proto typical process will be used to provide an extension of the original ideas of Yennie, Frautschi and Suura (YFS) [53, 54] to the parton model. In this derivation we will use the GPS conventions given in Ref. [55] for spinors $\{\mu, \nu, u\}$ and the corresponding photon and gluon polarization vectors:

$$(\epsilon_\sigma^\mu(\beta))^* = \frac{\bar{u}_\sigma(k)\,\gamma^\mu u_\sigma(\beta)}{\sqrt{2}\bar{u}_{-\sigma}(k)\,u_\sigma(\beta)}, \quad (\epsilon_\sigma^\mu(\zeta))^* = \frac{\bar{u}_\sigma(k)\,\gamma^\mu u_\sigma(\zeta)}{\sqrt{2}\bar{u}_{-\sigma}(k)\,u_\sigma(\zeta)}, \tag{2.48}$$

with $\beta^2 = 0$ and $\zeta_\uparrow = (1,0,0,1)$ and $\zeta_\downarrow = (1,0,0,-1)$. With these definitions, all the phase information of the amplitudes is known.

Recall that the renormalization group is a general property of renormalized perturbation theory based on its ultra violet behaviour. The YFS theory can be viewed as a general re-arrangement of renormalized perturbation theory based on

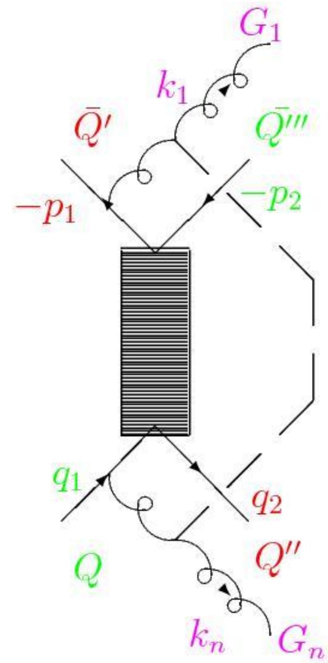

Figure 2.3: The process $\bar{Q}^{'}Q \rightarrow \bar{Q}^{'''} + Q^{''} + n(G)$. The four momenta are indicated in the standard manner: q_1 is the four momentum of the incoming Q, q_2 is the four momentum of the outgoing $Q^{''}$, etc., and $Q = u, d, s, c, , G$ [2].

its infrared behaviour. The results therefore apply to any renormalized perturbation theory in which the cross section is finite.

We begin by defining that the amplitude for the emission of n real gluons in the subprocess

$$Q^{\alpha} + \bar{Q}^{'\bar{\alpha}} \rightarrow Q^{''\gamma}\bar{Q}^{'''\bar{\gamma}} + n(G) \tag{2.49}$$

be represented by

$$\mathcal{M}^{(n)\alpha\bar{\alpha}}_{\gamma\bar{\gamma}} = \sum_{\ell} M^{(n)\alpha\bar{\alpha}}_{\gamma\bar{\gamma}\ell}, \tag{2.50}$$

where $M_{\ell}^{(n)}$ is the contribution to $\mathcal{M}^{(n)}$ from Feynman diagrams with ℓ virtual loops and $\alpha, \bar{\alpha}, \gamma$ and $\bar{\gamma}$ are colour indices. Symmetrization of M gives

$$M_{\ell}^{(n)} = \frac{1}{\ell!}\int \prod_{j=1}^{\ell} \frac{d^4k_j}{(2\pi)^4\left(k_j^2 - \lambda^2 + i\epsilon\right)}\rho_{\ell}^{(n)}\left(k_1, \cdots, k_{\ell}\right). \tag{2.51}$$

This last equation defines $\rho_l^{(n)}$ as a symmetric function of its arguments $k_1, \cdots, k_l$. The infrared gluon mass regulator for IR singularities is given by λ.

Let us now define the virtual IR emission factor $S_{\rm QCD}(k)$ for a gluon of 4-momentum k, for the $k \to 0$ regime such that

$$\lim_{k\to\infty} k^2 \left(\rho_{\gamma\bar{\gamma}1}^{(n)\alpha\bar{\alpha}}(k)\,|_{\text{leading Casmir contribution}} - S_{\rm QCD}(k)\,\rho_{\gamma\bar{\gamma}0}^{(n)\alpha\bar{\alpha}}\right) = 0. \tag{2.52}$$

This introduces a restriction on the leading colour Casmir terms at one loop.

We also define the residual amplitude $\beta_\ell^1(k_1, \cdots, k_{l-1}; k_\ell)$ through the equation

$$\rho_\ell^{(n)} = S_{\rm QCD}(k_\ell) \times \rho_{\ell-1}^{(n)}(k_1, \cdots, k_{\ell-1}) + \beta_\ell^1(k_1, \cdots, k_{\ell-1}; k_\ell)\,. \tag{2.53}$$

We obtained this equation by noting that the virtual gluons in $\rho_\ell^{(n)}$ are all on equal footing due to the symmetry of $\rho_\ell^{(n)}$. So, for a gluon ℓ, we may write for $k_\ell \to (0,0,0,0) \equiv O$ while the remaining k_i are fixed away from O, this gives eqn. (2.53). The residual amplitude has two noteworthy properties.

(1) It is symmetric in its first $\ell - 1$ arguments.

(2) It does not contain the IR singularities for gluon ℓ that are contained in $S_{\rm QCD}$.

If we keep applying eqn. (2.53), we get the rigorous exact rearrangement of the contribution to $\rho_\ell^{(n)}$ as

$$\rho_\ell^{(n)} = S_{\rm QCD}(k_1) \cdots S_{\rm QCD}(k_\ell)\,\beta_0^0 + \sum_{i=1}^{\ell} \prod_{j\neq i} S_{\rm QCD}(k_j)\,\beta_1^1(k_i) + \cdots + \beta_\ell^\ell(k_1, \cdots, k_\ell)\,, \tag{2.54}$$

where the virtual gluon residuals $\beta_i^i(k_1', \cdots, k_i')$ have the following properties

- They are symmetric functions of their arguments.
- They no longer contain the IR singularities which are contained in the product $S_{\rm QCD}(k_1') \cdots S_{\rm QCD}(k_i')$.

Equation (2.54) contains no approximations, it is an exact rearrangement of the contributions of the Feynman diagrams which contribute to $\rho_{\ell}^{(n)}$.

Substituting (2.54) into (2.50) we obtain

$$\mathcal{M}^{(n)} = e^{\alpha_s B_{\mathrm{QCD}}} \sum_{j=1}^{\infty} m_j^{(n)}, \tag{2.55}$$

where

$$\alpha_s(Q) B_{\mathrm{QCD}} = \int \frac{d^4k}{(k^2 - \lambda^2 + i\epsilon)} S_{\mathrm{QCD}}\,(k) \tag{2.56}$$

and

$$m_j^{(n)} = \frac{1}{j!} \int \prod_{i=1}^{j} \frac{d^4k_i}{(k_i^2 - \lambda^2 + i\epsilon)} \beta_j(k_1, \cdots, k_j) \tag{2.57}$$

where $\beta_j^j = \beta_j$. This result has an improved IR divergence structure over (2.50) since all of the IR singularities associated with $S_{\mathrm{QCD}}(k)$ are explicitly removed from the sum over the virtual IR improved loop contributions $m_j^{(n)}$ to all orders in $\alpha_s(Q)$.

We now need to perform an analogous rearrangement of the real IR singularities in the differential cross section associated with the $\mathcal{M}^{(n)}$. This cross section can be written as

$$\begin{aligned} d\hat{\sigma} \quad = \quad & \frac{e^{2\alpha_s \Re(B_{\mathrm{QCD}})}}{n!} \prod_{m=1}^{n} \frac{d^3k_m}{\sqrt{k_m^2 + \lambda^2}} \delta\left(p_1 + q_1 - p_2 - q_2 - \sum_{i=1}^{n} k_i\right) \\ & \bar{\rho}^{(n)}\left(p_1, q_1, p_2, q_2, k_1, \cdots, k_n\right) \frac{d^3p_2 d^3q_2}{p_2^0 q_2^0}, \end{aligned} \tag{2.58}$$

where

$$\bar{\rho}^{(n)}\left(p_1, q_1, p_2, q_2, k_1, \cdots, k_n\right) = \sum_{\text{colour, spin}} \left\| \sum_{j=0}^{\infty} m_j^{(n)} \right\|^2. \tag{2.59}$$

As before for $n = 1$ we define $\tilde{S}_{\mathrm{QCD}}(k)$ by

$$\lim_{|\vec{k}| \to 0} \vec{k}^2 \left(\bar{\rho}^{(1)}\,(k)\,|_{\text{leading Casmir contribution}} - \tilde{S}_{\mathrm{QCD}}\,(k)\,\bar{\rho}^{(0)}\right) = 0. \tag{2.60}$$

Repeating the steps we did for $S_{\rm QCD}$ yields

$$\begin{aligned} d\hat{\sigma}_{\rm exp} &= \sigma_n d\hat{\sigma}^n \\ &= e^{\sum_{IR}(QCD)} \sum_{n=0}^{\infty} \int \prod_{j=1}^{n} \frac{d^3k_j}{k_j^0} \int \frac{d^4y}{(2\pi)^4} e^{iy.(p_1+q_1-p_2-q_2-\sum k_j)+D_{\rm QCD}} \\ &\times \bar{\beta}_n\left(k_1,\cdots,k_n\right) \frac{d^3p_2}{p_2^0}\frac{d^3q_2}{q_2^0}, \end{aligned} \tag{2.61}$$

where

$$\sum_{IR}(QCD) = 2\alpha_s \Re\left(B_{\rm QCD}\right) + 2\alpha_s \tilde{B}_{\rm QCD}\left(K_{\rm max}\right), \tag{2.62}$$

with

$$2\alpha_s \tilde{B}_{\rm QCD}\left(K_{\rm max}\right) = \int \frac{d^3k}{k^0} \tilde{S}_{\rm QCD}\left(k\right) \theta\left(K_{\rm max} - k\right), \tag{2.63}$$

and

$$D_{\rm QCD} = \int \frac{d^3k}{k} \tilde{S}_{\rm QCD}\left(k\right) \left[e^{-iy.k} - \theta\left(K_{\rm max} - k\right)\right], \tag{2.64}$$

where $\bar{\beta}_n$ are the QCD hard gluon residuals defined above. Since the left hand side of (2.61) and $\sum_{IR}(QCD)$ [5, 6, 7, 8, 56, 9, 11, 12, 10] are infrared finite then

$$\sigma_{\rm exp}^{\bar{\hat{}}} \equiv e^{-\sum_{IR}(QCD)} d\hat{\sigma}_{\rm exp} \tag{2.65}$$

must also be infrared finite to all orders in α_s.

Let $\bar{\beta}_n^{(\ell)}$ denote the $\mathcal{O}(\alpha_s^{\ell}(Q))$ part of $\bar{\beta}_n$. Then we can write

$$\bar{\beta}_n^{(\ell)} = \tilde{\bar{\beta}}_n^{(\ell)} + D\bar{\beta}_n^{(\ell)}, \tag{2.66}$$

where this defines the left over non-abelian infrared divergence part of each contribution $\bar{\beta}_n^{(\ell)}$. The new function $\tilde{\bar{\beta}}_n^{(\ell)}$ is completely free of any infrared divergences. These left over infrared divergences are contained in the function $D\bar{\beta}_n^{(\ell)}$ which are of non-abelian origin.

At $\mathcal{O}(\alpha_s^n(Q))$ the infrared finiteness of the contribution to $d\bar{\hat{\sigma}}_{\rm exp}$ requires the contribution

$$
\begin{aligned}
d\bar{\hat{\sigma}}_{\rm exp} \quad \equiv & \quad \int \sum_{\ell=0}^{n} \prod_{j=1}^{\ell} \int_{k_j \geq K_{\rm max}} \frac{d^3 k_j}{k_j} \tilde{S}_{\rm QCD}(k_j) \sum_{i=0}^{n-\ell} \frac{1}{i!} \prod_{j=\ell+1}^{\ell+1} \\
\times & \quad \int \frac{d^3 k_j}{k_j^0} \bar{\beta}_i^{(n-\ell-i)}(k_{\ell+1}, \cdots, k_{\ell+i}) \frac{d^3 p_2}{p_2^0} \frac{d^3 q_2}{q_2^0}
\end{aligned}
\tag{2.67}
$$

to be finite.

We therefore also have that

$$
\begin{aligned}
Dd\bar{\hat{\sigma}}_{\rm exp} \quad \equiv & \quad \int \sum_{\ell=0}^{n} \prod_{j=1}^{\ell} \int_{k_j \geq K_{\rm max}} \frac{d^3 k_j}{k_j} \tilde{S}_{\rm QCD}(k_j) \sum_{i=0}^{n-\ell} \frac{1}{i!} \prod_{j=\ell+1}^{\ell+1} \\
& \quad \int \frac{d^3 k_j}{k_j^0} D\bar{\beta}_i^{(n-\ell-i)}(k_{\ell+1}, \cdots, k_{\ell+i}) \frac{d^3 p_2}{p_2^0} \frac{d^3 q_2}{q_2^0}
\end{aligned}
\tag{2.68}
$$

is finite. We can drop $D\bar{\beta}_n^{\ell}$ since they do not make a net contribution to the final parton cross section $\hat{\sigma}_{\rm exp}$. To see this, note that $D\bar{\beta}_n^{(\ell)}$ is defined by a minimal subtraction of the respective IR divergences in it; so that it only contains the actual pole and the constants $1/\epsilon - C_E$, where $1/\epsilon = \ln \lambda^2$ in the gluon mass regularization. That is

$$
\int dPhD\bar{\beta}_n^{(\ell)} \equiv \sum_{i=1}^{n+\ell} d_i^{n,\ell} \ln^i(\lambda^2),
\tag{2.69}
$$

dPh is the respective n-gluon Lorentz invariant phase space and the coefficients functions are independent of λ, for $\lambda \to 0$. Now since the integration region for the final particles is arbitrary, the independent powers of the IR regulator $\ln(\lambda^2)$ in eqn. (2.68) must give vanishing contributions.

Finally we have the rigorous result

$$
\begin{aligned}
d\hat{\sigma}_{\rm exp} \quad = & \quad \sum_n d\hat{\sigma}^n \\
= & \quad e^{\sum_{IR}(QCD)} \sum_{n=0}^{\infty} \left(\frac{1}{n!}\right) \int \prod_{j=1}^{n} \frac{d^3 k_j}{k_j} \int \frac{d^4 y}{(2\pi)^4} e^{iy.(p_1+q_1-p_2-q_2-\sum k_j)+D_{\rm QCD}} \\
\times & \quad \tilde{\bar{\beta}}_n(k_1, \cdots, k_n) \frac{d^3 p_2}{p_2^0} \frac{d^3 q_2}{q_2^0}
\end{aligned}
\tag{2.70}
$$

where the hard gluon residuals $\tilde{\bar{\beta}}_n\left(k_1, \cdots, k_n\right)$ are defined by

$$\tilde{\bar{\beta}}_n\left(k_1, \cdots, k_n\right) = \sum_{\ell=0}^{\infty} \tilde{\bar{\beta}}_n^{(\ell)}\left(k_1, \cdots, k_n\right) \tag{2.71}$$

are free of all infrared divergences to all orders in $\alpha_s(Q)$.

2.3 IR-Improved DGLAP-CS Theory

Using the result of the previous section we will now derive the IR improved kernels. Consider the kernel $P_{qq}(z)$

$$P_{qq}(z) = \frac{4}{3}\left(\frac{1+z^2}{1-z}\right) \quad (z < 1). \tag{2.72}$$

This kernel has an unintegrable IR singularity at $(z = 1)$, this corresponds to the point of zero energy gluon emission. This is regularized by the plus-function prescription (eqn. (2.33)). The regime $1 - \epsilon < z < 1$ has no probability, and at $z = 1$ we get a large negative integrable contribution. We would like to improve this mathematical artifact.

We note that LHC can produce 2 TeV partons so that at $z \approx 0.001$ we can obtain $\sim 2 - 3$ GeV soft gluons which can be detected. This can be compared with the LEP experiments where $z \approx 0.001$ implied ~ 100 MeV photons, which again could be detected. It was found that resummation was necessary to describe the data [57, 58, 59, 60, 61] cf. fig. (2.4). It may be argued that a similar view will have to be taken for the LHC data if we wish to improve the precision tags which can be achieved at a given fixed order in perturbation theory. Also the FNAL data on p_t spectra was improved at fixed order by resumming large logs associated with soft gluons [62, 63]. Finally, $P_{qq}(z)$ is set to 0 in the region $1 - \epsilon < z < 1$ where we expect it to have its largest value. This should not be.

As another example consider the $\mathcal{O}(\alpha_s)$ bremsstrahlung process. The differential spectrum is poorly represented by the $\mathcal{O}(\alpha_s)$ calculation. This is due to the fact that the behaviour of the spectrum for $z \to 1$ in $\mathcal{O}(\alpha_s)$ is unintegrable and has

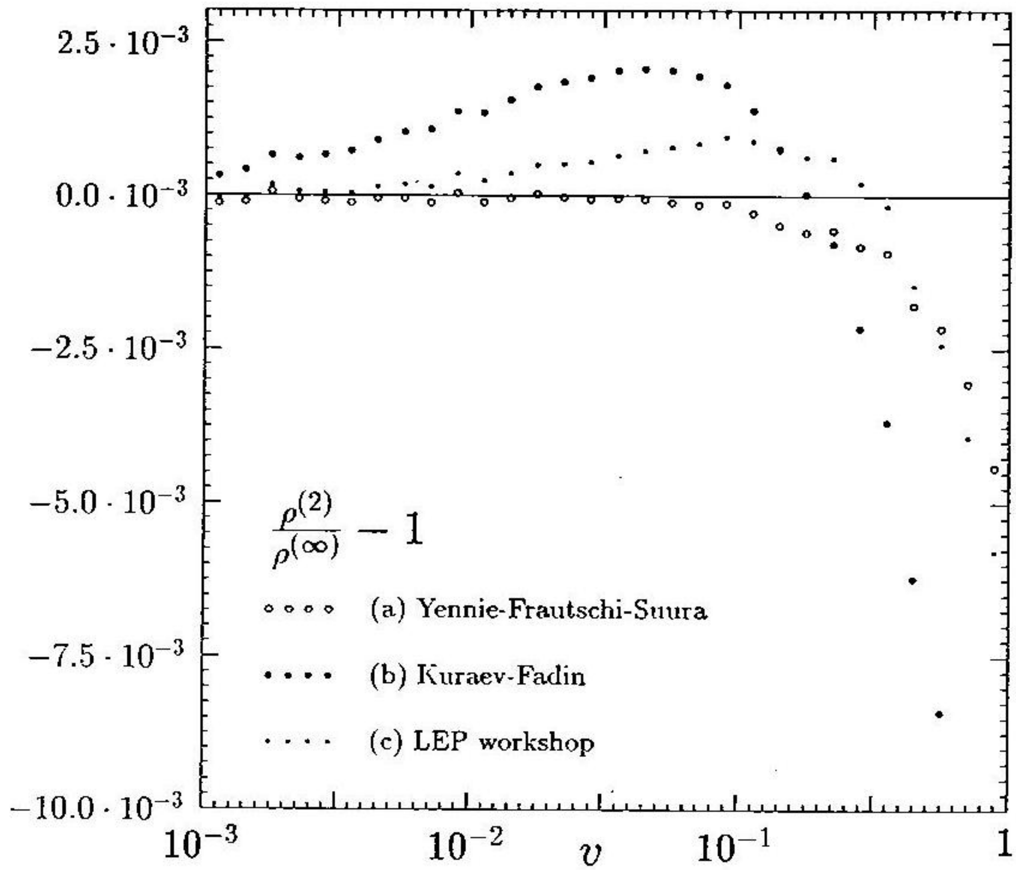

Figure 2.4: The ratio of the second order exponentiated distribution $\rho^{(2)}(\nu)$ and the infinite order solution $\rho^{(\infty)}$ by means of the Monte Carlo ($10^6 - 4.10^6$ M.C. events per point). Statistical error is below 2.10^4. Numerical input was set for e^+e^- beams at $\sqrt{s} = 92$ GeV. Three curves represent exponentiation of the type (a) YFS, (b) Kuraev-Fadin and (c) LEP workshop.

to be cut off. It was shown that resummation of the large soft higher-order effects changed the $z \to 1$ behaviour. The $(1-z)^{-1}$ behaviour was modified to $(1-z)^{\gamma-1}$, $\gamma > 0$. The exponentiated result has been tested in [57, 58, 59, 60, 61]. We wish to reproduce these results for QCD by summing up the leading IR terms in the correction to P_{qq}. This should make the IR singularity integrable and exhibit more accurately the true predictions of QCD.

We wish to sum up the leading IR terms in the corrections to P_{qq} with the aim of rendering integrable the IR singularity that is present in its lowest form. Our derivation starts from from eqn. (2.70). We will now derive the IR improved kernels

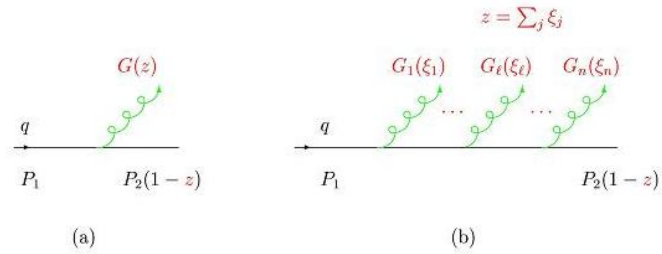

Figure 2.5: (a) The usual $q \to q(1-z) + G(z)$. (b) The multiple gluon improvement $q \to q(1-z) + G_1(\xi_1) + \cdots + G_n(\xi_n)$, $z = \sum_j \xi_j$.

[64]. We start with

$$\begin{aligned} \sum_{IR}(QCD) &= 2\alpha_s \Re(B_{\text{QCD}}) + 2\alpha_s \tilde{B}_{\text{QCD}}(K_{\max}) \\ &= \frac{1}{2}\left(2C_F\frac{\alpha_s}{\pi}t\ln\frac{k_{\max}}{E} + C_F\frac{\alpha_s}{2\pi}t + \frac{\alpha_s C_F}{\pi}\left(\frac{\pi^2}{3}-\frac{1}{2}\right)\right). \end{aligned} \tag{2.73}$$

Now the LHS of eqn. (2.70) is the sum over final states and an average over initial states of the respective process divided by the incident flux with that incident flux replaced by the respective initial state density for the process $q \to q(1-z) + G(z)$. In the context of hard scattering at scale Q as in eqn. (53) in ref. [49], the soft gluon effects for energy fraction $z \equiv K_{\max}/E$ working at the $\tilde{\bar{\beta}}$ level and using q_2 to represent the momentum conservation via other degrees of freedom for the hard process gives the result

$$\begin{aligned} &\int \frac{\alpha_s(t)}{2\pi} P_{BA}\, dt\, dz \\ =\;& e^{\sum_{IR}(QCD)(z)} \int \Bigg\{ \tilde{\bar{\beta}}_0 \int \frac{d^4y}{(2\pi)^4} e^{\left\{iy.(p_1-p_2)+\int^{k<K_{\max}}\left(d^3k/k\right)\tilde{S}_{\text{QCD}}(k)\left[e^{-iy.k}-1\right]\right\}} \\ +\;& \int \frac{d^3k_1}{k_1}\tilde{\bar{\beta}}_1(k_1) \int \frac{d^4y}{(2\pi)^4} e^{\left\{iy.(p_1-p_2-k_1)+\int^{k<K_{\max}}\left(d^3k/k\right)\tilde{S}_{\text{QCD}}(k)\left[e^{-iy.k}-1\right]\right\}} + \cdots \Bigg\} \frac{d^3p_2}{p_2^0}\frac{d^3q_2}{q_2^0} \\ =\;& e^{\sum_{IR}(QCD)(z)} \int \Bigg\{ \tilde{\bar{\beta}}_0 \int_{-\infty}^{\infty} \frac{dy}{(2\pi)} e^{\left\{iy.(E_1-E_2)+\int^{k<K_{\max}}\left(d^3k/k\right)\tilde{S}_{\text{QCD}}(k)\left[e^{-iy.k}-1\right]\right\}} \\ +\;& \int \frac{d^3k_1}{k_1}\tilde{\bar{\beta}}_1(k_1) \int_{-\infty}^{\infty} \frac{dy}{(2\pi)} e^{\left\{iy.\left(E_1-E_2-k_1^0\right)+\int^{k<K_{\max}}\left(d^3k/k\right)\tilde{S}_{\text{QCD}}(k)\left[e^{-iy.k}-1\right]\right\}} + \cdots \Bigg\} \frac{d^3p_2}{p_2^0 q_2^0}, \end{aligned} \tag{2.74}$$

where $E_i = p_i^0$, $i = 1, 2$.

The real infrared function $\tilde{s}_{\mathrm{QCD}}(k)$was calculated by [10, 11, 12]. The DGLAP-CS synthesization procedure in [6] was applied to remove its collinear singularities giving

$$\tilde{S}_{\mathrm{QCD}} = -\frac{\alpha_s C_F}{8\pi^2}\left(\frac{p_1}{kp_1}-\frac{p_2}{kp_2}\right)^2\Bigg|_{\mathrm{DGLAP-CS\ synthesized}}. \tag{2.75}$$

From [53, 54] we have the following integrals

$$\begin{aligned} I_{\mathrm{YFS}}\left(ze,0\right) &= \int_{-\infty}^{\infty}\frac{dy}{2\pi}e^{\left[iy(zE)+\int^{k<zE}\left(d^3k/k\right)\tilde{S}_{\mathrm{QCD}}(k)\left(e^{-iyk}\right)-1\right]} \\ &= F_{\mathrm{YFS}}\left(\gamma_q\right)\frac{\gamma_q}{ze}, \end{aligned} \tag{2.76}$$

and

$$\begin{aligned} I_{\mathrm{YFS}}\left(zE,k_1\right) &= \int_{-\infty}^{\infty}\frac{dy}{2\pi}e^{\left[iy(zE-k_1)+\int^{k<zE}\left(d^3k/k\right)\tilde{S}_{\mathrm{QCD}}(k)\left(e^{-iyk}\right)-1\right]} \\ &= \left(\frac{zE}{zE-k_1}\right)^{1-\gamma_q} I_{\mathrm{YFS}}\left(ZE,0\right). \end{aligned} \tag{2.77}$$

Substituting these results in (2.74) we arrive at

$$\int\left(\tilde{\bar{\beta}}_0\frac{\gamma_q}{zE}+\int dk_1k_1d\Omega_1\tilde{\bar{\beta}}_0\left(k_1\right)\left(\frac{zE}{zE-k_1}\right)^{1-\gamma_q}\frac{\gamma_q}{zE}\right)\frac{d^3p_2}{E_2q_2^0} = \int dt\frac{\alpha_s\left(t\right)}{2\pi}P_{BA}^0dz+\mathcal{O}\left(\alpha_s^2\right), \tag{2.78}$$

By differentiation

$$P_{BA} = P_{BA}^0 z^{\gamma_q}F_{\mathrm{YFS}}\left(\gamma_q\right)e^{\left(\frac{1}{2}\delta_q\right)}. \tag{2.79}$$

Finally we have

$$P_{BA} = P_{BA}^0 \equiv \frac{1}{2}z(1-z)\overline{\sum_{\mathrm{spins}}}\frac{\left|V_{A\to B+C}\right|^2}{p_\perp^2}, \tag{2.80}$$

which implies from eqn. (2.79)

$$P_{BA} = P_{BA}^0 = \frac{1}{2}z(1-z)\overline{\sum_{\mathrm{spins}}}\frac{\left|V_{A\to B+C}\right|^2}{p_\perp^2}z^{\gamma_q}F_{YFS}(\gamma_q)e^{\frac{1}{2}\delta_q}. \tag{2.81}$$

where $A=q$, $B=G$, $C=q$ and $V_{A\to B+C}$ is the lowest order amplitude for $q\to G(z)+q(1-z)$. This gives the un-normalized exponentiated result

$$P_{qq}(z) = C_F F_{YFS}(\gamma_q)e^{\frac{1}{2}\delta_q}\frac{1+z^2}{1-z}(1-z)^{\gamma_q} \tag{2.82}$$

where

$$\gamma_q = C_F \frac{\alpha_s}{\pi} t = \frac{4C_F}{\beta_0} \tag{2.83}$$

$$\delta_q = \frac{\gamma_q}{2} + \frac{\alpha_s C_F}{\pi}\left(\frac{\pi^2}{3} - \frac{1}{2}\right). \tag{2.84}$$

Also

$$F_{\text{YFS}}(\gamma_q) = \frac{e^{C_E \gamma_q}}{\Gamma(1+\gamma_q)}. \tag{2.85}$$

and,

$$\beta_0 = 11 - \frac{2}{3} n_f, \tag{2.86}$$

where n_f is the number of active quark flavors,

$$C_E = 0.5772\cdots$$

is Euler's constant and $\Gamma(w)$ is Euler's gamma function.

The normalization condition of eqn. (2.35) gives the IR-Improved kernel for NS DGLAP-CS evolution in QCD.

$$P_{qq}(z) = C_F F_{YFS}(\gamma_q) e^{\frac{1}{2}\gamma_q}\left[\frac{1+z^2}{1-z}(1-z)^{(\gamma_q)} - f_q(\gamma_q)\delta(1-z)\right], \tag{2.87}$$

where

$$f_q(\gamma_q) = \frac{2}{\gamma_q} - \frac{2}{\gamma_q+1} + \frac{1}{\gamma_q+2}. \tag{2.88}$$

From eqn. (2.20) we know that $P_{Gq}(z) = P_{qq}(1-z)$ for $z < 1$ therefore we have

$$P_{Gq}(z) = P_{qq}(1-z) = C_F F_{YFS}(\gamma_q) e^{\frac{1}{2}\delta_q} \frac{1+(1-z)^2}{z} z^{\gamma_q}. \tag{2.89}$$

Let us now use eqn. (2.36) to check momentum conservation. So we need to check if

$$\int_0^1 dz z(P_{Gq}(z) + P_{qq}(z)) = 0. \tag{2.90}$$

Therefore, using eqn. (2.87) and (2.89). we need to check

$$I = C_F F_{YFS} e^{\frac{1}{2}\delta_q} \int_0^1 dz z\left[\frac{1+z^2}{1-z}(1-z)^{\gamma_q} - f_q(\gamma_q)\delta(1-z) + \frac{1+(1-z)^2}{z} z^{(}\gamma_q)\right]. \tag{2.91}$$

This can be written as

$$I = C_F F_{YFS} e^{\frac{1}{2}\delta_q} \int_0^1 dz \left[(1+(1-z)^2) z^{\gamma_q} - (1+z^2)(1-z)^{\gamma_q}\right], \tag{2.92}$$

where we have used

$$\frac{z}{1-z} = \frac{z-1+1}{1-z} = -1 + \frac{1}{1-z}. \tag{2.93}$$

By making the change of variable $z \to 1-z$ we see that these terms exactly cancel. Thus the quark momentum sum rule is satisfied.

Let us now improve $P_{GG}(z)$ which is given by

$$P_{GG}(z) = 2C_G \left[\frac{1-z}{z} + \frac{z}{1-z} + z(1-z)\right]. \tag{2.94}$$

This function has unintegrable IR singularities at both $z = 1$ and $z = 0$. Repeating the QCD exponentiation calculation using the colour representation for gluons to the process $G \to G(z) + G(1-z)$ we obtain the un-normalized exponentiated result

$$P_{GG}(z) = 2C_G F_{YFS}(\gamma_G) e^{\frac{1}{2}\delta_G} \left[\frac{1-z}{z} z^{\gamma_G} \frac{z}{1-z}(1-z)^{\gamma_G} \ \frac{1}{2}\left(z^{1+\gamma_G}(1-z) + z(1-z)^{1+\gamma_G}\right)\right], \tag{2.95}$$

where

$$\gamma_G = C_G \frac{\alpha_s}{\pi} t = \frac{4C_G}{\beta_0}, \tag{2.96}$$

and

$$\delta_G = \frac{\gamma_G}{2} + \frac{\alpha_s C_G}{\pi}\left(\frac{\pi^2}{3} - \frac{1}{2}\right). \tag{2.97}$$

Here γ_G and δ_G were obtained from the expression for γ_q and δ_q by making the substitution $C_F \to C_G$. The exponentiation has made the singularities at $z = 0$ and $z = 1$ integrable as desired.

We now normalize P_{GG} by taking into account the virtual corrections such that the momentum sum rule

$$\int_0^1 dz z(2n_f P_{qG}(z) + P_{GG}(z)) = 0 \tag{2.98}$$

is satisfied. We finally obtain

$$\begin{aligned} P_{GG}(z) &= 2C_G F_{YFS}(\gamma_G) e^{\frac{1}{2}\delta_G} \Bigg[\frac{1-z}{z} z^{\gamma_G} + \frac{z}{1-z}(1-z)^{\gamma_G} \\ &+ \frac{1}{2}(z^{1+\gamma_G}(1-z) + z(1-z)^{1+\gamma_G}) - f_G(\gamma_G)\delta(1-z) \Bigg], \end{aligned} \tag{2.99}$$

where

$$\begin{aligned} f_G(\gamma_G) &= \frac{n_f}{6C_G F_{YFS}(\gamma_G)} e^{-\frac{1}{2}\delta_G} + \frac{2}{\gamma_G(1+\gamma_G)(2+\gamma_G)} + \frac{1}{(1+\gamma_G)(2+\gamma_G)} \\ &+ \frac{1}{2(3+\gamma_G)(4+\gamma_G)} + \frac{1}{(2+\gamma_G)(3+\gamma_G)(4+\gamma_G)}. \end{aligned} \tag{2.100}$$

Finally we improve P_{qG} by applying eqn. (2.70) to the process $G \to q + \bar{q}$ to get the following exponentiated result

$$P_{qG}(z) = F_{YFS}(\gamma_G) e^{\frac{1}{2}\delta_G} \frac{1}{2} \left[z^2 (1-z)^{\gamma_G} + (1-z)^2 z^{\gamma_G} \right]. \tag{2.101}$$

We will then obtain a new normalization constant for P_{GG} using the gluon momentum sum rule. The result is

$$\begin{aligned} \bar{f}_G(\gamma_G) &= \frac{n_f}{C_G} \frac{1}{(1+\gamma_G)(2+\gamma_G)(3+\gamma_G)} + \frac{2}{\gamma_G(1+\gamma_G)(2+\gamma_G)} + \frac{1}{(1+\gamma_G)(2+\gamma_G)} \\ &+ \frac{1}{2(3+\gamma_G)(4+\gamma_G)} + \frac{1}{(2+\gamma_G)(3+\gamma_G)(4+\gamma_G)}. \end{aligned} \tag{2.102}$$

This constant $\bar{f}_G$ should be used for f_G in P_{GG} whenever eqn. (2.101) is used.

The IR-improved kernels are a follows:

$$P_{qq}(z)^{exp} = C_F F_{YFS}(\gamma_q) e^{\frac{1}{2}\delta_q} \left[\frac{1+z^2}{(1-z)}(1-z)^{\gamma_q} - f_q(\gamma_q)\delta(1-z) \right], \tag{2.103}$$

$$P_{Gq}(z)^{exp} = C_F F_{YFS}(\gamma_q) e^{\frac{1}{2}\delta_q} \left[\frac{1+(1-z)^2}{z} z^{\gamma_q} \right], \tag{2.104}$$

$$P_{qG}(z)^{exp} = F_{YFS}(\gamma_G) e^{\frac{1}{2}\delta_G} \left[z^2(1-z)^{\gamma_G} + (1-z)^2 z^{\gamma_G} \right], \tag{2.105}$$

$$\begin{aligned} P_{GG}(z)^{exp} &= 2C_G F_{YFS}(\gamma_G) e^{\frac{1}{2}\delta_G} \Bigg[\frac{(1-z)}{z} z^{\gamma_G} + \frac{z}{(1-z)}(1-z)^{\gamma_G} \\ &+ \frac{1}{2}(z^{1+\gamma_G}(1-z) + z(1-z)^{1+\gamma_G}) - f_G(\gamma_G)\delta(1-z) \Bigg]. \end{aligned} \tag{2.106}$$

In conclusion, by using an exact rearrangement of the QCD Feynman series to isolate and resum the leading IR contributions to the physical processes that generate the evolution kernels in DGLAP-CS theory, there is no longer any need for a regularization procedure such as the plus-function procedure since the higher order corrections tame these singularities. We will implement these kernels in the HERWIG6.5 Monte Carlo and investigate the phenomological consequences.

CHAPTER THREE

Monte Carlo Event Generator

Monte Carlo methods are used to simulate physical and mathematical systems by repeated random sampling. Due to the inherent random nature of quantum chromodynamics, Monte Carlo techniques are well suited for its simulation. The goal is to use computers to generate events that mimic those that can be observed in a detector. The output of these generators are in the form of events with the same average behaviour and the same fluctuations as the real data. These fluctuations are due to the quantum mechanics of the underlying theory. Monte Carlo techniques are used to select the relevant variables according to the desired probability distributions.

The five main applications of Monte Carlo event generators in QCD are:

(1) To give an idea of the kind of events one expects to find in real detectors and at what rates.

(2) To help in the design and optimization of new detectors.

(3) To devise analyzing strategies that could be used on real data to optimize signal to background conditions.

(4) To estimate detector acceptance.

(5) They give a framework within which to interpret the observed phenomena in terms of a more fundamental theory (Standard Model, etc.).

To see how a typical QCD Monte Carlo event generator works, let us consider an experiment that collides a 700 GeV u-quark with a 700 GeV $\bar{u}$-quark to produce a $d\bar{d}$ quark through the decay of a Z boson [65]. The elementary hard subprocess is given by $u\bar{u} \to Z \to d\bar{d}$ and the cross section for this process is given by

$$d\sigma(u\bar{u} \to Z^0 \to d\bar{d}) = \frac{1}{2\hat{s}} \left|\mathcal{M}(u\bar{u}) \to Z^0 \to d\bar{d}\right|^2 \frac{d\cos\theta d\phi}{8\,(2\pi)^2}, \tag{3.1}$$

where $\mathcal{M}$ is the matrix element and $\hat{s}$ is the center of mass energy squared. The two degrees of freedom in this problem are the decay angles of Z (θ, ϕ).

This equation can now be used to write an event generator. The first step is to sample the multidimensional hyper cube phase space which spans all the relevant degrees of freedom. In this case, it is a two dimensional space $-1 < \cos\theta < 1$, $0 < \phi < 2\pi$. A candidate event is then chosen by selecting $\cos\theta$ and ϕ variables from a uniformly distributed random number generator. The candidates event's differential cross section (event weight) $d\sigma$ is then calculated from eqn. (3.1), and this is directly related to the probability of the event occurring. An approximation to the integral $\int d\sigma$ is done by averaging over many candidate events.

The next step is to extract physics information from these candidates events which are distributed in flat space. There are two ways which can be used to accomplish this goal. The event weights are used to create histograms representing physical distributions. For example a histogram for the transverse momentum of the d quark is filled with the event weights from a large number of candidate events. For a large number of events, this distribution should reproduce the one predicted by eqn. (3.1). Alternately, we can use unweighted events that are distributed according to the theoretical value. Unlike the first method, unweighted events produce genuine simulation of the experiment. It produces events with the frequency predicted by the theory being modeled.

To generate unweighted events, the acceptance-rejection or Von Neumann method is normally used. We first find the maximum event weight $d\sigma_{\mathrm{MAX}}$. In this example, $d\sigma_{\mathrm{MAX}}$ occurs when one of the final state quarks is collinear with one of the initial quarks i.e. $\cos\theta = \pm 1$. For more complicated processes we can approximate $d\sigma_{\mathrm{MAX}}$ by randomly scanning the parameter space. Then for each candidate event, the ratio of the event weight over the maximum event weight ($\frac{d\sigma}{d\sigma_{MAX}}$) is compared to a random number $\mathcal{R}$ uniformly distributed in the interval $(0, 1)$. We accept events for which $\frac{d\sigma}{d\sigma_{MAX}} > \mathcal{R}$, and reject the others. These accepted events will have the frequency and distribution predicted by eqn. (3.1).

This gives an overview of the basics of an event generator. The process given in eqn. (3.1) is not physical since the kinematics of the process is too simple, i.e. the Z has zero transverse momentum. This is due to the fact that in this example the number of initial and final state particles is fixed but in a real world example there may be radiation that creates extra particles. This is especially pertinent in QCD processes due to the strength of the coupling constant. This extra radiation corresponds to higher order corrections in perturbation theory and is responsible for generating transverse momentum for the Z boson.

Also quark beams cannot be prepared and it is not possible to detect isolated quarks. We therfore need a way to create bound states from the individual quarks. This process is called hadronization. Thus for a realistic event generator we need a way to compute exactly or to estimate the effect of higher order corrections in perturbation theory and a way to describe hadronization effects.

3.1 Hadron Event Generators

Two of the most popular Monte Carlo event generators are Herwig [13, 14] and Pythia [66]. These start with a leading order sub-process such as $u\bar{u} \to Z \to d\bar{d}$ as discussed earlier. We then add higher order effects by evolving the event using the parton shower, i.e. the partons branch by splitting. Finally, the partons are hadronized into colour singlet hadrons and the resonances are decayed. To complete the simulation, the underlying structure of the event is generated : beam remnants (coloured remains of the proton which are left behind when the parton which participates in the hard subprocess is taken out), interaction from other partons in the hadrons and collisions between other hadrons in the colliding beam (pile up).

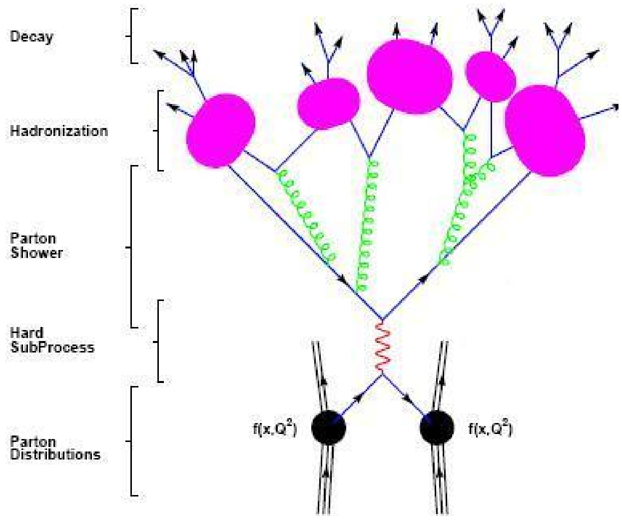

Figure 3.1. The basic structure of a showering and hadronization event generator.

Figure (3.1) shows the general structure of the final event from a SHG [67]. In this diagram time goes from bottom to top. Two protons collide and a parton is resolved on a scale Q and momentum fraction x in each one. In this example, a valence quark is resolved in the proton shown on the left, while an antiquark is resolved from the proton on the right. The phenomenology of the partons resolution is encoded in the parton distribution function $f(x, Q^2)$. The hard sub process then follows. The quark and antiquark annihilate into an s-channel resonance. This resonance then decays into a fermion antifermion pair. In our toy model, the resonance is a Z and the initial and final state fermions are $u\bar{u}$ and $d\bar{d}$ respectively.

Higher order QCD effects are incorporated by allowing the (anti)quark to branch into $q\bar{q}$ pairs, and the gluons may branch into $q\bar{q}$ or $g\bar{g}$ pairs. These resultant partons may also branch resulting in a cascade of partons. This is called the parton shower. The initial state partons also go through the showering process. The event now consists of quarks, antiquarks and gluons which, due to colour confinement, cannot exists in isolation. Next, through the process of hadronization, these coloured partons are grouped into colour singlet composite hadrons using a phenomological model. This hadronization takes place in the non-perturbative regime and the model contains several parameters that have to be tuned using experimental data. Since the hadronization scale is much smaller than the hard scales(s), the choice of hadronization models is negligible for most physical processes. After hadronization the short lived resonances are decayed.

Other features are also added to the underlying event. There is a small (≈ 1 GeV) primordial transverse momentum due to the motion of the partons inside the proton, against which the beam remnants collide. These beam remnants are colour connected to the hard subprocess and so are included in the hadronization system. Multiple parton parton interactions and pile up from other collisions in the same bunch crossing are also accounted for.

We note that SHG's produce events with the frequency predicted by the theory. Also with a few minor exceptions the hard subprocess is the only process dependent part. Everything else is (almost) completely generic and implementing a new physics process usually only involves implementing the computer code for the hard subprocess. This hard subprocess is the only event that has a weight associated with it. Everything else is implemented with unit probability. Therefore, after selecting a hard subprocess using the hit-and-miss method, all other aspects of the generation are added onto the accepted event without ever rejecting the event. Thus during the simulation of the hard subprocess a large number of candidate events are attempted, but only a fraction are accepted. However, for each hard subprocess event that is chosen, one fully simulated event will be generated.

SHG's provide an *exclusive* description of the events. Let us consider the production of Z^0 bosons in the hard sub process. Prior to the shower (at the leading order) the transverse momentum of the Z will always be zero, because there is nothing for the Z to recoil against. The SHG's though produce transverse momentum for the Z through the parton showers, since the final state particle energy from the hard subprocess must recoil against those produced by the shower due to momentum conservation. This prediction of the Z transverse momentum is termed exclusive because of the detailed listing of the particles recoiling against the Z is provided. These exclusive calculations provided by SHG's are ideal for the simulation of experiments, because the full event is necessary for a detailed detector simulation.

3.2 The Parton Shower

The parton shower in Monte Carlo event generators formed by the splitting of partons serves two main purposes[68]:

- To provide estimates of higher order corrections that are enhanced by large kinematic logarithms. These occur in the phase space regions of collinear parton branching and/or soft gluon emission

- To generate high-multiplicity partonic states which can readily be converted into the observed hadrons by a soft hadronization mechanism, i.e. one that involves only modest transfers of momentum or quantum numbers between neighbouring regions of phase space.

The parton shower is a Markov process in which successive values of an evolution variable t, a momentum fraction z and an azimuthal angle ϕ are generated, together with the flavours of the partons emitted during showering. A markov process is a random process whose future probabilities are determined by its most recent values, that is, if $t_1 < \cdots < t_n$, we have

$$P(x(t_n) < x_n | x(t_{n-1}), \cdots, x(t_1)) = P(x(t_n) < x_n | x(t_{n-1})). \tag{3.2}$$

The evolution variable t starts at some high value Q, characteristic of the hard process, and the next value is selected by solving the equation

$$\Delta_i(Q, t_0) = \mathcal{R}\Delta_i(t, t_0) \tag{3.3}$$

where Δ_i is the Sudakov form factor for partons of the relevant flavour i, t_0 is an infrared cutoff and $\mathcal{R} \in [0,1]$ is a random number. The Sudakov form factor is

$$\Delta_i(Q,t_0) = \exp\left[-\sum_j \int_{t_0}^{Q} \frac{dt}{t} \int_0^1 dz \mathcal{P}_{ji}(z,t,t_0)\right] \tag{3.4}$$

where $\mathcal{P}_{ji}$ is the probability distribution for the parton branching $i \to j$. We expect this to be given by $\alpha_s P_{ji}(z)/2\pi$ where P_{ji} is the corresponding DGLAP splitting function. These parton branching probabilities are modified in practice for example the splitting functions have infrared singularities at $z = 0$ and/or 1, which have to be regularized. This is normally done by cutting out the singular part of the integration region in a way that depends on the evolution variable t and the cutoff t_0. In HERWIG for the splitting $g \to gg$ we have $\sqrt{t_0/t} < z < 1 - \sqrt{t_0/t}$ [69].

If $\mathcal{R} < \Delta_i(Q,t_0)$ then the evolution of parton i has finished since the selected value of t is now less than the cutoff value t_0. It can emit no more resolvable partons and the program goes on to the hadronization phase. Otherwise the next value of the evolution variable t and the type of branching $i \to j$ is selected, then the momentum fraction z of the branching is chosen by solving

$$\int_0^z dz^{'} \mathcal{P}_{ji}(z^{'},t,t_0) = \mathcal{R} \int_0^1 dz^{'} \mathcal{P}_{ji}(z^{'},t,t_0) \tag{3.5}$$

where $\mathcal{R}^{'} \in [0,1]$ is another random number.

To see how eqn. (3.4) comes about consider that in some order of pertubation theory we have evaluated an amplitude A_N^a with an outgoing gluon a of momentum k_a and polarization ϵ_a. Let there be a branching $a \to b + c$ giving a correction to this amplitude as shown in fig. (3.2). Let the momenta of gluons b and c be at small angles θ_b and θ_c to that of a. If ω_i represents the energy of gluons i,$z = \omega_b/\omega_a$ the energy fraction of gluon b, and $t = k_a^2$ the virtuality of gluon a, we have

$$\theta \equiv \theta_b + \theta_c = \frac{\theta_b}{1-z} = \frac{\theta_c}{z} = \frac{1}{\omega_a}\sqrt{\frac{t}{z\,(1-z)}} \tag{3.6}$$

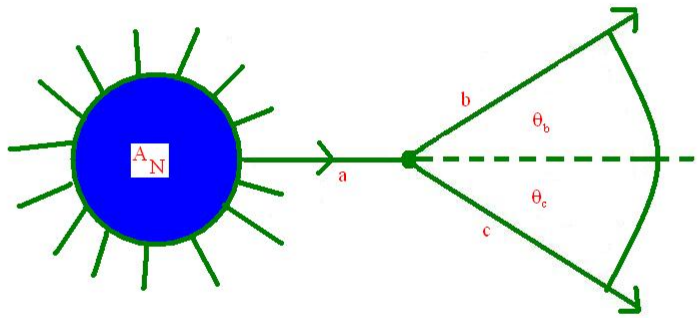

Figure 3.2. Branching of an outgoing parton $a \to b + c$.

We are interested in the collinearly divergent terms so we only need to consider the transverse polarization states, for which the triple gluon vertex gives

$$A^{bc}_{N+1} = A^{a}_{N}.\frac{g_s}{t}.2f^{abc}\left(\epsilon_a.\epsilon_b\epsilon_c.k_b - \epsilon_b.\epsilon_c\epsilon_a.k_b - \epsilon_c.\epsilon_a\epsilon_b.k_c\right). \tag{3.7}$$

Choosing ϵ_i^0 and using plane polarization states polarized in and out of the plane of branching, then for a polarized in the plane we have

$$\epsilon_a.k_b = -\omega_b\theta_b = -\sqrt{z\left(1-z\right)t}, \tag{3.8}$$

and for $\epsilon_{b,c}$ in the plane

$$\begin{aligned} \epsilon_b.k_c &= \omega_c\theta = \sqrt{\left(1-z\right)t/z}, \\ \epsilon_c.k_b &= -\omega_b\theta = -\sqrt{zt/\left(1-z\right)}, \end{aligned} \tag{3.9}$$

giving

$$A^{bc}_{N+1} = A^{a}_{N}.\frac{g_s}{\sqrt{t}}.f^{abc}K_{gg}(\epsilon_a, \epsilon_b, \epsilon_c, z), \tag{3.10}$$

where the K_{gg} are listed in table (1) in ref. ([69]).

Using the invariant phase space element

$$\frac{dtd\phi dz}{4(2\pi)^3}, \tag{3.11}$$

where ϕ is the azimuthal angle between the plane of the branching and the polarization a we obtain the contribution to the cross section

$$d\sigma_{N+1} = d\sigma_N\frac{dt}{t}\frac{d\phi}{2\pi}dz.\frac{\alpha_s}{2\pi}.\frac{C_A}{2}\left|k_{gg}\right|^2, \tag{3.12}$$

where $C_A = N_C = 3$. We note that there is a collinear singularity (dt/t) and an infrared (dz/z) singularity when a gluon is emitted with polarization in the plane of branching.

Integrating over ϕ, averaging over polarizations of a and summing over those of b and c gives

$$d\bar{\sigma}_{N+1} = d\bar{\sigma}_N \frac{dt}{t} dz . \frac{\alpha_s}{2\pi} . P_{GG}(z), \tag{3.13}$$

where P_{GG} is the usual DGLAP evolution kernel. The amplitude A_N^a may also involve an outgoing quark, which branches into a quark b and a gluon c. We will again obtain a collinear singularity of A_{N+1}^{bc}. This is governed by the splitting function $P_{qq}(z)$. Finally an outgoing gluon may branch into a quark-antiquark instead of gluon-gluon. The corresponding splitting function is $P_{qG}(z)$

$$\frac{1}{2}\left[z^2 + (1-z)^2\right]. \tag{3.14}$$

We see that there are no infrared singularities since no soft gluons can be emitted in this branching.

Assume that the sequence of branching continues, for example, parton $b \to d + e$ with virtuality $k_b^2 = t^{'}$ and energy fraction $\omega_d/\omega_b = z^{'}$. The corresponding contribution of order α_s^{N+2} is

$$d\bar{\sigma}_{N+2} = d\bar{\sigma}_N \frac{dt}{t}\frac{dt^{'}}{t^{'}} dz dz^{'} \left(\frac{\alpha_s}{2\pi}\right)^2 P_{ba}(z) P_{db}(z^{'}). \tag{3.15}$$

This sequence of branchings may be formulated as a simple Markov process [70, 71, 72] in which each step i has a probability depending on the parton virtuality t_i, the type of splitting involved and the energy fraction z_i for that step. It is assumed that each t_i is small compared with the preceeding one, so that the sequence of virtualities is strongly decreasing as we move away from the hard subprocess:

$$Q^2 \gg t_1 \gg t_2 \cdots \gg t_n \gg Q_0^2, \tag{3.16}$$

where Q^2 is the momentum transfer scale of the subprocess and Q_0^2 is the cutoff scale at which we stop using pertubation theory. This strongly ordered region is the one in which the largest number of logarithms will arise to enhance the contribution to the cross section in this order:

$$\sigma_n \propto \sigma_0 \alpha_s^n \int_{Q_0^2}^{Q^2} \frac{dt_1}{t_1} \int_{Q_0^2}^{t_1} \frac{dt_2}{t_2} \cdots \int_{Q_0^2}^{t_{n-1}} \frac{dt_n}{t_n} = \sigma_0 \frac{\alpha_s^n}{n!} \left(\ln \frac{Q^2}{Q_0^2} \right)^n . \tag{3.17}$$

The parton branching process can be more conveniently described in terms of a generating functional

$$\Phi_a \left[W, Q^2; f(\omega) \right] = \frac{1}{\sigma_{\text{tot}}} \sum_{N=0}^{\infty} \int d\bar{\sigma}_N \left(\omega_1, \cdots, \omega_N \right) f(\omega_1) \cdots f(\omega_N), \tag{3.18}$$

corresponding to the ensemble of parton cascades initiated by a parton a of energy W produced in a hard process at scale Q^2. We now need to find the evolution equation for this functional. To do this consider the distribution of the first branching of the initial parton. Let $\Delta_a(Q^2, t)$ represent the probability that no branching occurs at virtuality higher than t. Then using fig. (3.3) and eqn. (3.13) and (3.18) we have

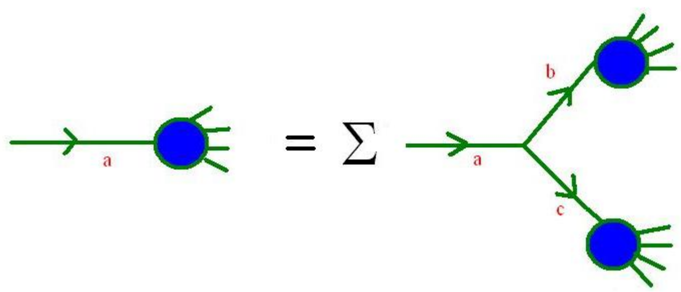

Figure 3.3. Evolution equation for outgoing parton cascades.

$$\begin{aligned} \Phi_a \left[W, Q^2 \right] &= \Delta_a \left(Q^2, Q_0^2 \right) \Phi_a \left[W, Q_0^2 \right] + \int_{Q_0^2}^{Q^2} \frac{dt}{t} \Delta_a \left(Q^2, t \right) \sum_b \int dz \frac{\alpha_s}{2\pi} P_{ba}(z) \\ &\times \Phi_b \left[zW, t \right] \Phi_c \left[(1-z) W, t \right], \end{aligned} \tag{3.19}$$

where the sum is over all possible branchings $a \to b + c$. The probability that no branching whatsoever occurs above the virtuality cutoff Q_0^2, which is called the Sudakov form factor of parton a, is given by $\Delta_a(Q^2, Q_0^2)$. It must satisfy the differential equation

$$d\Delta_a\left(t, Q_0^2\right) = -\frac{dt}{t}\Delta_a\left(t, Q_0^2\right)\sum_b \int dz \frac{\alpha_s}{2\pi} P_{ba}(z), \tag{3.20}$$

which has the solution

$$\Delta_a\left(Q^2, Q_0^2\right) = \exp\left[-\int_{Q_0^2}^{Q^2} \frac{dt}{t}\sum_b \int dz \frac{\alpha_s}{2\pi} P_{ba}(z)\right]. \tag{3.21}$$

The values of t and z at each branching is then used to construct the kinematics of the parton shower except for the angle. In HERWIG t represents $E^2(1-\cos\theta)$ where E is the energy of the parent parton and θ is the opening angle, while z is the energy fraction, so that $q_t^2 = 2z^2(1-z)^2 t$. To completely determine the branch we need to fix the azimuthal angle ϕ, which fixes the direction of the relative transverse momentum q_t.

After the branching $i \to jk$ takes place at scale t_i, we need to generate the evolution of the daughter parton j and k. Naively we expect the evolution to start at t_i and the next values of t_k and t_k to be obtained from eqn. (3.4) using the appropriate Sudakov form factors Δ_j and Δ_k with Q replaced by t_i. This however implies that t_j and t_k can be both be arbitrarily close to t_i which is not possible. There is also a stronger constraint in HERWIG due to *angular ordering*. In HERWIG $t_i = E_i^2(1-\cos\theta_i)$, where θ_i is the opening angle in the branching $i \to jk$. By angular ordering we mean that the opening angle θ_j of any subsequent branching of parton j is less than θ_i. This implies $t_j = E_j^2(1-\cos\theta_i) < z^2 t_i$, where $z = E_j/E_i$. Hence the evolution of parton j starts at $(1-z^2)t_i$ rather than t_i. Similarly, the evolution of parton k starts at $(1-z)^2 t_i$. For further evolution to be possible, we require $z^2 t_i(1-z)^2 t_i > t_0$. This leads to the condition $\sqrt{(}t_0/t_i) < 1 - \sqrt{t_0/t_i}$.

Angular ordering is an attempt to simulate with more accuracy those higher order contributions that are enhanced due to soft gluon emission (and associated virtual corrections). For example, consider the branching $q \to qg$. A soft gluon emitted by one of the daughter partons can only resolve the individual outgoing quark and gluon colour charges if its angle of emission is less than the opening angle of the branching. Otherwise, it is emitted by the coherent sum of their colour charges, which is equal to that of the parent quark. Therefore, any emission at larger angles are generated from the parent and not the daughters. This is called angular ordering.

The outcome of these branchings is to create a parton shower in which each initial parton from the hard process is replaced by a jet of partons moving in roughly the same direction, together with some relatively soft wide-angle partons between jets. This shower exhibits preconfinement [73, 74] i.e. the distribution of colour and flavour is organized in such a way to form non-exotic colour singlet objects. This shower is then used as an input to a hadronization model.

3.3 HERWIG

HERWIG is a general purpose Monte Carlo event generator for the simulation of lepton-lepton, lepton-hadron and hadron-hadron collisions. This program includes a large range of hard scattering processes together with initial and final state radiation using the angular ordered parton shower, hadronization and hadron decays, and underlying event simulation [13].

HERWIG contains a large library of hard $2 \to n$ scattering processes for both the Standard Model and its supersymmetric extensions. The main features of a generic hard process simulated by HERWIG can be divided into five components:

(1) Elementary hard subprocesses: Start from the hard elementary distribution $\sigma_{ab\to f_i}$, with ab the pair of incoming particles which interact to produce one or more primary outgoing fundamental objects, f_i. This can be computed exactly in perturbation theory.

(2) Initial state parton showers: Each incident parton of the individual beam hadron with low spacelike virtuality ($m^2 < 0$), branches into a number of

timelike ($m^2 > 0$) partons. In this process, the incident parton's energy is decreased to a fraction x of that of the beam and its spacelike virtuality is increased. This mass is bounded by the scale Q of the hard subprocess. This initial state emission process leads to the evolution of the structure function $f(x, Q)$ of the incident hadron.

(3) Final state parton showers: The outgoing virtual partons with a large timelike mass generate a shower of partons with lower virtuality. The amount of emission depends on the upper limit on the virtuality of the initiating parton which is controlled by the momentum transfer scale Q. Timelike partons from the initial state emission may also initiate parton showering.

(4) Heavy object decays: The massive produced particles (top quarks, Higgs bosons, etc.) can decay on time scales that may be shorter than that of the QCD parton showers. These may also initiate parton showers before and/or decaying.

(5) Hadronization process: The emitted partons are combined together to generate the final hadrons by using a hadronization model. Since the hadronization process takes place at low momentum transfer scale ($Q_0 < 1$ Gev), α_s is large and perturbation theory is no longer applicable. It therefore has to be described a phenomological model. The preconfinement property of perturbative QCD is used by Herwig as the basis for a simple hadronization model (cluster model) which is local in colour and independent of the hard process and energy [75, 76]. After the parton shower phase, any gluons are split non-pertubatively into $q\bar{q}$ pairs. In the $N_c \to \infty$ limit, all quarks and antiquarks can be uniquely formed into colour singlet clusters due to colour pre-confinement, the mass spectrum of these clusters is strongly peaked at low mass and falls off rapidly. The high mass clusters are first split into low

mass clusters using a string like mechanism. The constituent partons which do not participate in the hard subprocess undergo a soft "underlying event" interaction modeled on soft minimum bias hadron-hadron collisions.

HERWIG has the following processes:

- QCD: $2 \rightarrow 2$ scattering processes including heavy flavour production
- Electroweak: $\gamma/\gamma^*/Z^0/W^\pm/H^0$ production either singly or in pairs and often with additional jets.
- SUSY: A large range of MSSM production processes in lepton-lepton and hadron-hadron collisions.
- New gauge bosons and resonant graviton production.

3.4 PYTHIA

PYTHIA [77] is a general purpose generator for hadronic events in pp, e^+e^- and ep colliders. It contains a subprocess library and generation machinery, initial and final state parton showers, underlying events, hadronization and decays and analysis tools.

The final state shower in PYTHIA [78, 79] is based on forward evolution in terms of a decreasing timelike virtuality m^2, with angular ordering imposed by veto. The initial state shower [80, 81] is based on backward evolution i.e. starting at the hard scattering scale and moving backwards in time to the shower initiators, in terms of a decreasing spacelike virtuality Q^2. Partons radiated in the initial state may also initiate final state showers.

For the hadronization process PYTHIA uses the Lund string model [82, 83]. It is based on a picture with linear confinement, where (anti)quarks or other colour (anti)triplets are located at the ends of the string, and gluons are energy and momentum carrying kinks on the string. Thereby a gluon is attached to two string pieces, one related to its colour and the other its anticolour, and experiences a confinement force twice that of a quark. The string breaks by the production of new $q\bar{q}$ pairs, and a quark from one break can combine with an antiquark from an adjacent one to form a colour singlet meson.

PYTHIA has around 240 different $2 \to n$ subprocesses, all at leading order. These include:

- QCD: $2 \to 2$ partonic scattering, heavy flavour, elastic and diffractive processes.
- Standard Model: $\gamma/\gamma^*/Z^0/W^{\pm}$ singly or in pairs, or with a quark or gluon, Higgs
- SUSY: two Higgs doublets, sfermion and gaugino pairs, R-parity-violating decays.
- Exotics: technicolour, new gauge bosons, compositeness, leptoquarks, doubly charged Higgses. extra dimensions.

CHAPTER FOUR

Implementation in HERWIG6.5

We will now discuss our implementation of the IR-Improved kernels. This was done by modifying the following functions in HERWIG6510 [13]: **HWBSUG**, **HWBSU1**, **HWBSU2**, **HWBRAN**. These modifications will now be discussed.

4.1 Gluon Quark Splitting Function

Suppose we know a function P_{ab} which is nonnegative in the allowed z range $z_{min} \leq z \leq z_{max}$. We need to select an z at random so that the probability in a small interval dz around a given z is proportional to $P_{ab}(z)dz$. The integral of $P_{ab}(z)$ does not have to be explicitly normalized to unity since by the Monte Carlo procedure of picking exactly one accepted z value, normalization is implicit in the final result. Then z can be found as follows

$$\int_{z_{min}}^{z} P_{ab}(z)dz = \mathcal{R}\int_{z_{min}}^{z_{max}} P_{ab}(z)dz. \tag{4.1}$$

Consider the

$$\begin{aligned} P_{Gq}^{exp}(z) &= C_F F_{YFS}(\gamma_q)e^{\frac{1}{2}\delta_q}\left[\frac{1+(1-z)^2}{z}z^{\gamma_q}\right] \\ &= C_F F_{YFS}(\gamma_q)e^{\frac{1}{2}\delta_q}[1+(1-z)^2)z^{\gamma_q-1}] \end{aligned} \tag{4.2}$$

splitting function. Using eqn. (4.1) we can calculate the next value of the evolution variable. We deal with the singular part by integrating the denominator as follows:

$$\int_{z_{min}}^{z_1} z^{\gamma_q-1}dz = \mathcal{R}\int_{z_{min}}^{z_{max}} z^{\gamma_q-1}dz, \tag{4.3}$$

where $\mathcal{R}$ is a random number uniformly distributed between 0 and 1. Therefore

$$z_1^{\gamma_q} - z_{min}^{\gamma_q} = \mathcal{R}(z_{max}^{\gamma_q} - z_{min}^{\gamma_q}). \tag{4.4}$$

Thus we have

$$\left(\frac{z_1}{z_{min}}\right)^{\gamma_q} - 1 = \mathcal{R}\left[z_{rat}^{\gamma_q} - 1\right], \tag{4.5}$$

where

$$z_{rat} = \frac{z_{max}}{z_{min}}. \tag{4.6}$$

As a test, let $\gamma_q \to 0$, which gives

$$1 + \gamma_q \ln\left(\frac{z_1}{z_{min}}\right) - 1 = \mathcal{R}[1 + \gamma_q \ln(z_{rat}) - 1], \tag{4.7}$$

which implies

$$\ln\left(\frac{z_1}{z_{min}}\right) = \ln(z_{rat}^{\mathcal{R}}). \tag{4.8}$$

Finally we get

$$z_1 = z_{min} \times z_{rat}^{\mathcal{R}} \tag{4.9}$$

as in HERWIG6.5.

To implement the IR improved kernel in HERWIG6.5, we replace eqn. (4.9) with

$$z_1 = z_{min}[\mathcal{R}(z_{rat}^{\gamma_q} - 1) + 1)]^{\frac{1}{\gamma_q}}. \tag{4.10}$$

The original HERWIG6.5 code was given by procedure (4.1).

Table 4.1. Quark or antiquark branching

if ID2 = 13 **then**
  $Z_{\rm max}$ = 1 - HWBVMC(ID)/QNOW
  $W_{\rm min}$ = MIN($Z_{\rm min} \times (1 - Z_{\rm min})$, $Z_{\rm max} \times (1 - Z_{\rm max})$)
  $E_{\rm test} = (1 + Z_{\rm max}^2) \times \alpha_s$(5-SUDORD×2,QNOW×$W_{\rm min}$)
  $Z_{\rm rat} = Z_{\rm max}/Z_{\rm min}$
  repeat
    $Z_1 = Z_{\rm min} \times Z_{\rm rat}^{\mathcal{R}}$
    $Z_2 = 1 - Z_1$
    PGQ =$(1 + Z_2^2)$
    $Z_{\rm test}$ = PGQ $\times\alpha_s$(5-SUDORD× 2,QNOW×$Z_1 Z_2$)
  until ($Z_{\rm test} < (E_{\rm test} \times \mathcal{R})$)
end if

This was replaced by procedure (4.2), where $Z_{max} = 1 - Z_{min}$ and $n_f = 5$ sets the number of quark flavours at 5. This was done to be consistent with the calculation of the running coupling α_s, which is calculated with $n_f = 5$ in HERWIG6.5

Table 4.2. Quark or antiquark branching with IR-Improved kernels

if ID2 = 13 **then**
  $n_f = 5$
  $\beta_0 = 11 - 2/3 n_f$
  $\gamma_q = 16/(3 \times \beta_0)$
  $Z_{\text{max}} =$ 1 - HWBVMC(ID)/QNOW
  $W_{\text{min}} = \text{MIN}(Z_{\text{min}} \times (1 - Z_{\text{min}}), Z_{\text{max}} \times (1 - Z_{\text{max}}))$
  $E_{\text{test}} = (1 + Z_{\text{max}}^2) \times \alpha_s(\text{5-SUDORD}\times 2,\text{QNOW}\times W_{\text{min}})$
  $Z_{\text{rat}} = Z_{\text{max}}/Z_{\text{min}}$
  repeat
    $Z_1 = Z_{\text{min}}[\mathcal{R}(Z_{\text{rat}}^{\gamma_q} - 1) + 1)]^{\frac{1}{\gamma_q}}$
    $Z_2 = 1 - Z_1$
    $\delta_q = 1/2 \times \alpha_s(\text{5-SUDORD}\times 2,\text{QNOW}\times Z_1 Z_2) \times 1.184056810$
    PGQW $=(1 + Z_2^2) \times \exp(.5\delta_q) \times \text{FYFS}_q(n_f)$
    $Z_{\text{test}} =$ PGQW $\times \alpha_s(\text{5-SUDORD}\times 2,\text{QNOW}\times Z_1 Z_2)$
  until $(Z_{\text{test}} < (E_{\text{test}} \times \mathcal{R}))$
end if

4.2 Gluon Gluon Splitting Function

As before, we deal with the singular part of $P_{GG}(z)^{exp}$ by solving for z_1 in the equation

$$\int_{z_1}^{z_{max}} \frac{1}{z\,(1-z)} dz = \mathcal{R} \int_{z_{min}}^{z_{max}} \frac{1}{z\,(1-z)}. \tag{4.11}$$

Integrating both sides gives

$$\ln\left[\frac{z_{max}\,(1-z_1)}{(1-z_{max})\,z_1}\right] = \ln\left[\frac{z_{max}\,(1-z_{min})}{(1-z_{max})\,z_{min}}\right] = \ln z_{rat}^{\mathcal{R}} \tag{4.12}$$

where

$$z_{rat} = \frac{z_{max}\,(1-z_{min})}{(1-z_{max})\,z_{min}} \tag{4.13}$$

as in HERWIG6.5. Here

$$z_{rat}^{\mathcal{R}} = \frac{z_{max}\,(1-z_1)}{(1-z_{max})\,z_1} \tag{4.14}$$

giving

$$z_1 = \frac{z_{max}}{z_{max} + (1 - z_{max})\, z_{rat}^{\mathcal{R}}} \tag{4.15}$$

Table 4.3. Gluon gluon branching

$W_{\min} = Z_{\min} \times Z_{\max}$
$E_{\text{test}} = (1 - W_{\min})^2 \times \alpha_s(5 - \text{SUDORD} \times 2,\ \text{QNOW}\ \times W_{\min})$
$Z_{\text{rat}} = (Z_{\max}\,(1 - Z_{\min}))/(Z_{\min}\,(1 - Z_{\max}))$
repeat
   $Z_1 = Z_{\max}/\left(Z_{\max} + (1 - Z_{\max})\, Z_{\text{rat}}^{\mathcal{R}}\right)$
   $Z_2 = 1 - Z_1$
   PGG$= (1 - (Z_1 Z_2))^2$
   $Z_{\text{test}} = \text{PGG} \times \alpha_s(\text{5-SUDORD}\ \times 2,\ \text{QNOW}\ \times (Z_1 Z_2))$
until $Z_{\text{test}} < E_{\text{test}} \times \mathcal{R}$

Table 4.4. Gluon gluon branching with IR-Improved kernels

$n_f = 5$
$\beta_0 = 11 - 2/3 n_f$
$\gamma_G = 12/\beta_0$
$W_{\min} = Z_{\min} \times Z_{\max}$
$\delta_G = \gamma_G/2 + \alpha_s(5 - \text{SUDORD} \times 2, \text{QNOW} \times W_{\min}) \times 2.664127824$
$E_{\text{test}} = \left[Z_{\max}^2 Z_{\min}^{\gamma_G} + Z_{\min}^2 Z_{\max}^{\gamma_G} + 1/2\left(Z_{\min}^{2+\gamma_G} Z_{\max}^2 + Z_{\max}^{2+\gamma_G} Z_{\min}^2\right)\right]$
   $\times \alpha_s\,(5 - \text{SUDORD} \times 2, \text{QNOW} \times W_{\min}) \times \exp(.5\delta_G)\text{FYFS}_G(n_f)$
$Z_{\text{rat}} = (Z_{\max}\,(1 - Z_{\min}))/(Z_{\min}\,(1 - Z_{\max}))$
repeat
   $Z_1 = Z_{\max}/\left(Z_{\max} + (1 - Z_{\max})\, Z_{\text{rat}}^{\mathcal{R}}\right)$
   $Z_2 = 1 - Z_1$
   $\delta_G = \gamma_G/2 + \alpha_s(5 - \text{SUDORD} \times 2, \text{QNOW} \times Z_1 Z_2) \times 2.664127824$
   PGGW $= Z_2^2 Z_1^{\gamma_G} + Z_1^2 Z_2^{\gamma_G} + 1/2\left(Z_1^{2+\gamma_G} Z_2^2 + Z_1^2 Z_2^{2+\gamma_G}\right) \times \exp(.5\delta_G) \times \text{FYFS}_G(n_f)$
   $Z_{\text{test}} = \text{PGGW} \times \alpha_s(\text{5-SUDORD}\ \times 2,\ \text{QNOW}\ Z_1 Z_2)$
until $Z_{\text{test}} < E_{\text{test}}\mathcal{R}$

Now

$$\begin{aligned} P_{GG}(z) &= 6\left[\frac{1-z}{z} + \frac{z}{1-z} + z\,(1-z)\right] \\ &= 6\frac{(1 - z(1-z))^2}{z\,(1-z)}, \end{aligned} \tag{4.16}$$

and

$$P_{GG}(z)^{exp} \propto \left[\frac{(1-z)}{z} z^{\gamma_G} + \frac{z}{(1-z)}(1-z)^{\gamma_G} + \frac{1}{2}(z^{1+\gamma_G}(1-z) + z(1-z)^{1+\gamma_G})\right]$$
$$= \frac{(1-z)^2 z^{\gamma_G} + z^2(1-z) + \frac{1}{2}(z^{2+\gamma_G}(1-z)^2 + z^2(1-z)^{2+\gamma_G})}{z(1-z)}. \quad (4.17)$$

To implement $P_{GG}^{exp}(z)$ in HERWIG6.5, the original procedure (4.3) was replaced by procedure (4.4).

4.3 Quark Gluon Splitting Function

A similar implementation was done for the quark gluon splitting function.

Table 4.5. Gluon quark branching

$E_{\text{test}} = Z_{\text{min}}^2 Z_{\text{max}}^2 + Z_{\text{max}}^2 Z_{\text{min}}^2$
repeat
  $Z_1 = \text{HWRUNI}(0, Z_{\text{min}}, Z_{\text{max}})$
  $Z_2 = 1 - Z_1$
  $\text{PQG} = Z_1^2 + Z_2^2$
  $Z_{\text{test}} = \text{PQG}$
until $Z_{\text{test}} < E_{\text{test}}\mathcal{R}$

Table 4.6. Gluon quark branching with IR-Improved kernels

$n_f = 5$
$\beta_0 = 11 - 2/3n_f$
$\gamma_G = 12/\beta_0$
$\delta_G = \gamma_G/2 + \alpha_s(5 - \text{SUDORD} \times 2, \text{QNOW} \times \text{WMIN}) \times 2.664127824$
$E_{\text{test}} = Z_{\text{min}}^2 Z_{\text{max}}^{\gamma_G} + Z_{\text{max}}^2 Z_{\text{min}}^{\gamma_G} \times \exp(.5\delta_G) \times \text{FYFS}_G(n_f)$
repeat
  $Z_1 = \text{HWRUNI}(0, Z_{\text{min}}, Z_{\text{max}})$
  $Z_2 = 1 - Z_1$
  $\delta_G = \gamma_G/2 + \alpha_s(5 - \text{SUDORD} \times 2, \text{QNOW} \times Z_1 Z_2) \times 2.664127824$
  $\text{PQGW} = Z_1^2 Z_2^{\gamma_G} + Z_2^2 Z_1^{\gamma_G} \times \exp(.5\delta_G) \times \text{FYFS}_G(n_f)$
  $Z_{\text{test}} = \text{PQGW}$
until $Z_{\text{test}} < E_{\text{test}}\mathcal{R}$

4.4 Parton Branching Process

Following [69], the probability that no branching occurs above the virtuality cutoff Q_0^2 is given by $\Delta_a(Q^2, Q_0^2)$. It must satisfy the differential equation

$$d\Delta_a(t, Q_0^2) = \frac{-dt}{t}\Delta(t, Q_o^2)\sum_b \int dz \frac{\alpha_s}{2\pi} P_{ba}(z), \tag{4.18}$$

which can be solved to give

$$\Delta_a(Q^2, Q_0^2) = \exp\left[-\int_{Q_0^2}^{Q^2} \frac{dt}{t}\sum_b \int dz \frac{\alpha_s}{2\pi} P_{ba}(z)\right]. \tag{4.19}$$

The non-branching probability appearing in the evolution equation may be written as

$$\Delta(Q^2, t) = \frac{\Delta_a(Q^2, Q_o^2)}{\Delta_a(t, Q_o^2)}, \quad t = k_a^2 \quad \text{the virtuality of gluon } a. \tag{4.20}$$

The virtuality of parton a is generated with the correct distribution by solving the equation

$$\Delta_a(Q^2, t) = \mathcal{R}, \tag{4.21}$$

where $\mathcal{R}$ is a random number uniformly distributed between 0 and 1.

Recall

$$\alpha_s(Q) = \frac{2\pi}{b_0 \log\left(\frac{Q}{\Lambda}\right)}, \tag{4.22}$$

so

$$\begin{aligned}\int_0^1 dz \frac{\alpha_s(Q^2)}{2\pi} P_{qG}(z) &= \frac{2\pi}{2\pi b_0 \ln\left(\frac{Q^2}{\Lambda^2}\right)} \int_0^1 dz \frac{1}{2}\left[z^2 + (1-z)^2\right] \\ &= \frac{1}{3}\frac{1}{b_0 \ln\left(\frac{Q^2}{\Lambda^2}\right)}.\end{aligned} \tag{4.23}$$

Therefore

$$\begin{aligned}&\int_{Q_0^2}^{Q^2} \frac{1}{3}\frac{dt}{t}\frac{1}{b_0 \ln\left(\frac{t}{\Lambda^2}\right)}, \quad t = Q^2 \\ =\ & \frac{1}{3b_0} \ln\ln \frac{t}{\Lambda^2}\Big|_{Q_0^2}^{Q^2} \\ =\ & \frac{1}{3b_0}\left[\ln\left(\frac{\ln\left(\frac{Q^2}{\Lambda^2}\right)}{\ln\left(\frac{Q_0^2}{\Lambda^2}\right)}\right)\right].\end{aligned} \tag{4.24}$$

Finally

$$\Delta_a(Q^2,Q_0^2) = \exp\left[-\frac{2}{3b_0}\ln\left(\frac{\ln\left(\frac{Q^2}{\Lambda^2}\right)}{\ln\left(\frac{Q_0^2}{\Lambda^2}\right)}\right)\right]$$
$$= \left[\frac{\ln\left(\frac{Q^2}{\Lambda^2}\right)}{\ln\left(\frac{Q_0^2}{\Lambda^2}\right)}\right]^{-\frac{2}{3b_0}}. \tag{4.25}$$

Let $\Delta_a(Q^2,t) = \mathcal{R}$, then

$$\left[\frac{\ln\left(\frac{t}{\Lambda^2}\right)}{\ln\left(\frac{Q^2}{\Lambda^2}\right)}\right]^{\frac{2}{3b_0}} = \mathcal{R}, \tag{4.26}$$

which implies

$$t = \Lambda^2\left(\frac{Q^2}{\Lambda^2}\right)^{\mathcal{R}^{\frac{3b_0}{2}}}. \tag{4.27}$$

Recall

$$b_0 = \left(\frac{11}{3}n_c - \frac{2}{3}n_f\right)$$
$$= \frac{1}{3}\left(11n_c - 10\right), \quad n_f = 5$$
$$= \frac{2}{3}\mathbf{BETAF}. \tag{4.28}$$

The momentum available after a $q\bar{q}$ split in HERWIG is given by

$$QQBAR = QCDL3\left(\frac{QLST}{QCDL3}\right)^{\mathcal{R}^{BETAF}}. \tag{4.29}$$

Let us now repeat the above calculation for the IR-Improved kernels. Recall

$$P_{qG}(z)^{exp} = F_{YFS}(\gamma_G)e^{\frac{1}{2}\delta_G}\left[z^2(1-z)^{\gamma_G} + (1-z)^2 z^{\gamma_G}\right] \tag{4.30}$$

so

$$\int_0^1 dz\frac{\alpha_s\left(Q^2\right)}{2\pi}P_{qG}(z)^{exp} = \frac{4F_{YFS}(\gamma_G)e^{\frac{1}{2}\delta_G}}{b_0\ln\left(\frac{t}{\Lambda^2}\right)\left(\gamma_G+1\right)\left(\gamma_G+2\right)\left(\gamma_G+3\right)}. \tag{4.31}$$

Therefore

$$\int_{Q_0^2}^{Q^2}\frac{dt}{t}\frac{4F_{YFS}(\gamma_G)e^{\frac{1}{2}\delta_G}}{b_0\ln\left(\frac{Q^2}{\Lambda^2}\right)\left(\gamma_G+1\right)\left(\gamma_G+2\right)\left(\gamma_G+3\right)}, \quad t = Q^2$$
$$= \frac{4F_{YFS}(\gamma_G)e^{0.25\gamma_G}}{b_0\left(\gamma_G+1\right)\left(\gamma_G+2\right)\left(\gamma_G+3\right)}Ei\left(1,\frac{8.369604402}{b_0\ln\left(\frac{t}{\Lambda^2}\right)}\right)\Bigg|_{Q_0^2}^{Q^2}. \tag{4.32}$$

Here we have used

$$\delta_G = \frac{\gamma_G}{2} + \frac{\alpha_s C_G}{\pi}\left(\frac{\pi^2}{3} - \frac{1}{2}\right), \tag{4.33}$$

with $C_G = 3$ the gluon quadratic Casimir invariant. Finally

$$\Delta_a(Q^2, t) = \exp\left[-2\left(F\left(Q^2\right) - F\left(t\right)\right)\right], \tag{4.34}$$

where

$$F(Q^2) = \frac{4F_{YFS}(\gamma_G)e^{0.25\gamma_G}}{b_0\left(\gamma_G+1\right)\left(\gamma_G+2\right)\left(\gamma_G+3\right)} Ei\left(1, \frac{8.369604402}{b_0 \ln\left(\frac{Q^2}{\Lambda^2}\right)}\right), \tag{4.35}$$

and Ei as defined in appendix A.

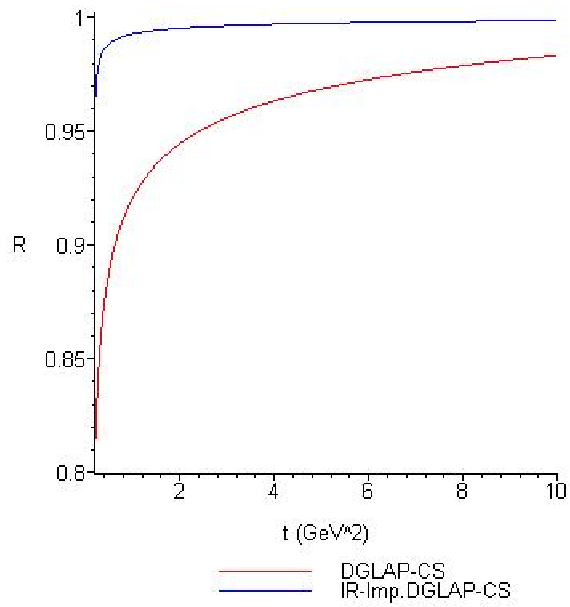

Figure 4.1: Graph of $\Delta_a(Q^2, t)$ for the DGLAP-CS and IR.Imp.DGLAP-CS kernels (4.25, 4.34)

As before, we set $\Delta_a(Q^2, t) = \mathcal{R}$ and solve for t. We accomplished this by setting

$$f(t) = F(t) - \frac{\ln(\mathcal{R})}{2} - F(Q^2), \quad \text{from} \quad (4.34) \tag{4.36}$$

and using the Newton-Raphson method with

$$f'(t) = \frac{4F_{YFS}(\gamma_G)e^{0.25\gamma_G}}{b_0\left(\gamma_G+1\right)\left(\gamma_G+2\right)\left(\gamma_G+3\right)} \frac{e^{\frac{8.369604402}{b0\ln\left(\frac{t}{\Lambda^2}\right)}}}{t\ln\left(\frac{t}{\Lambda^2}\right)} \tag{4.37}$$

Fig. 4.1 shows the difference between the two results $\Delta_a(Q^2, t)$. We see that they agree within a few % except for softer values of t, as expected.

These new functions were implemented in HERWIG6.5. Our results are given in the next chapter.

CHAPTER FIVE

HERWIRI Results

We will now discuss the phenomological implications of our new Monte Carlo HERWIRI1.0 [84, 85, 86]. Specifically, we compared $pp \to$ 2-jets $+ X$ via $2 \to 2$ hard process and $pp \to Z/\gamma^* + X \to \ell^+\ell^- + X'$, with $\ell = e, \mu$, results obtained by HERWIG6.5 and HERWIRI1.0. The three main quantities that we compared were the p_t, energy fraction and rapidity distributions. We made these comparisons at $\sqrt{s} = 14$ TeV, LHC energies. Comparisons were also made for π^+ production in $2 \to 2$ hard processes at these energies. As a test of HERWIRI1.0, we also did a comparison of the p_t and rapidity distribution at $\sqrt{s} = 1.96$ TeV for the process $p\bar{p} \to Z/\gamma^* \to e^+e^- + X$.

We choose these processes due to their importance at LHC. At LHC the dominant process is the $2 \to 2$ hard process and the Z bosons will be produced in large amounts as well. The Z boson cross sections, like the $2 \to 2$ hard subprocess, can be accurately calculated in perturbative QCD due to their large mass scale and also due to the fact their fermionic couplings are well known. The Z decay modes produce distinct experimental signatures that are easy to separate from the background $2 \to 2$ hard subprocesses. At the LHC, their cross sections have been proposed as a standard candle for measuring collider integrated luminosities. These two types of hard processes are then very representative testing processes for HERWIRI1.0 as HERWIG6.5.

As one of our first tests we will plot the Z mass distribution. We know $m_Z = 91.1875 \pm 0.0021$ [87] so we expect the peak to be around this number. From fig. (5.1) we see that this is the case. Within error bars the result of HERWIG6.5 and HERWIRI1.0 give the same result. This was the expected result, because we have

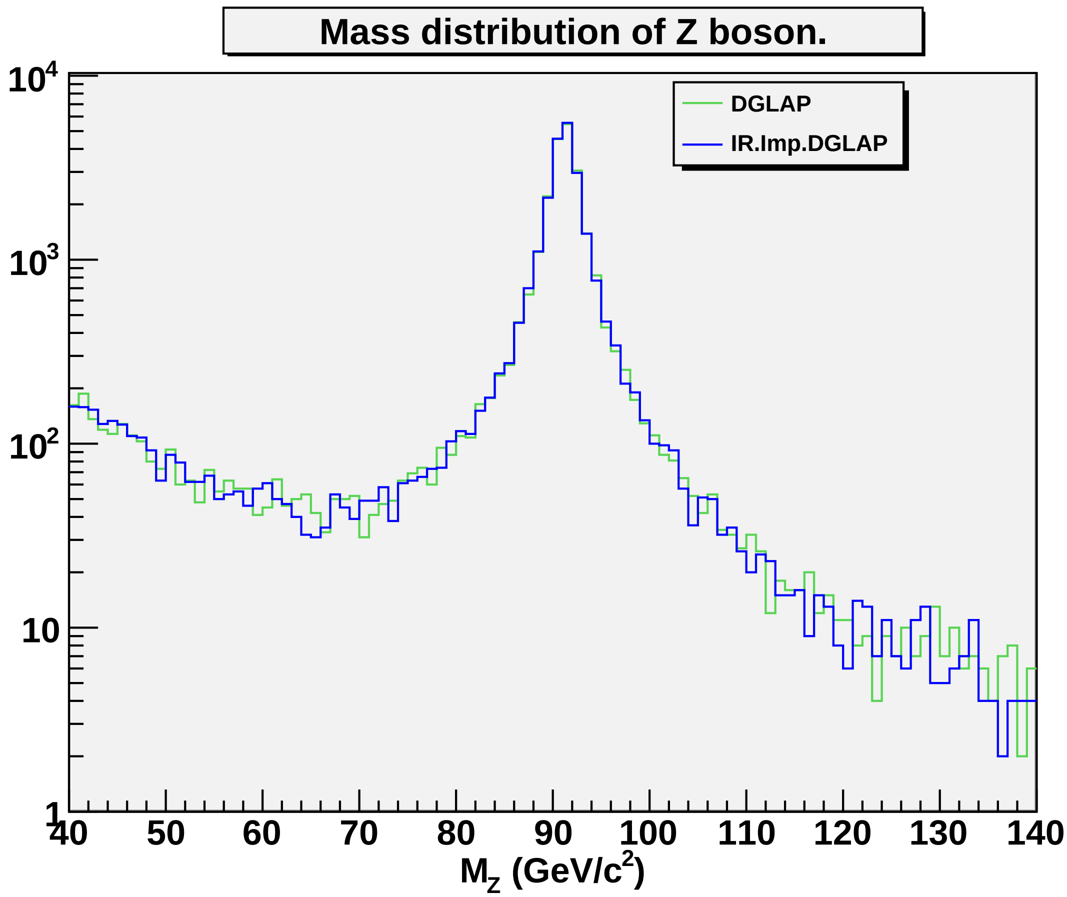

Figure 5.1. Z mass distribution.

not changed the hard scale physics in the calculation.

5.1 LHC comparison

For another of our comparisons, we ran **IPROC**=1500, QCD $2 \rightarrow 2$ hard parton scattering, for both Monte Carlos at $\sqrt{s} = 14$ TeV. In fig. (5.2(a)) we show our results for the distribution of p_t^2 for the parton shower. We ran one million events at the default values of the Monte Carlos. The efficiency was about 10% giving approximately 100 thousand events. Due to the resummation of the low p_t gluons, we expect the low p_t region to be more populated. This is exactly what we observed. We see a similar result for the energy fraction parton shower constituents.

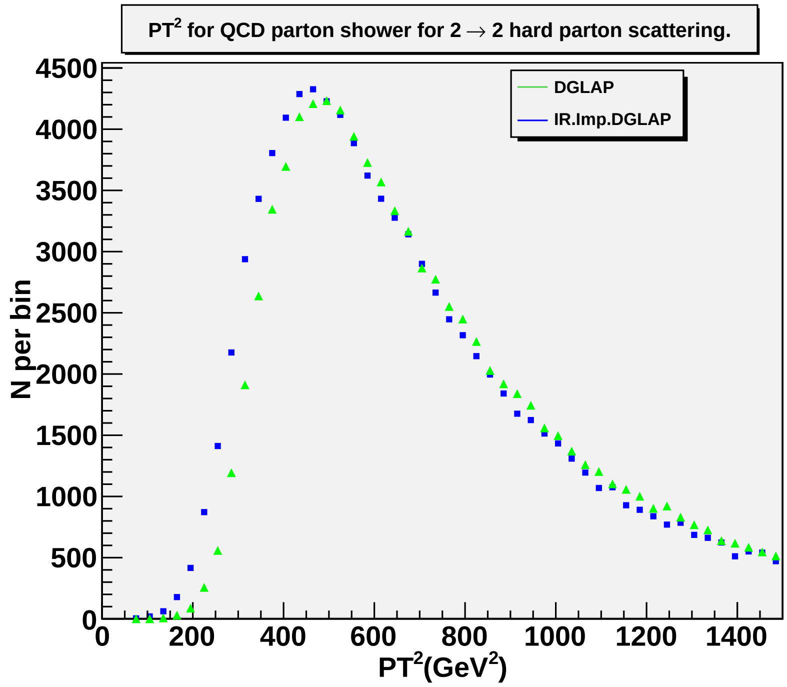

(a)

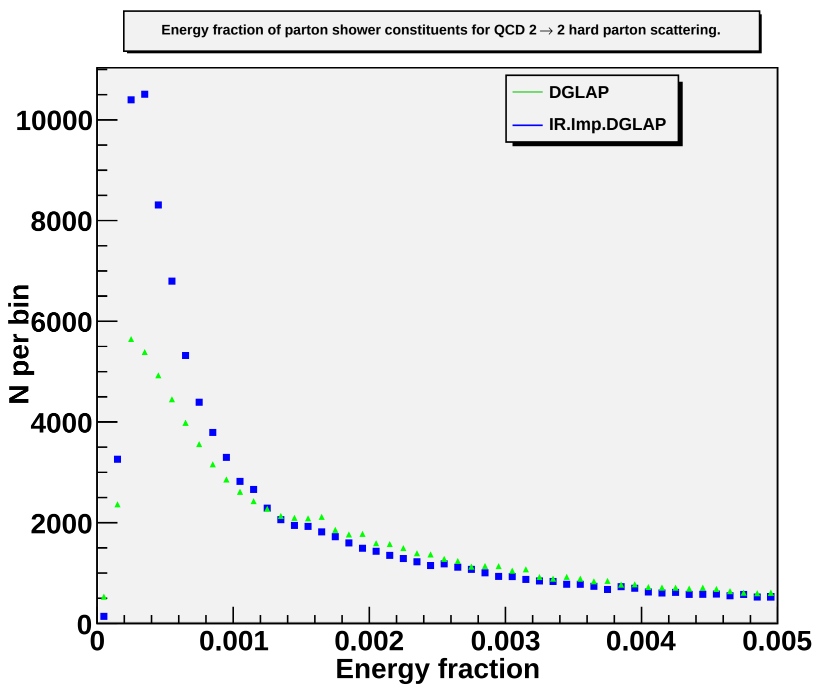

(b)

Figure 5.2: Comparison of p_t^2 and energy fraction distributions for QCD $2 \to 2$ hard parton scattering.

Now the parton shower constituents are not directly observable. To test our Monte Carlo on an observable particle we considered π^+. We see that HERWIRI1.0 modifies the distributions. The shapes are different for various values of **PTMIN** cf. fig. (5.3) and (5.4), where **PTMIN** is the minimum p_t in hadronic jet production. To compare these spectra to the real data, some tuning will be necessary.

For a final comparison at LHC energies, we compared the p_t and energy fraction distributions for IPROC=1353, $q\bar{q} \to Z \to \mu\mu^+$. The cuts on acceptance used were $m_Z > 40$ GeV, $p_t^l > 5$ GeV and $|\eta_\ell| < 50$. These results are shown in (5.5). As expected, for parton energy spectra, our results with HERWIRI1.0 are softer. A similar result holds for the generated Z p_t spectra.

In fig. (5.6), we investigate the IR-cut sensitivity of HERWIG6.5 versus HERWIRI1.0 Z-distribution, by varying the IR-cut parameters by a factor of 0.7 and 1.44 relative to their values. We see that while HERWIG6.5 does not respond very much to the change in phase space, as expected, HERWIRI1.0 shows the expected response of a convergent integral. This already suggests that HERWIRI1.0 should have a better description of soft phenomenon than does HERWIG6.5.

We also compared the Z rapidity distribution at 14 TeV as shown in fig. (5.7). The rapidity Y is a function of energy and longitudinal momentum given by

$$Y = \frac{1}{2} \ln \frac{E + p_Z}{E - p_Z}. \tag{5.1}$$

We see that HERWIRI1.0 moves some events to larger values of rapidity. This will then affect precision theory predictions for the Z rapidity for a given exact finite order in perturbation theory.

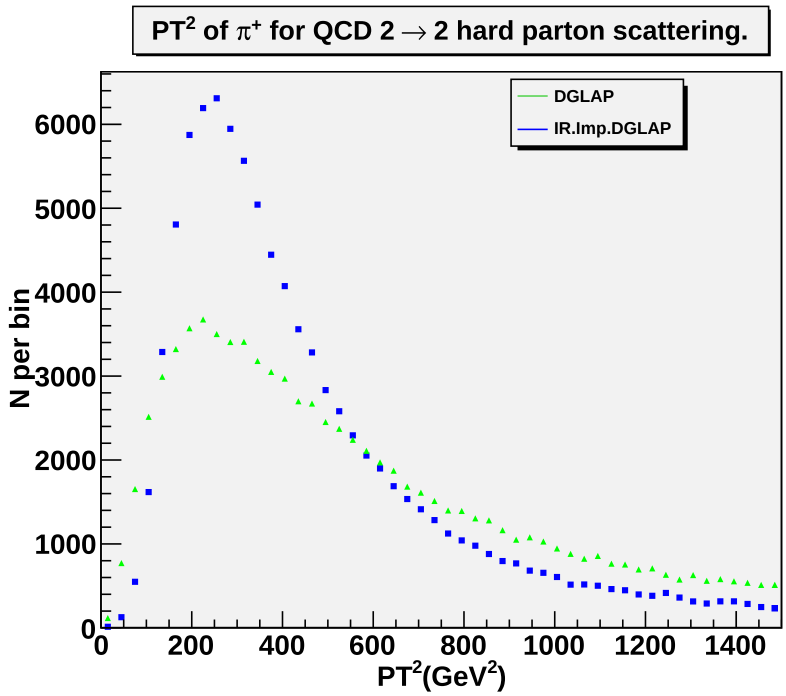

(a)

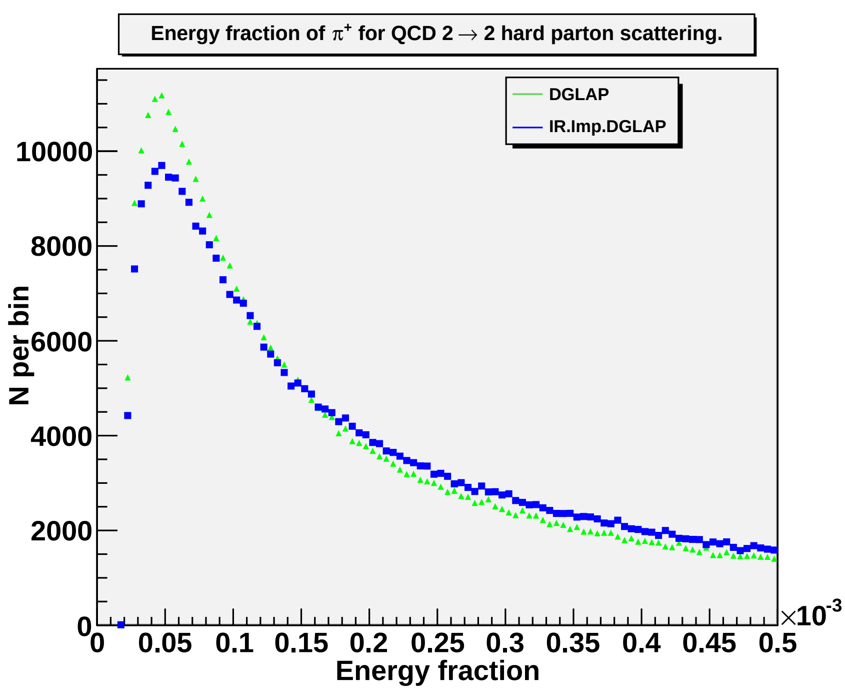

(b)

Figure 5.3: Comparison of p_t^2 and energy fraction distributions for π^+ generated for QCD $2 \rightarrow 2$ hard parton scattering for **PTMIN**=100.

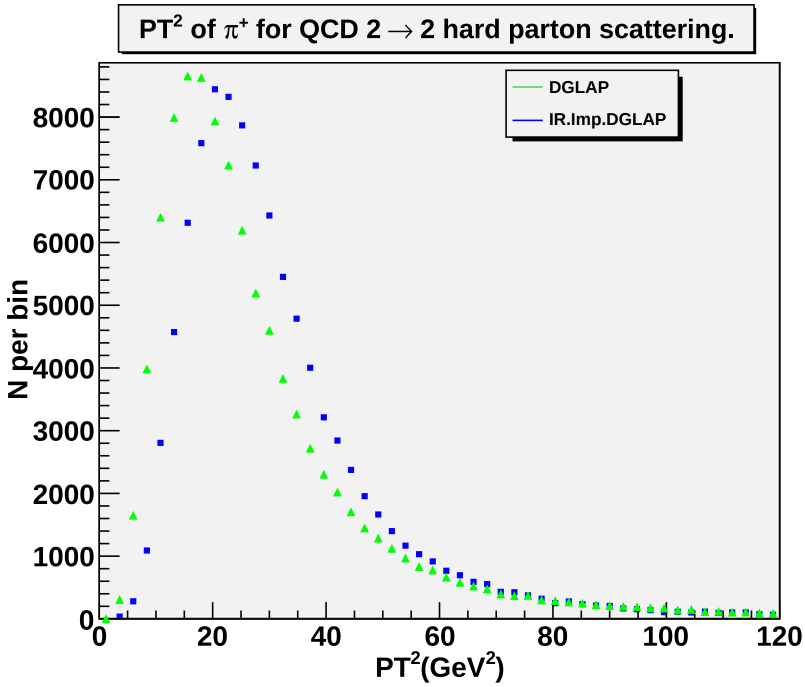

(a)

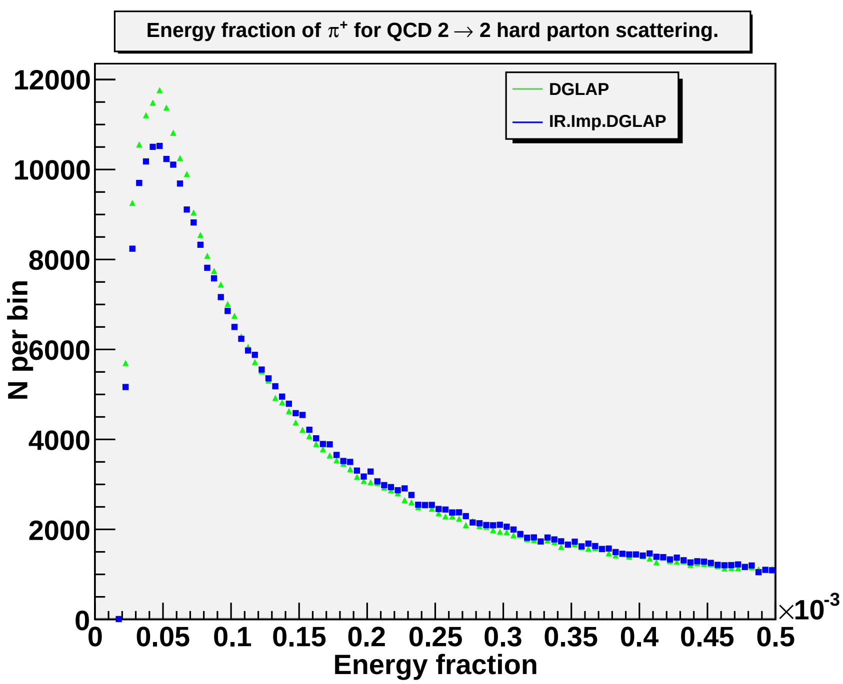

(b)

Figure 5.4: Comparison of p_t^2 and energy fraction distributions for π^+ generated for QCD $2 \rightarrow 2$ hard parton scattering for **PTMIN**=10.

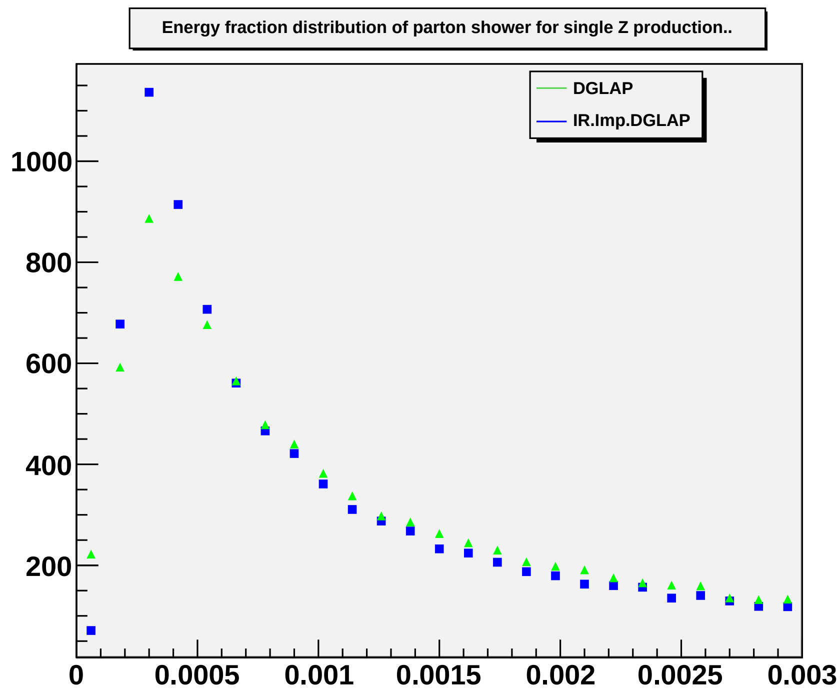

(a)

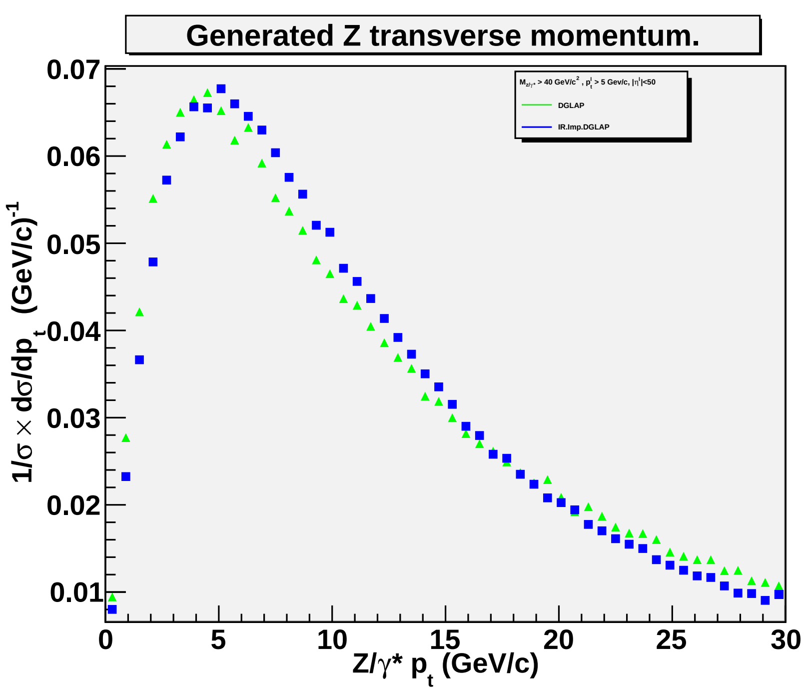

(b)

Figure 5.5. Comparison of Z p_t and energy fraction distributions for $q\bar{q} \rightarrow Z/\gamma \rightarrow \mu\mu^+$.

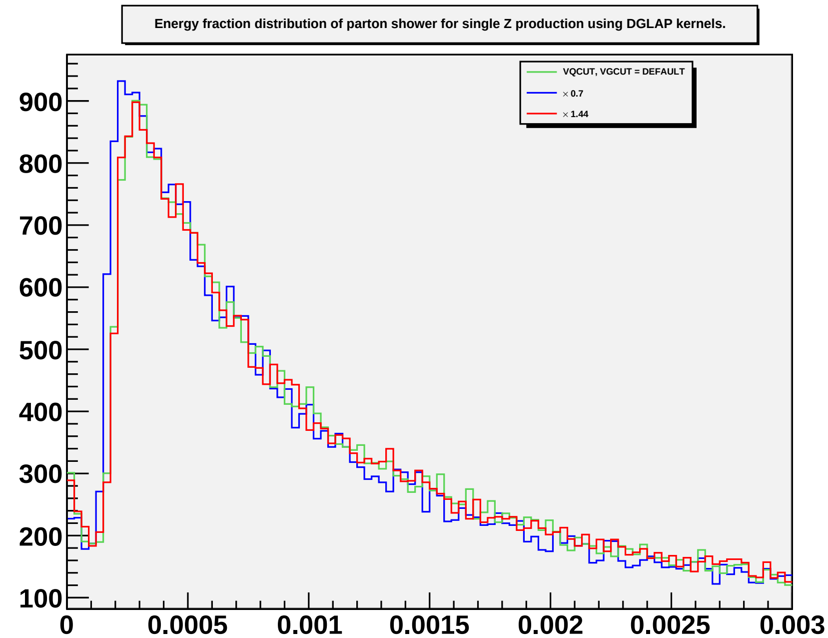

(a)

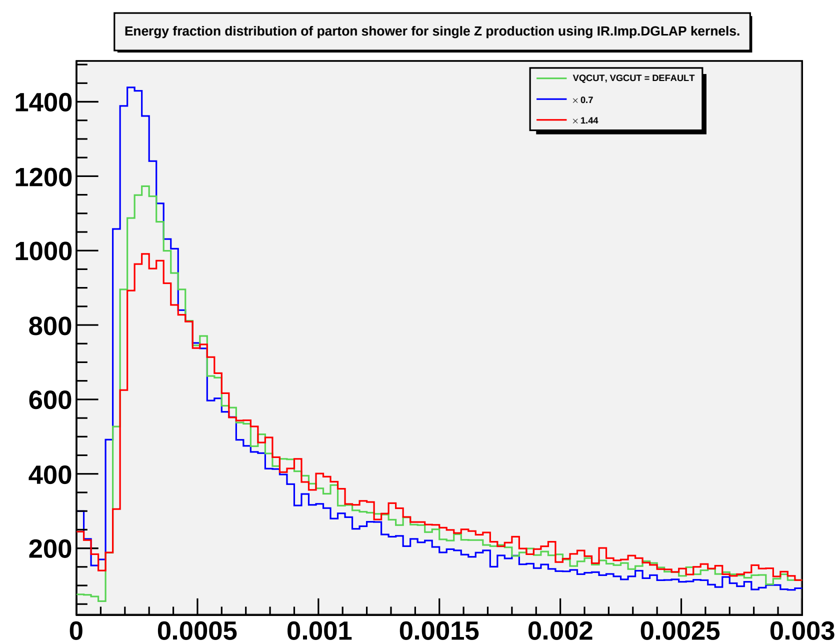

(b)

Figure 5.6: IR-cut-off sensitivity in Z distributions to the ISR parton energy fraction: (a) DGLAP-CS (b) IR-Improved DGLAP-CS - for the single Z hard subprocess.

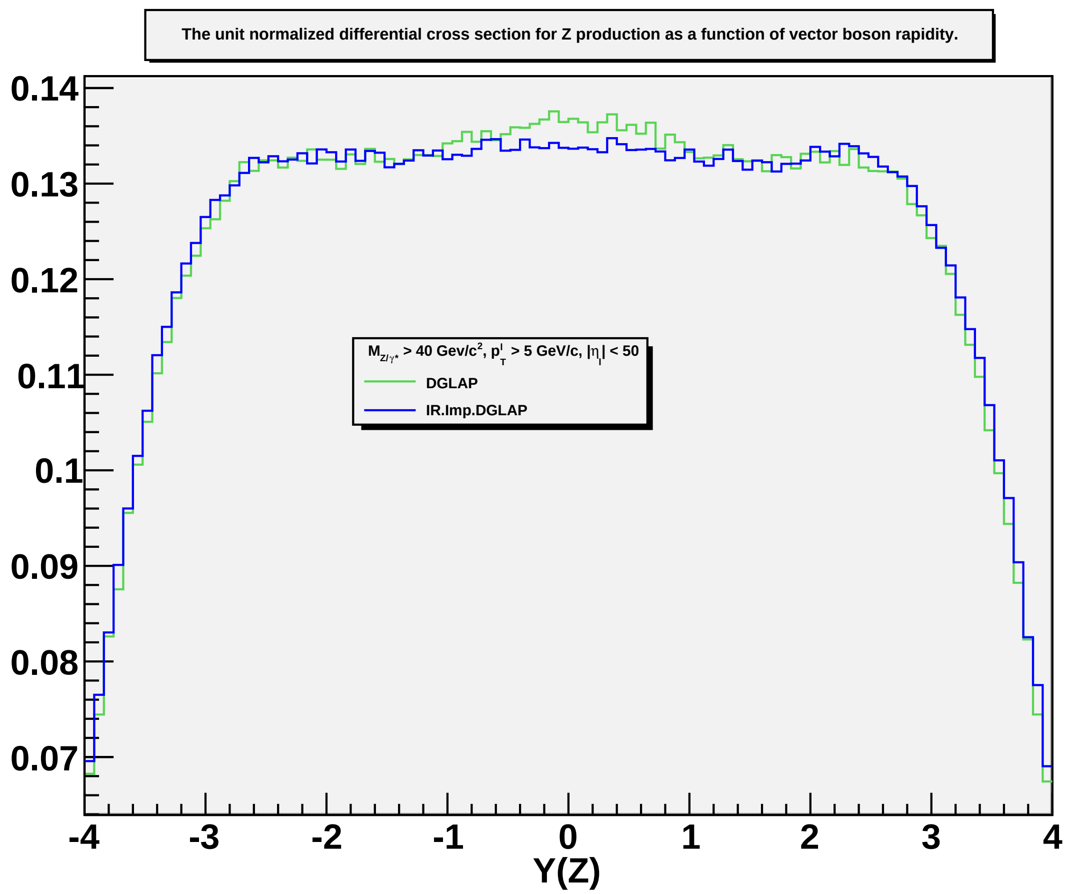

Figure 5.7. The Z rapidity distribution (ISR parton shower) comparison.

5.2 FNAL comparison

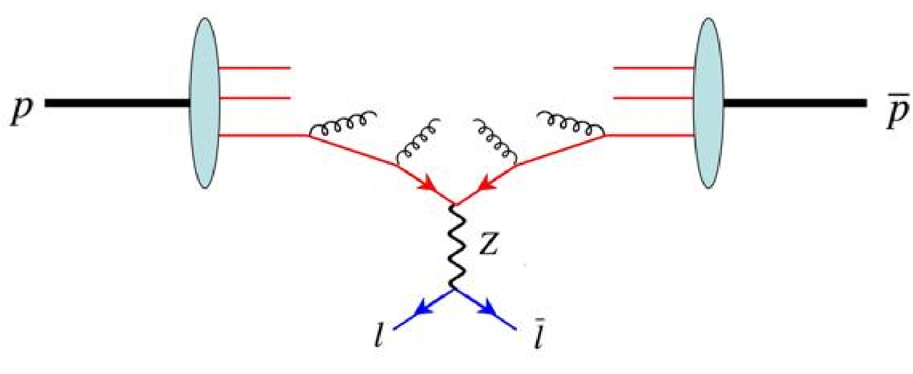

Figure 5.8: A schematic of vector boson production in high energy proton-antiproton collisions. Energetic quark-antiquark pairs annihilate to produce a Z boson, which subsequently decays to a lepton-antilepton pair.

To test our predictions that HERWIRI1.0 better describes softer phenomenon, we look at recent FNAL data in single Z production with Z decays to e^+e^- at 1.96 TeV. This process is shown in fig. (5.8) [88]. We compare both the CDF rapidity data [89] in table (E.1) and the DØ p_t data below 15 GeV in table (E.2) [90] with both HERWIG6.5 and HEWRWIRI1.0. We see that the HERWIRI1.0 and HERWIG6.5 χ^2/d.o.f. for the rapidity data are similar cf. fig. (5.9), 1.76 and 1.86 for HERWIG6.5 and HERWIRI1.0 respectively, with HERWIRI1.0 somewhat closer to the data for smaller values of the data, save the first two points at and next to $Y = 0$. For the the re-normalized p_t DØ spectrum between 0 and 15 GeV, we see that HERWIRI1.0 gives a better χ^2/d.o.f. (~ 0.29 versus 0.40) cf. fig.(5.10), showing that it does better represent the soft physics.

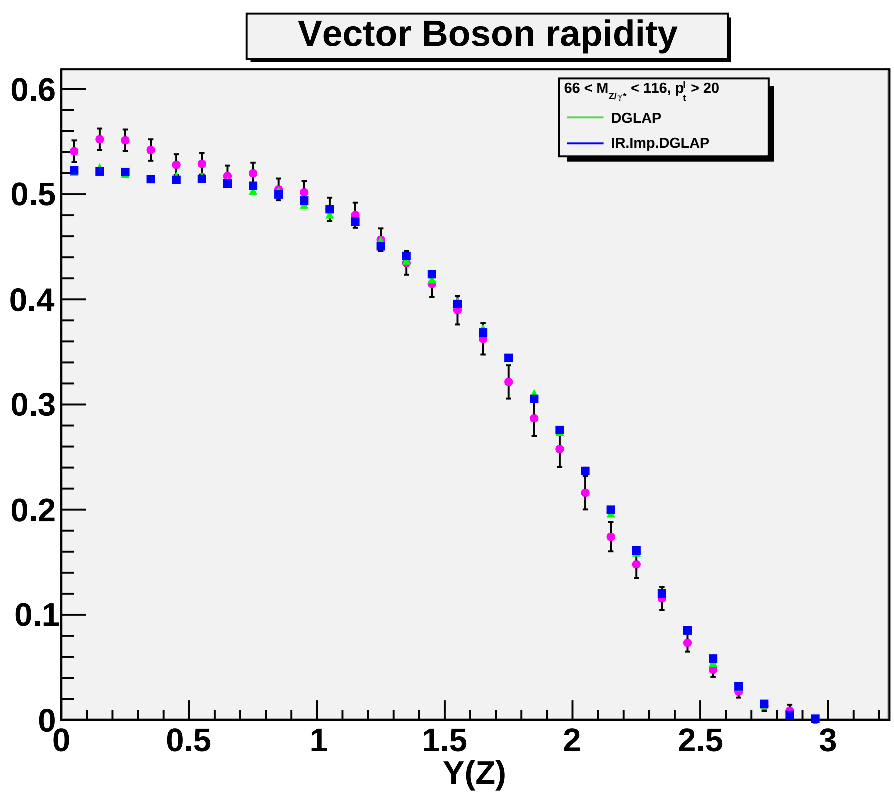

Figure 5.9: CDF rapidity data on (Z/γ^*) production to e^+e^- pairs. The dots represent the data in table (E.1).

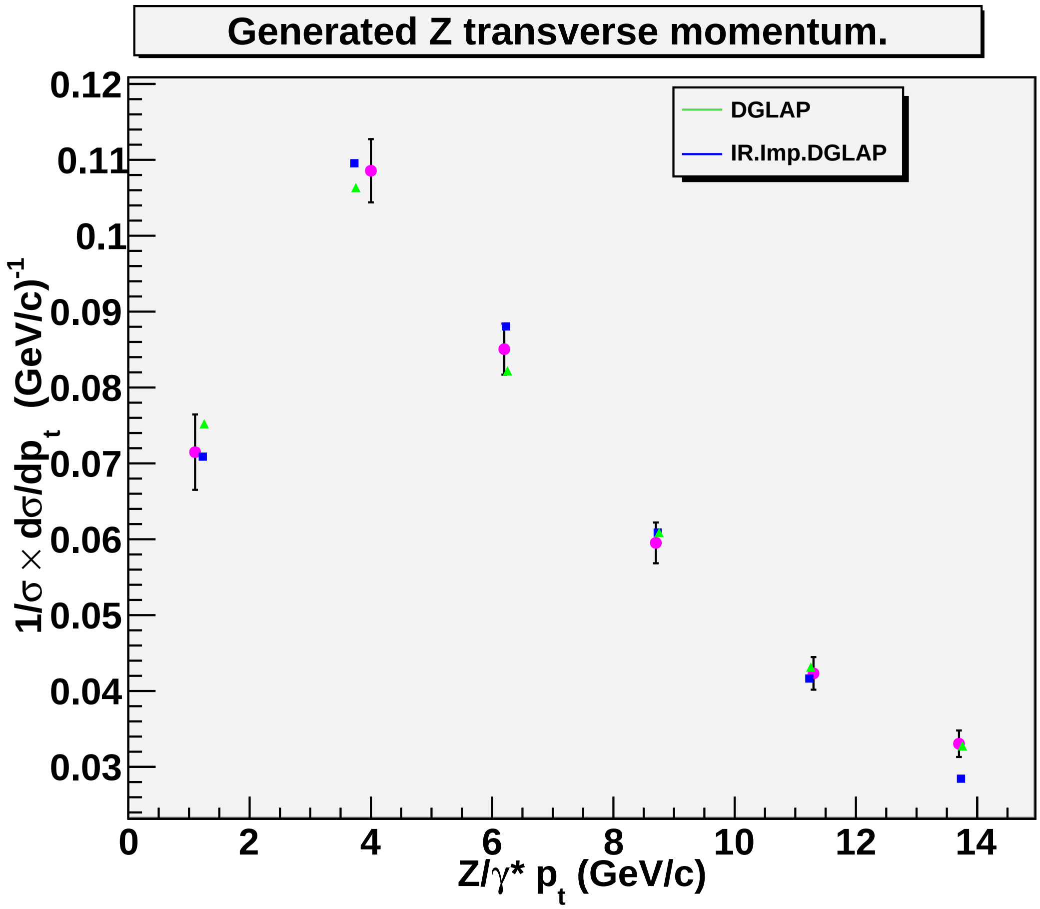

Figure 5.10: DØ p_t spectrum data on (Z/γ^*) production on e^+e^- pairs. The dots represent the data in table (E.2).

This sets the stage for a new class of hadron-hadron MC event generators which do not require an explicit IR-cut-off. Incorporation of the NLO and other exact higher order corrections give a clear path to $^2/_3 - 1\%$ precision QCD prediction on an event-by-event basis. Our research is a foundational step toward this goal.

APPENDICES

APPENDIX A

Exponential Integral

The exponential integrals , $Ei(n,z)$, are defined for $\Re > 0$;

$$Ei(n,z) = \int_1^\infty \frac{e^{-tz}}{t^n} dt. \tag{A.1}$$

The derivative is given by the following formula

$$Ei'(n,z) = -Ei(n-1,z) \quad (n = 1, 2, 3, \cdots). \tag{A.2}$$

So

$$\begin{aligned} Ei'(1,z) &= -Ei(0,z) \\ &= -\int_1^\infty e^{-tz} dt \\ &= -\frac{e^{-z}}{z}. \end{aligned} \tag{A.3}$$

APPENDIX B

Standard Model Properties

Table B.1. Fermions

Leptons			Quarks		
Flavour	Mass (Gev/c^2)	Charge	Flavour	Mass (Gev/c^2)	Charge
ν_e electron neutrino	$< 1 \times 10^{-8}$	0	u up	0.003	2/3
e electron	0.000511	-1	d down	0.006	$-1/3$
ν_μ muon neutrino	< 0.0002	0	c charm	1.3	1/3
μ muon	0.106	-1	s strange	0.1	$-1/3$
ν_τ tau neutrino	< 0.02	0	t top	172.6	2/3
τ tau	1.7771	-1	b bottom	4.3	$-1/3$

Table B.2. Bosons

Unified electroweak			Strong		
Name	Mass (Gev/c^2)	Charge	Name	Mass (Gev/c^2)	Charge
γ photon	0	0	g gluon	0	0
W^{-1}	80.398	-1			
W^+	80.398	$+1$			
Z	91.1875	0			

APPENDIX C

HERWIRI

HERWIRI 1.0 is one aspect of the HERWIRI (High Energy Radiation With IR Improvement) project to incorporate various sets of infrared improvements into a parton shower generator for hadronic physics. It is authored by: S Joseph, S. Majhi, B.F.L Ward and S. Yost. HERWIRI 1.0 incorporates IR-improved DGLAP-CS kernels in the HERWIG6.5 event generator. The program is available at http://thep03.baylor.edu as a 529 kB gzip'ed tar file herwiri1.0.tar.gz.

HERWIRI 1.0 is written in fortran 77, and has been compiled with gfortran under linux (suse10.2, fedora 6,10, and others). A Makefile is provided. The main program has the same form as described in the HERWIG manual. For more information visit the official HERWIG information page http://hepwww.rl.ac.uk/theory/seymour/herwig/. An example hwmain.f is provided in the package. In the example, the user routine HWRAP calculates the rapidity distribution of the Z boson.

HWMAIN.f

```
      PROGRAM HWIGPR
C---COMMON BLOCKS ARE INCLUDED AS FILE HERWIG65.INC
      INCLUDE 'HERWIG65.INC'
      INTEGER N
      EXTERNAL HWUDAT
C---MAX NUMBER OF EVENTS THIS RUN
      MAXEV= 1000
C---BEAM PARTICLES
      PART1='P'
      PART2='P'
```

```
      open (unit = 1, file = "output.dat")
C---BEAM MOMENTA
      PBEAM1=7000.
      PBEAM2=7000.
C---PROCESS
      IPROC=1353
C---INITIALISE OTHER COMMON BLOCKS
      CALL HWIGIN
C---USER CAN RESET PARAMETERS AT THIS POINT, OTHERWISE DEFAULT
C   VALUES IN HWIGIN WILL BE USED.
      NOWGT = .TRUE.
      PRVTX = .FALSE.
      MAXPR = 5
      PTMIN = 5
C---COMPUTE PARAMETER-DEPENDENT CONSTANTS
      CALL HWUINC
C---CALL HWUSTA TO MAKE ANY PARTICLE STABLE
      CALL HWUSTA('PI0     ')
C---USER'S INITIAL CALCULATIONS
      CALL HWABEG
C---INITIALISE ELEMENTARY PROCESS
      CALL HWEINI
C---LOOP OVER EVENTS
      DO 100 N=1,MAXEV
C---INITIALISE EVENT
      CALL HWUINE
C---GENERATE HARD SUBPROCESS
      CALL HWEPRO
C---GENERATE PARTON CASCADES
```

```
      CALL HWBGEN
C---FINISH EVENT
      CALL HWUFNE
C---USER'S EVENT ANALYSIS
      CALL HWRAP
  100 CONTINUE
C---TERMINATE ELEMENTARY PROCESS
      CALL HWEFIN
C---USER'S TERMINAL CALCULATIONS
      CALL HWAEND
      close(1)
      STOP
      END
C----------------------------------------------------------------------
      SUBROUTINE HWRAP
C     USER'S ROUTINE TO CALCULATE THE RAPIDITY DISTRIBUTION OF THE Z
C     ZLOW    : MINIMUM VALUE OF Z FOR CUT
C     PTLCUT  : CUT ON LEPTON MOMENTUM
C     ETACUT  : CUT ON LEPTON RAPIDITY
C-----------------------------------------------------------------------
      INCLUDE 'HERWIG65.INC'
      INTEGER IST, I
      LOGICAL ZCUT, PTTEST, PLUS, MINUS
      DOUBLE PRECISION ZLOW, PX, PY, PT, PTLP,PTLM, ETAL,
     &  PTLCUT, MUPLUS, MUMINUS, E, PZ, ETA,
     &  ETAFNL, ETACUT

      ETACUT = 50
      ZLOW = 40
```

```
      PTLCUT = 5
      IF (IERROR.NE.0) RETURN
      ZCUT = .FALSE.
      PLUS = .FALSE.
      MINUS =.FALSE.
         DO 30 I=1, NHEP
            IST = ISTHEP(I)
C MAKE CUT ON Z
            IF((IST .EQ. 120) .AND. (IDHEP(I) .EQ. 23)) THEN
              IF(PHEP(5,I) .GT. ZLOW)  THEN
                E = PHEP(4,I)
                PZ= PHEP(3,I)
                ETAFNL =  0.5*LOG((E+PZ)/(E-PZ))
                ZCUT = .TRUE.
              ENDIF
            ENDIF
C MAKES CUT ON PT and Y FOR E-MINUS
            IF ((IST .EQ. 190) .AND.(IDHEP(I) .EQ. 11) ) THEN
               PX = PHEP(1,I)
               PY = PHEP(2,I)
               E = PHEP(4,I)
               PZ = PHEP(3,I)
               ETA = 0.5*LOG((E+PZ)/(E-PZ))
               PTLM = SQRT(PX*PX + PY*PY)
               IF((PTLM .GT. PTLCUT) .AND. (ABS(ETA) .LT.ETACUT )) THEN
                 PLUS = .TRUE.
               ENDIF
            ENDIF
C MAKES CUT ON PT and Y FOR E-PLUS
```

```
            IF ((IST .EQ. 190) .AND.(IDHEP(I) .EQ. -11) ) THEN
               PX = PHEP(1,I)
               PY = PHEP(2,I)
               E = PHEP(4,I)
               PZ = PHEP(3,I)
               ETA = 0.5*LOG((E+PZ)/(E-PZ))
               PTLP = SQRT(PX*PX + PY*PY)
               IF((PTLP .GT. PTLCUT) .AND. (ABS(ETA) .LT.ETACUT)) THEN
                  MINUS = .TRUE.
               ENDIF
            ENDIF
   30    CONTINUE
         IF(ZCUT) THEN
C ONYLY WRITE EVENTS THAT PASS LEPTON TEST
            IF(PLUS .AND. MINUS) THEN
              WRITE(1,*), ETAFNL
            ENDIF
          ENDIF
      END
```

APPENDIX D

Sample Output

HERWIRI1.0		Beam 1:	Beam 2:	Seeds:	Status:	40
Process:	1351	980.00 GeV/c	980.00 GeV/c	17673	Error:	0
Event:	1	p	$\bar{\mathrm{p}}$	63565	Weight:	1.1597E+00

—INITIAL STATE—								
IHEP	ID	IDPDG	IST	P-X	P-Y	P-Z	ENERGY	MASS
1	p	2212	101	0.00	0.00	980.00	980.00	0.94
2	$\bar{\mathrm{p}}$	−2212	102	0.00	0.00	−980.00	980.00	0.94
3	CoM	0	103	0.00	0.00	0.00	1960.00	1960.00
—HARD SUBPROCESS—								
IHEP	ID	IDPDG	IST	P-X	P-Y	P-Z	ENERGY	MASS
4	u	2	121	0.00	0.00	0.07	0.33	0.32
5	$\bar{\mathrm{u}}$	−2	122	0.00	0.00	−173.09	173.09	0.32
6	$\mathrm{Z}^0/\gamma^\star$	23	120	2.98	6.04	−173.01	173.54	11.76
—H/W/Z BOSON DECAYS—								
IHEP	ID	IDPDG	IST	P-X	P-Y	P-Z	ENERGY	MASS
7	e^-	11	123	5.46	1.88	−102.72	102.88	0.00
8	e^+	−11	124	−5.46	−1.88	−70.29	70.53	0.00
—PARTON SHOWERS—								
IHEP	ID	IDPDG	IST	P-X	P-Y	P-Z	ENERGY	MASS
9	u	94	141	2.98	6.04	10.59	−10.06	−7.50
10	Cone	0	100	−0.52	0.85	−16.25	16.28	0.00
11	g	21	149	−2.98	−6.04	−9.22	11.44	0.75

12	ud	2101	147	0.00	0.00	978.62	978.62	−0.34
13	ū	94	142	0.00	0.00	−183.61	183.61	0.37
14	$\bar{u}\bar{d}$	−2101	148	0.00	0.00	−796.39	796.39	0.37
15	e^-	11	190	7.18	5.36	−133.80	134.10	0.00
16	e^+	−11	190	−4.20	0.67	−39.22	39.45	0.00

HERWIRI1.0		Beam 1:	Beam 2:	Seeds:	Status:	40
Process:	1351	980.00 GeV/c	980.00 GeV/c	188159330	Error:	0
Event:	2	p	p̄	459163350	Weight:	1.1597E+00

—INITIAL STATE—								
IHEP	ID	IDPDG	IST	P-X	P-Y	P-Z	ENERGY	MASS
1	p	2212	101	0.00	0.00	980.00	980.00	0.94
2	p̄	−2212	102	0.00	0.00	−980.00	980.00	0.94
3	CoM	0	103	0.00	0.00	0.00	1960.00	1960.00
—HARD SUBPROCESS—								
IHEP	ID	IDPDG	IST	P-X	P-Y	P-Z	ENERGY	MASS
4	u	2	121	0.00	0.00	0.38	0.50	0.32
5	ū	−2	122	0.00	0.00	−58.01	58.01	0.32
6	$Z^0/\gamma^\star$	23	120	5.71	2.37	−57.63	58.83	10.09
—H/W/Z BOSON DECAYS—								
IHEP	ID	IDPDG	IST	P-X	P-Y	P-Z	ENERGY	MASS
7	e^-	11	123	3.63	−1.22	−9.76	10.48	0.00
8	e^+	−11	124	−3.63	1.22	−47.87	48.02	0.00
—PARTON SHOWERS—								
IHEP	ID	IDPDG	IST	P-X	P-Y	P-Z	ENERGY	MASS

9	u	94	141	5.71	2.37	12.02	−10.81	−8.10
10	Cone	0	100	−0.96	0.29	−6.60	6.68	0.00
11	ud	2101	147	0.00	0.00	911.91	911.91	0.39
12	u	2	149	−2.24	−0.22	67.10	67.14	0.32
13	ū	−2	149	−3.46	−2.15	−11.03	11.76	0.32
14	ū	94	142	0.00	0.00	−69.64	69.64	0.21
15	$\bar{\mathrm{u}}\bar{\mathrm{d}}$	−2101	148	0.00	0.00	−910.36	910.36	0.47
16	e^-	11	190	7.22	0.27	−23.03	24.14	0.00
17	e^+	−11	190	−1.51	2.10	−34.59	34.69	0.00

APPENDIX E

FNAL Data

Table E.1. Rapidity data

y	δ	stat. δ	sys. δ
0.05	69.84	0.74	0.59
0.15	71.31	0.74	0.58
0.25	71.18	0.74	0.59
0.35	69.99	0.72	0.59
0.45	68.06	0.70	0.58
0.55	68.29	0.70	0.61
0.65	66.79	0.69	0.60
0.75	67.13	0.70	0.61
0.85	65.15	0.69	0.65
0.95	64.79	0.68	0.71
1.05	62.72	0.67	0.75
1.15	61.99	0.66	0.88
1.25	58.97	0.65	0.74
1.35	56.12	0.64	0.80
1.45	53.55	0.63	0.98
1.55	50.32	0.62	1.14
1.65	46.79	0.60	1.32
1.75	41.50	0.58	1.46
1.85	37.03	0.56	1.62
1.95	33.26	0.54	1.65
2.05	27.89	0.52	1.53
2.15	22.48	0.50	1.29
2.25	19.09	0.51	1.14
2.35	14.91	0.51	0.90
2.45	9.47	0.48	0.61
2.55	6.16	0.48	0.39
2.65	3.47	0.47	0.27
2.75	1.69	0.45	0.13
2.85	1.11	0.64	0.11
2.95	0.00	0.00	0.00

Table E.2: The normalized differential cross section for Z events produced in bins of p_T. The first uncertainty is statistical and the second is systematic.

$\langle p_T \rangle$ (GeV/c)	$1/\sigma \times d\sigma/dp_T$ (GeV/c)$^{-1}$
1.1	$(5.32 \pm 0.13 \pm 0.24) \times 10^{-2}$
4.0	$(8.08 \pm 0.12 \pm 0.19) \times 10^{-2}$
6.2	$(6.33 \pm 0.11 \pm 0.14) \times 10^{-2}$
8.7	$(4.43 \pm 0.09 \pm 0.11) \times 10^{-2}$
11.3	$(3.15 \pm 0.08 \pm 0.08) \times 10^{-2}$
13.7	$(2.46 \pm 0.07 \pm 0.06) \times 10^{-2}$
16.2	$(1.86 \pm 0.06 \pm 0.05) \times 10^{-2}$
18.7	$(1.42 \pm 0.05 \pm 0.05) \times 10^{-2}$
21.3	$(1.09 \pm 0.04 \pm 0.03) \times 10^{-2}$
23.7	$(9.40 \pm 0.40 \pm 0.20) \times 10^{-3}$
26.4	$(6.90 \pm 0.30 \pm 0.20) \times 10^{-3}$
28.5	$(5.50 \pm 0.30 \pm 0.10) \times 10^{-3}$
34.6	$(3.90 \pm 0.10 \pm 0.10) \times 10^{-3}$
44.6	$(2.10 \pm 0.07 \pm 0.06) \times 10^{-3}$
54.6	$(1.10 \pm 0.05 \pm 0.03) \times 10^{-3}$
64.6	$(7.30 \pm 0.40 \pm 0.20) \times 10^{-4}$
73.4	$(4.20 \pm 0.30 \pm 0.20) \times 10^{-4}$
85.4	$(2.50 \pm 0.20 \pm 0.10) \times 10^{-4}$
95.1	$(1.60 \pm 0.17 \pm 0.08) \times 10^{-4}$
117.5	$(6.00 \pm 0.50 \pm 0.30) \times 10^{-5}$
157.5	$(1.10 \pm 0.20 \pm 0.07) \times 10^{-5}$
195.5	$(3.00 \pm 1.00 \pm 0.30) \times 10^{-6}$
245.5	$(7.10 \pm 6.10 \pm 0.60) \times 10^{-7}$

[1] J. F. de Troconiz and F. J. Yndurain, "The hadronic contributions to the anomalous magnetic moment of the muon," *Phys. Rev.* **D71** (2005) 073008, `arXiv:hep-ph/0402285`.

[2] B. F. L. Ward, "IR-Improved DGLAP Theory: Kernels, Parton Distributions, Reduced Cross Sections," *Annals Phys.* **323** (2008) 2147–2171, `arXiv:0707.3424 [hep-ph]`.

[3] M. Dittmar, F. Pauss, and D. Zurcher, "Towards a precise parton luminosity determination at the CERN LHC," *Phys. Rev.* **D56** (1997) 7284–7290, `arXiv:hep-ex/9705004`.

[4] B. F. L. Ward and S. Jadach, "YFS MC approach to QCD soft gluon exponentiation," *Acta Phys. Polon.* **B33** (2002) 1543–1558, `arXiv:hep-ph/0205062`.

[5] B. F. L. Ward and S. Jadach, "QCD soft gluon exponentiation: YFS MC approach. ((X))," `arXiv:hep-ph/0210357`.

[6] B. F. L. Ward and S. Jadach, "Dokshitzer-Gribov-Lipatov-Altarelli-Parisi evolution and the renormalization group improved Yennie-Frautschi-Suura theory in QCD," *Mod. Phys. Lett.* **A14** (1999) 491–500.

[7] D. DeLaney *et al.*, "Multiple gluon effects in $q + \bar{q} \to t + \bar{t} + X$ at FNAL energies: Semianalytical results," *Mod. Phys. Lett.* **A12** (1997) 2425–2434, `arXiv:hep-ph/9506302`.

[8] C. Glosser, S. Jadach, B. F. L. Ward, and S. A. Yost, "QED x QCD threshold corrections at the LHC," *Mod. Phys. Lett.* **A19** (2004) 2113–2120, `arXiv:hep-ph/0404087`.

[9] B. F. L. Ward, C. Glosser, S. Jadach, and S. A. Yost, "Threshold corrections in precision LHC physics: QED x QCD," *Int. J. Mod. Phys.* **A20** (2005) 3735–3738, `arXiv:hep-ph/0411047`.

[10] D. B. DeLaney, S. Jadach, C. Shio, G. Siopsis, and B. F. L. Ward, "Multiple gluon effects in fermionanti-fermion scattering at SSC / CERN LHC energies," *Phys. Rev.* **D52** (1995) 108–115, `arXiv:hep-ph/9403204`.

[11] D. B. DeLaney, S. Jadach, C. Shio, G. Siopsis, and B. F. L. Ward, "Renormalization group improved exponentiation of soft gluons in QCD," *Phys. Lett.* **B342** (1995) 239–244, `arXiv:hep-ph/9304320`.

[12] D. B. DeLaney, S. Jadach, C. Shio, G. Siopsis, and B. F. L. Ward, "Erratum: Multiple gluon effects in fermion-(anti)fermion scattering at and beyond cern lhc energies [phys. rev. d 52, 108 (1995)]," *Phys. Rev. D* **66** (Jul, 2002) 019903.

[13] G. Corcella *et al.*, "HERWIG 6.5: an event generator for Hadron Emission Reactions With Interfering Gluons (including supersymmetric processes)," *JHEP* **01** (2001) 010, `arXiv:hep-ph/0011363`.

[14] G. Marchesini *et al.*, "HERWIG: A Monte Carlo event generator for simulating hadron emission reactions with interfering gluons. Version 5.1 - April 1991," *Comput. Phys. Commun.* **67** (1992) 465–508.

[15] S. L. Glashow, "Partial Symmetries of Weak Interactions," *Nucl. Phys.* **22** (1961) 579–588.

[16] S. Weinberg, "A Model of Leptons," *Phys. Rev. Lett.* **19** (1967) 1264–1266.

[17] A. Salam, "Elementary Particle Theory,". edited by N. Svartholm (Almquist and Wrksell, Stokholm, 1968), p. 367.

[18] G. 't Hooft and M. J. G. Veltman, "Regularization and Renormalization of Gauge Fields," *Nucl. Phys.* **B44** (1972) 189–213.

[19] G. 't Hooft and M. J. G. Veltman, "Combinatorics of gauge fields," *Nucl. Phys.* **B50** (1972) 318–353.

[20] G. 't Hooft, "RENORMALIZABLE LAGRANGIANS FOR MASSIVE YANG-MILLS FIELDS," *Nucl. Phys.* **B35** (1971) 167–188.

[21] M. J. G. Veltman, "Perturbation theory of massive Yang-Mills fields," *Nucl. Phys.* **B7** (1968) 637–650.

[22] D. J. Gross and F. Wilczek, "ULTRAVIOLET BEHAVIOR OF NON-ABELIAN GAUGE THEORIES," *Phys. Rev. Lett.* **30** (1973) 1343–1346. CITATION = PRLTA,30,1343;.

[23] H. D. Politzer, "RELIABLE PERTURBATIVE RESULTS FOR STRONG INTERACTIONS?," *Phys. Rev. Lett.* **30** (1973) 1346–1349. CITATION = PRLTA,30,1346;.

[24] F. Wilczek, "Status of QCD," `arXiv:hep-ph/9311302`.

[25] G. ALTARELLI, "The standard model of particle physics," `arXiv:hep-ph/0510281`.

[26] P. W. Higgs, "BROKEN SYMMETRIES AND THE MASSES OF GAUGE BOSONS," *Phys. Rev. Lett.* **13** (1964) 508–509.

[27] F. Englert and R. Brout, "BROKEN SYMMETRY AND THE MASS OF GAUGE VECTOR MESONS," *Phys. Rev. Lett.* **13** (1964) 321–322.

[28] **Super-Kamiokande** Collaboration, Y. Ashie *et al.*, "Evidence for an oscillatory signature in atmospheric neutrino oscillation," *Phys. Rev. Lett.* **93** (2004) 101801, `arXiv:hep-ex/0404034`.

[29] G. Altarelli, "A QCD primer," `arXiv:hep-ph/0204179`.

[30] M. H. Seymour, "Quantum ChromoDynamics," `arXiv:hep-ph/0505192`.

[31] F. Wilczek, "Asymptotic freedom: From paradox to paradigm," *Proc. Nat. Acad. Sci.* **102** (2005) 8403–8413, `arXiv:hep-ph/0502113`.

[32] S. Bethke, "Experimental tests of asymptotic freedom," *Prog. Part. Nucl. Phys.* **58** (2007) 351–386, `arXiv:hep-ex/0606035`.

[33] D. Stump *et al.*, "Inclusive jet production, parton distributions, and the search for new physics," *JHEP* **10** (2003) 046, `arXiv:hep-ph/0303013`.

[34] A. D. Martin, R. G. Roberts, W. J. Stirling, and R. S. Thorne, "Uncertainties of predictions from parton distributions. 1: Experimental errors," *Eur. Phys. J.* **C28** (2003) 455–473, `arXiv:hep-ph/0211080`.

[35] D. Amati, R. Petronzio, and G. Veneziano, "Relating Hard QCD Processes Through Universality of Mass Singularities," *Nucl. Phys.* **B140** (1978) 54.

[36] R. K. Ellis, H. Georgi, M. Machacek, H. D. Politzer, and G. G. Ross, "Perturbation Theory and the Parton Model in QCD," *Nucl. Phys.* **B152** (1979) 285.

[37] S. B. Libby and G. Sterman, "Jet and Lepton Pair Production in High-Energy Lepton- Hadron and Hadron-Hadron Scattering," *Phys. Rev.* **D18** (1978) 3252.

[38] A. H. Mueller, "Cut Vertices and their Renormalization: A Generalization of the Wilson Expansion," *Phys. Rev.* **D18** (1978) 3705.

[39] C. T. Sachrajda, "INCLUSIVE PRODUCTION AT LARGE TRANSVERSE MOMENTUM IN QCD," *Phys. Lett.* **B76** (1978) 100.

[40] T. Eichten *et al.*, "MEASUREMENT OF THE NEUTRINO - NUCLEON ANTI-NEUTRINO - NUCLEON TOTAL CROSS-SECTIONS," *Phys. Lett.* **B46** (1973) 274–280.

[41] **Gargamelle Neutrino** Collaboration, F. J. Hasert *et al.*, "Observation of neutrino-like interactions without muon or electron in the Gargamelle neutrino experiment," *Phys. Lett.* **B46** (1973) 138–140.

[42] **UA1** Collaboration, G. Arnison *et al.*, "Experimental observation of isolated large transverse energy electrons with associated missing energy at s**(1/2) = 540-GeV," *Phys. Lett.* **B122** (1983) 103–116.

[43] **UA1** Collaboration, G. Arnison *et al.*, "Experimental observation of lepton pairs of invariant mass around 95-GeV/c**2 at the CERN SPS collider," *Phys. Lett.* **B126** (1983) 398–410.

[44] **UA2** Collaboration, M. Banner *et al.*, "Observation of single isolated electrons of high transverse momentum in events with missing transverse energy at the CERN anti-p p collider," *Phys. Lett.* **B122** (1983) 476–485.

[45] **LEP** Collaboration, J. Alcaraz *et al.*, "Precision Electroweak Measurements and Constraints on the Standard Model," `arXiv:0712.0929 [hep-ex]`.

[46] **CDF** Collaboration, A. Abulencia *et al.*, "Measurements of Inclusive W and Z Cross Sections in p-pbar Collisions at sqrts =1.96 TeV," *J. Phys.* **G34** (2007) 2457–2544, `arXiv:hep-ex/0508029`.

[47] J. Callan, Curtis G., "Broken scale invariance in scalar field theory," *Phys. Rev.* **D2** (1970) 1541–1547.

[48] K. Symanzik, "Small distance behavior in field theory and power counting," *Commun. Math. Phys.* **18** (1970) 227–246.

[49] G. Altarelli and G. Parisi, "Asymptotic Freedom in Parton Language," *Nucl. Phys.* **B126** (1977) 298. CITATION = NUPHA,B126,298;.

[50] Y. L. Dokshitzer, "Calculation of the Structure Functions for Deep Inelastic Scattering and e+ e- Annihilation by Perturbation Theory in Quantum Chromodynamics. (In Russian)," *Sov. Phys. JETP* **46** (1977) 641–653.

[51] L. N. Lipatov, "The parton model and perturbation theory," *Sov. J. Nucl. Phys.* **20** (1975) 94–102.

[52] V. N. Gribov and L. N. Lipatov, "e+ e- pair annihilation and deep inelastic e p scattering in perturbation theory," *Sov. J. Nucl. Phys.* **15** (1972) 675–684.

[53] D. R. Yennie, S. C. Frautschi, and H. Suura, "The infrared divergence phenomena and high-energy processes," *Ann. Phys.* **13** (1961) 379–452.

[54] K. T. Mahanthappa, "Multiple production of photons in quantum electrodynamics," *Phys. Rev.* **126** (1962) 329–340.

[55] S. Jadach, B. F. L. Ward, and Z. Was, "Global positioning of spin GPS scheme for half-spin massive spinors," *Eur. Phys. J.* **C22** (2001) 423–430, `arXiv:hep-ph/9905452`.

[56] B. F. L. Ward and S. A. Yost, "QED x QCD exponentiation and shower / ME matching at the LHC," `arXiv:hep-ph/0509003`.

[57] D. Y. Bardin *et al.*, "Z LINE SHAPE,". Presented at the 2nd General Meeting of the LEP Physics Workshop 89, Geneva, Switzerland, May 8-9, 1989.

[58] S. Jadach, M. Skrzypek, and B. F. L. Ward, "Analytical results for low angle Bhabha scattering with pair production," *Phys. Rev.* **D47** (1993) 3733–3741.

[59] S. Jadach, E. Richter-Was, B. F. L. Ward, and Z. Was, "High precision improved analytic exponentiation results for multiple photon effects in low angle Bhabha scattering at SLC and LEP," *Phys. Rev.* **D44** (1991) 2669–2677.

[60] S. Jadach, M. Skrzypek, and B. F. L. Ward, "Is there a better way of exponentiating QED corrections?," *Phys. Lett.* **B257** (1991) 173–178.

[61] S. Jadach and B. F. L. Ward, "EXCLUSIVE EXPONENTIATION IN THE MONTE CARLO YENNIE- FRAUTSCHI-SUURA APPROACH,". Contribution to Workshop on Radiative Corrections, Brighton, England, Jul 9-14, 1989.

[62] C. Balazs, E. L. Berger, P. M. Nadolsky, and C. P. Yuan, "All-orders resummation for diphoton production at hadron colliders," *Phys. Lett.* **B637** (2006) 235–240, `arXiv:hep-ph/0603037`.

[63] **CDF** Collaboration, D. E. Acosta *et al.*, "Measurement of the cross section for prompt diphoton production in $p\bar{p}$ collisions at $\sqrt{s} = 1.96$ TeV," *Phys. Rev. Lett.* **95** (2005) 022003, `arXiv:hep-ex/0412050`.

[64] B. F. L. Ward, "IR-Improved DGLAP-CS Theory," *Advances in High Energy Physics* **2008** (2008) .

[65] M. A. Dobbs *et al.*, "Les Houches guidebook to Monte Carlo generators for hadron collider physics," `arXiv:hep-ph/0403045`.

[66] T. Sjostrand, S. Mrenna, and P. Skands, "A Brief Introduction to PYTHIA 8.1," *Comput. Phys. Commun.* **178** (2008) 852–867, `arXiv:0710.3820 [hep-ph]`.

[67] M. Dobbs and J. B. Hansen, "The HepMC C++ Monte Carlo event record for High Energy Physics," *Comput. Phys. Commun.* **134** (2001) 41–46.

[68] R. K. Ellis, W. J. Stirling, and B. R. Webber, "QCD and collider physics," *Camb. Monogr. Part. Phys. Nucl. Phys. Cosmol.* **8** (1996) 1–435.

[69] B. R. Webber, "Monte Carlo Simulation of Hard Hadronic Processes," *Ann. Rev. Nucl. Part. Sci.* **36** (1986) 253–286. CITATION = ARNUA,36,253;.

[70] A. Giovannini, "QCD JETS AS MARKOV BRANCHING PROCESSES," *Nucl. Phys.* **B161** (1979) 429–448.

[71] P. Cvitanovic, P. Hoyer, and K. Konishi, "PARTONS AND BRANCHING," *Phys. Lett.* **B85** (1979) 413.

[72] P. Cvitanovic, P. Hoyer, and K. Zalewski, "PARTON EVOLUTION AS A BRANCHING PROCESS," *Nucl. Phys.* **B176** (1980) 429.

[73] D. Amati and G. Veneziano, "Preconfinement as a Property of Perturbative QCD," *Phys. Lett.* **B83** (1979) 87.

[74] Y. I. Azimov, Y. L. Dokshitzer, V. A. Khoze, and S. I. Troyan, "Similarity of Parton and Hadron Spectra in QCD Jets," *Z. Phys.* **C27** (1985) 65–72.

[75] G. Marchesini and B. R. Webber, "Simulation of QCD Jets Including Soft Gluon Interference," *Nucl. Phys.* **B238** (1984) 1.

[76] G. Marchesini and B. R. Webber, "Monte Carlo Simulation of General Hard Processes with Coherent QCD Radiation," *Nucl. Phys.* **B310** (1988) 461.

[77] T. Sjostrand *et al.*, "High-energy physics event generation with PYTHIA 6.1," *Comput. Phys. Commun.* **135** (2001) 238–259, `arXiv:hep-ph/0010017`.

[78] M. Bengtsson and T. Sjostrand, "A Comparative Study of Coherent and Noncoherent Parton Shower Evolution," *Nucl. Phys.* **B289** (1987) 810.

[79] E. Norrbin and T. Sjostrand, "QCD radiation off heavy particles," *Nucl. Phys.* **B603** (2001) 297–342, `arXiv:hep-ph/0010012`.

[80] G. Miu and T. Sjostrand, "W production in an improved parton shower approach," *Phys. Lett.* **B449** (1999) 313–320, `arXiv:hep-ph/9812455`.

[81] T. Sjostrand, "A Model for Initial State Parton Showers," *Phys. Lett.* **B157** (1985) 321.

[82] B. Andersson, G. Gustafson, G. Ingelman, and T. Sjostrand, "Parton Fragmentation and String Dynamics," *Phys. Rept.* **97** (1983) 31–145.

[83] T. Sjostrand, "JET FRAGMENTATION OF NEARBY PARTONS," *Nucl. Phys.* **B248** (1984) 469.

[84] S. Joseph, S. Majhi, B. F. L. Ward, and S. A. Yost, "HERWIRI1.0: MC Realization of IR-Improved DGLAP-CS Parton Showers," `arXiv:0906.0788 [hep-ph]`.

[85] H. Jung *et al.*, "Proceedings of the workshop: HERA and the LHC workshop series on the implications of HERA for LHC physics," `arXiv:0903.3861 [hep-ph]`.

[86] B. F. L. Ward, S. Joseph, S. Majhi, and S. A. Yost, "Precision QED $\otimes$ QCD Resummation Theory for LHC Physics: IR-Improved Scheme for Parton Distributions, Kernels, Reduced Cross Sections with Shower/ME Matching," `arXiv:0810.0723 [hep-ph]`.

[87] **ALEPH** Collaboration, "Precision Electroweak Measurements and Constraints on the Standard Model," `arXiv:0811.4682 [hep-ex]`.

[88] **CDF and D0** Collaboration, D. S. Waters, "W and Z production and asymmetries at the Tevatron," `arXiv:0707.1709 [hep-ex]`.

[89] **CDF and DO** Collaboration, C. Galea, "Measurements of Z Production at the Tevatron," *Proc. DIS* (2008) .

[90] **D0** Collaboration, V. M. Abazov *et al.*, "Measurement of the shape of the boson transverse momentum distribution in $p\bar{p} \to Z/\gamma^* \to e^+e^- + X$ events produced at $\sqrt{s} = 1.96$-TeV," *Phys. Rev. Lett.* **100** (2008) 102002, `arXiv:0712.0803 [hep-ex]`.